Modelling and Control of Surfing Kites for Power Generation

Han Yan (Ashley)

A thesis submitted to

Auckland University of Technology

in partial fulfillment of the requirements for the degree

of

Master of Engineering (ME)

2017

School of Engineering

Abstract

Wind power is the second largest renewable resource from which we can obtain electricity, besides hydropower. Wind farms have had significant growth in past decades; however, they require a massive investment to setup including heavy towers, large land scale, and huge blades. Meanwhile, due to Betz's law, the maximum power that the wind turbine can harvest is only 59.3%. Therefore, surfing kites have been proposed as a promising alternative way to generate electricity. This project aims to build a suitable simulation platform to study the modelling and control of kites for power generation.

In this thesis, different types of the kite and their controlling methods have been reviewed, and two line surf kites have been identified as the subjects for the study. By analysing and comparing Newtonian mechanics theory and Kane' method, the dynamic model of a kite is established. The kite power generation cycle and retraction cycle is then explained according to the model. Glider mode from AeroSim simulation blockset in Simulink library provides a set of tools to develop this non-linear six degree of the freedom kite dynamic model.

The simulation results demonstrate the power generation ability of a surf kite. Considering the input constraints, a linear control system is proposed and simulated to make the kite achieve a figure eight configuration needed for power generation. The Simulink toolbox has then been employed to simulate the linear control scheme to determine its stability and performance.

Table of Contents

List of Figures

Attestation of Authorship

"I hereby declare that this submission is my own work and that, to the best of my knowledge and belief, it contains no material previously published or written by another person (except where explicitly defined in the acknowledgements), nor material which to a substantial extent has been submitted for the award of any other degree or diploma of a university or other institution of higher learning."

_____

Han Yan (Ashley)

_____/_____/_____

Acknowledgements

There have been many people who have encouraged and supported me through this research.

I would like to thank my supervisor, Dr Loulin Huang, for his support and guidance, without which my research would not have proceeded as quickly and promptly in order to finish in reasonable time.

I would like to thank my father who has encouraged me to improve my own learning through research and taught me the value of commitment. I would like to thank my mother who has motivated me to find my own pathway in life and has supported me throughout my highs and lows during my endeavour.

I would like to thank Dr. Dylan Thorpe from RMIT, who has provided me with invaluable advice, consultation, and materials for my research.

1.0 Introduction

Since the innovation of electricity, its use in AC and DC motors and its application to something as essential as an electrical light bulb, human society's reliance on and consumption of electricity has grown at a steady rate from 7,323 billion watt-hours in 1980 to 19,710 billion watt-hours in 2012 [1]. This means electricity consumption globally is increasing at a rate of approximately 2% per annum. However, conventional power generation technologies can no longer cope with this growth. Meanwhile, there has also been concern about the reliance on fossil fuel-based electricity generation because of its impact on the environment, and renewable technologies have become the favoured method for power generation [2].

1.1 Power Generation History

When the principle of electricity generation was conceived by Michael Faraday [2] in 1820, electricity became the mainstream energy choice of developed countries due to its ease of distribution and application in various pieces of equipment. The consumption of electrical power steadily increased as more requests for electricity were discovered and used. However, it was not until the first demonstration and commercialisation of hydroelectric power generation at the Schoellkopf Power Plant in 1882 that the use and further research into power generation started in earnest [3].

The first large scale commercialisation of electricity generation was hydroelectric and coal power plants. To this day these two types of power generation are the most mature generation technologies with an energy extraction efficiency of 85% to 90% for hydroelectric and 32% to 42% for coal [4]. With coal providing 40% of the world's electricity and hydroelectric providing 17% [5] in 2015, they are still very relevant in today's electricity industry.

From the 1950s, due to the concern about dwindling non-renewable resources such as coal and oil, electricity generation research has been prioritised to studying renewable methods. Meanwhile, generation from wind and geothermal innovations grew in production size.

1.2 Motivation

Wind generation through the use of wind turbines was fully developed on a mass scale in 1941 with the commissioning of the Smith-Putnam wind turbine in Castleton, Vermont, but the disadvantage of a wind turbine was immediately apparent as it was only operational for 1100 hours in total before a failure on the wind turbine blade occurred [6].

On the other hand, kite energy harvest is a new field in the renewable energy generation realm. Since it has been proposed, it has been quickly accepted by the public due to significantly fewer materials and weight compared with the conventional wind turbines. It can offer a much cheaper option of utilising wind power. Meanwhile, a kite can reach much higher altitudes than wind turbines where the wind speed, density, and stability are more suitable for electricity generation. This suggests that a kite will collect more energy and produce more steady output. Furthermore, according to the Betz' limitation, no turbine can capture more than 59% of wind kinetic energy on the horizontal axis. However, the high altitude kite is not subject to this limitation [8]. Figure 1 shows the wind speed and wind density at different elevation levels:

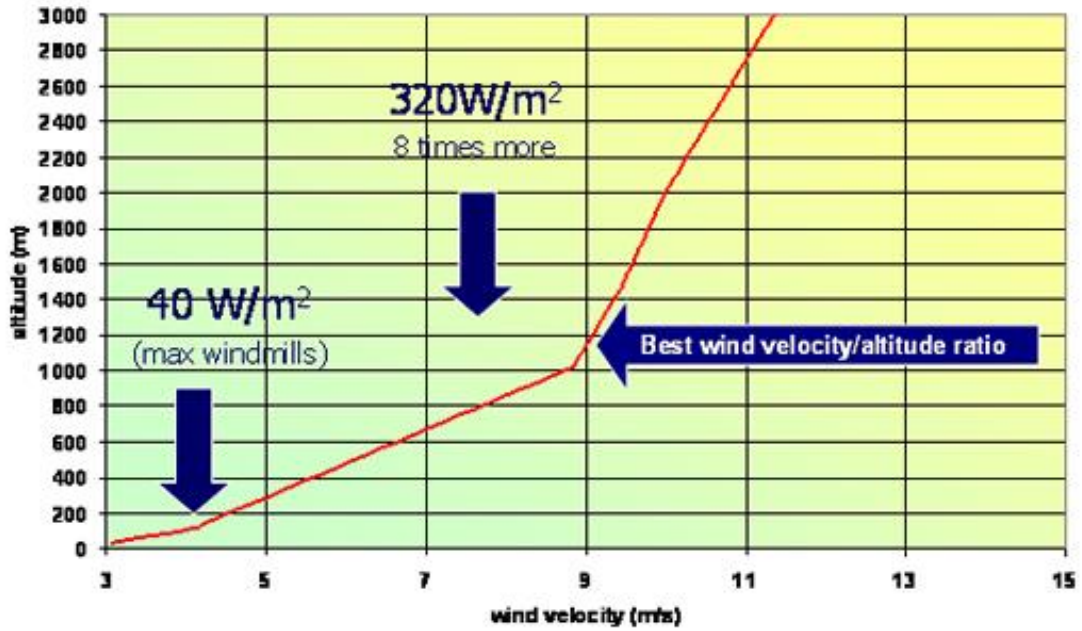

Figure 1. Wind velocity and density at various elevations. From Airborne Wind Energy. Retrieved from http://www.antonellocherubini.com/why-airborne-wind-energy.html Adapted with permission.

This new technology of kite energy harvesting offers an excellent opportunity as well as presenting difficult challenges. Even though a variety of realistic projects are being worked on internationally, the lack of test rigs in New Zealand limits this to a simulation. It is necessary to explore the character of different types of kites, reviewing the kite motion in the air in order to build a basic computer model for the chosen types of kite for further advanced development.

1.3 Thesis Objective

The current development of a kite generation system is heavily based on intensive mathematic models, which can hardly be implemented on the actual system. The primary objective of this project is to build a practical and reduced approach platform to simulate the modelling and control of a kite for power generation by employing tools such as MatLab Aerospace and Simscape. This platform should provide strong suitability so that a more complex modelling system can be developed based on this model in the future.

1.4 Thesis Structure

This thesis is organised in the following way: Chapter 2 summarises the current research in this field, studies different types of kites and chooses a suitable type for this project explaining the aerodynamic force of the surf kite. Chapter 3 develops the mathematical approaches to model the kite based on Newton's second law, followed by chapter 4 which develops mathematical methods based on Kane equation of motion. The simulation based on Newton's law model is presented in Chapter 5. Chapter 6 implements Kane's equation models by using MatLab Aerospace/Aerosim and of kite Simscape. Chapter 7 presents the simulation results and findings. The final conclusions and suggestions for future work are described in chapter 8 and 9.

2.0 Kite Literature Review

2.1 Current Research

Many ideas have been proposed to harvest electricity from kites including ladder mill, pumping mill and ship tethering kites. In 1990, Ockels first introduced the concept of generating power by using single cross wind kites, and Delft University built the first prototypes in 2007. However, the published detailed information has been limited since this, and it is still a new area of research, which is quite commercially driven [10]. Therefore, the following sections summarise the information found in the literature that is relevant to this project, including the configuration of the kites and their operation principles.

2.2 Types of Kite

Different kites have different interactions with the wind and various mechanical motions. A kite that can produce an efficient upward thrust while at the same time retains a simple structure would be ideal for this project [11]. Other factors for consideration are price, availability, shape, mass, and surface area. A variety of kites were considered for selection:

- **Diamond Shape Kite**

As a classic design that has been proven to be popular throughout the years, a kite in a diamond shape is an excellent choice. With predictable upward lift and drag based upon a single flat surface plane with minimal thickness, it is straightforward to model the interaction between this kite and the wind vector [11]. Costs of design and building of the kite are small. The mass can also be kept minimal by using metal bars as frames and nylon as the surface. However, the gain in the lift of the kite per increased surface area is not as efficient as other kites. Also, they are relatively uncontrollable for power generation purposes and the wind speed operation range is comparatively narrower.

Figure 2. Diamond Kite. From Types of Kites. Retrieved from http://www.my-best-kite.com/types-of-kites.html. Reprinted with permission.

- **Barn Door Kite**

The barn door kite is a large, pentagon-shaped kite with sides elongated to form a stout body for flight. This kite has a slight curvature towards the centre of the original pentagon shape where all the frames cross over. Giving it a larger, tortoise shell-like appearance, this protrusion mimics the behaviour of an airplane wing where the pressure difference created is larger, thereby giving it bigger lift compared to the diamond kite. The reinforced frames are required to keep the kite from ripping from being ripped. The cost is slightly higher than for the diamond

kite. The mass is also within an acceptable standard as the lift counters the increased weight. However, the increased mass means a higher wind speed is required to initially start the kite, coupled with the growing complication of five point joints to control the kite in a predictable manner [11].

Figure 3. Barn Door Kite. From Barn Door Kite Plans. Retrieved from http://www.kiteplans.org/planos/MBKbarndoor/barn-door-kite-plans.html. Reprinted with permission.

- **Rokkaku Kite**

This hexagonal kite, like the barn door, has a curvature near the frame convergence points, but there the similarity ends as the rokkaku kite is a symmetrical design. The lift on this is again increased compared to the barn door kite due to the two convergence points giving an overall greater curvature across the whole surface area of the kite. This improves the lift generated per surface area ratio to a point where relatively lighter wind can keep the rokkaku kite up in the air using two lines, making this kite somewhat easier to control by ground actuators. However, the rokkaku kite is not easy to setup. It is slightly heavier and can easily tear up in stronger winds [12].

Figure 4. Rokkaku Kite. From American Kitefliers Association. Retrieved from http://kite.org/education/styles/single-line/rokkaku-kites. Reprinted with permission.

- **Sode Kite**

As shown in figure 5, the sode kite adds the curvature into the square shaped form with a square shaped tail. This form means that the lift to the surface area ratio is highly efficient. The frame also holds up extremely well under wind stress. However, it is too costly to set up this kite for power generation. The controllability of the kite body is a complex operation as the tail can be a proven additional element of interaction to the wind force when generating power [11].

Figure 5. Sode Kite. From The Drachen Foundation. Retrieved from http://www.drachen.org/collections/sode-surprise. Reprinted with permission.

- **Delta Kite**

The delta kite is the first of the triangular kites that were considered. It retains all the characteristics of the diamond kite while adding in the stability curvature of the Rokkaku. This is by far the best kite that we have seen to date regarding ease of construction and low price. However, the delta kite can only fly well in low winds [13].

Figure 6. Delta Kite. From Delta Kite Gallery. Retrieved from **http://www.bckites.ca/images/stowaway-delta.jpg.** Reprinted with permission.

- **Roller kite**

The roller kite design was based upon old light gliders and airplane models with a nice large body with slight curvature [14]. The critical consideration was what the tail fin added to the design. The fin gave the design an extreme advantage over other kites in controllability and overall flexibility in harsher winds. The repair and maintenance on this kite would also be easier as the points likely to tear would be the fins. But, the roller kite is expensive and can only be found in the very niche market in New Zealand. Also, the kite is not easy to control.

Figure 7. Roller Kite. From into the Wind. Retrieved from http://intothewind.com/Item--i-5685. Reprinted with permission.

- **Dopero Kite**

This kite combines the Rokkaku kite's large surface area with curvature roller kite's stabilising fin. It can sustain higher winds speeds yet at the same time has a large surface area so it can pick up and fly in a light breeze [11].

Figure 8. Dopero Kite. From Kite Builders Knowledge Base. Retrieved from http://www.kitebuilder.com/wiki/pmwiki.php/KitePlans/00022. Reprinted with permission.

- **Surf Kite**

This kite is unique in that it contains no frames. It is essentially a floating canvas tied to two strings. This type of kite can be controlled by two lines, whereas the single line kites above are highly uncontrollable for the flight trajectory. With two-line control, the operator can steer the kite by pulling on one line to create a roll angle; the angle will then cause the kite to yaw toward

to the pulling side. Meanwhile, the two-line control of power kite can generate a crosswind motion by altering the flight trajectory moving towards to the non-parallel normal wind's direction. This crosswind component increases the apparent wind on the kite [15].

Due to the material and the form of the kite shape, surf kites can generate more lift force and less drag force than other types of kites. This means that the kite can glide in the air for longer periods of time and can travel further to the edge of the wind window. Furthermore, this arc shape power kite can be quickly re-launched from the ground by pulling on one of the tethering lines to turn on the kite wingtip. Thus, the power kite was chosen as the kite model to be used [16].

Figure 9. Surf **Kite.** From Prism Kite Technology. Retrieved from https://prismkites.com/product/tensor. Reprinted with permission.

2.3 Kite Force

The motion of the kite depended on four forces and one angle: lift force, drag force, tension, weight, and angle of attack. Lift and drag force can be considered as one overall force called wind force. The diagram below shows how the forces act on the kite. Each of these forces will be discussed in detail below:

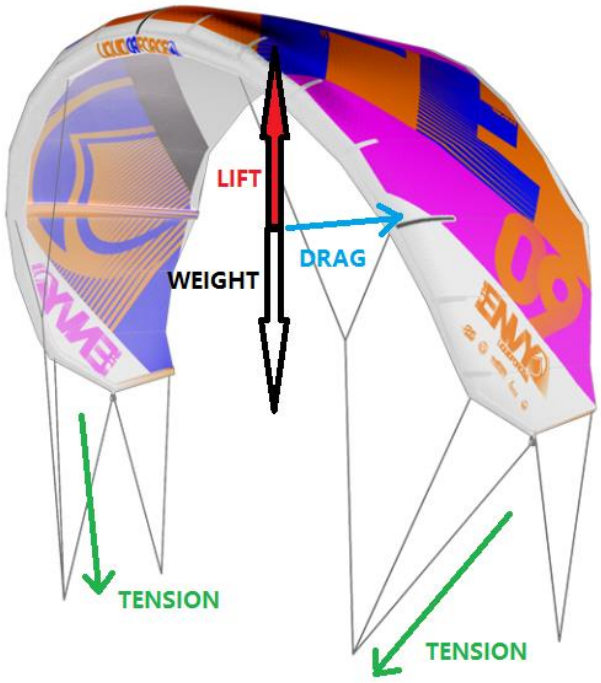

Figure 10 Kite Aerodynamic Forces

2.3.1 Wind force components

Overall, the wind force consists of lift force and drag force as figure 10 illustrated. The lift force is in the upward direction (the red arrow), and drag force is in the horizontal direction opposite to the moving orientation of the kite (the blue arrow). The lift vector is perpendicular to the apparent wind. Apparent wind is the vector subtraction of true wind velocity deducted from the kite velocity. As figure 11 shown, a kite flying with velocity V_k on a rigid rope with

variable length r_t and an inclination angle β. The origin o of the wind reference frame of X_w, Y_w, Z_w is located at the rope attachment point, and the axis X_w is pointing in the direction of the wind velocity V_w. The apparent wind velocity V_a is defined as the relative velocity at the wing

$$V_a=V_w-V_k \tag{2.1}$$

For the sake of deriving the equation in the future, the wind velocity V_w is assumed to be uniform and constant, parallel to the ground plane.

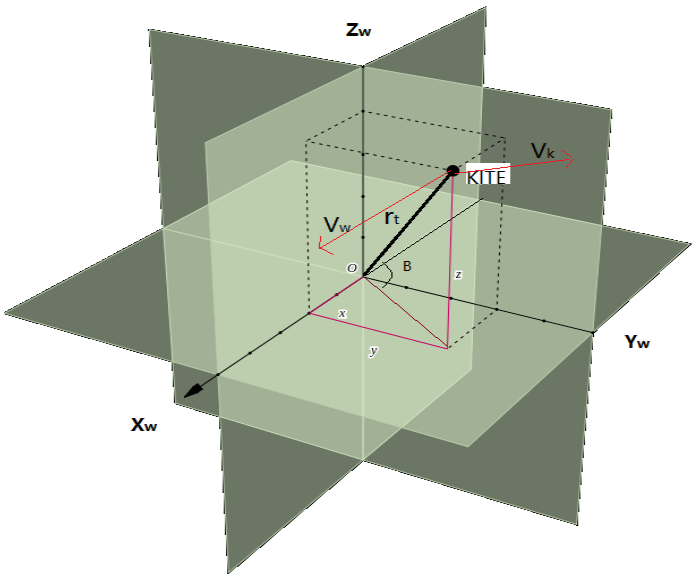

Figure 11 Wind Velocity

Lift and drag forces and the angle of attack play a major role in keeping the kite in the sky. The details of these forces are explained below:

- **Lift force**

Newton's third law states that "*to every action, there is always opposed an equal reaction; or the mutual actions of two bodies upon each other are always equal and directed to contrary*

parts." In this case, the air exerts an equal and opposite force called lift on the kite due to their interactions, and it is these forces that cause the kite to stay in the air.

According to Newton's second law of motion, he defined that: "the *change of momentum of a body is proportional to the impulse impressed on the body, and happens along the straight line on which that impulse is impressed*." This expressed as force equals mass times acceleration (F=m*a); the acceleration is the rate of change in velocity (v) with respect to the change in time (t), F=m*(dv/dt) [22].

For a kite immersed in a moving air, the air always surrounds the surface of the kite; when the kite moves, it creates deflections of the air flow. The molecules of the air are free to move, so it always moves around the kite body to produce the net force on the body. The shape of the kite has a significant influence on the amount of lift force size [22], [23].

Lift force (denoted as F_L) depends on the air density, airborne object's true velocity, the viscosity in the air and the air compressibility. It also depends on the overall surface area via air flow, the shape of the object and its inclination towards air flow.

All these effects can be described with a single variable called *lift coefficient*, noted as C_L in the equation as follows:

$$F_L = \frac{1}{2} \times \rho \times V^2 \times A \times C_L \quad (2.1)$$

where, F_L is the lift force, ρ is the air density, V is the true velocity, A is the effective kite surface area and C_L is the lift coefficient.

- **Drag force**

The drag force (denoted as F_D) is known as air resistance, which is an opposite force acting on its relative motion to surrounding air. The Drag force is not generated by the gravitational field;

if the object is not in contact with air, there will be no drag force. Like the lift force, drag force also needs the changing velocity (vector quantity) between the objective and air to be created. This force can be set up either by the changing the surrounding air (wind) or moving the body in the static fluid [22], [23].

Skin friction, form drag, and induced drag are three sources of drag force. Firstly, the skin friction between the molecules of the air and the kite surface provide drag force, and the magnitude of the skin friction depends on properties of both the kite and air [22], [23]. In this project, the material of surf kite is much smoother than other types of kite. Therefore, it will have less friction. The property of viscosity of the air is not in the scope of this project.

Secondly, the form drag is related to the shape of the object. As the air flows through the object, the local velocity and pressure are changed. The pressure defined as force/Area; the pressure is a measure of linear momentum of gas molecules and a change in momentum produces a force, a different pressure distribution will provide a force on the object. The suitable concave-convex arc of surf kite provides less form drag.

Thirdly, as the name indicates, the induced drag is caused by life force. It happens because the distribution of the lift force is not uniform on the body. In summary, the drag force is affected by cross-section area, shapes and surface smoothness [22], [23], [24].

Similar to the lift force, the drag force is also subject to a lot of complex dependencies such as the density of the air, the size and shape of the object, and body inclination to the flow. To solve the problem, the drag coefficient is introduced to reduce the complexity. It is noted as C_D. It combined all the effects, simple and complex, into a single equation:

$$F_D = \frac{1}{2} \times \rho \times V^2 \times A \times C_D \qquad (2.2)$$

where

F_D is the drag force, ρ is the air density, V is the true airspeed, A is the kite effective surface area and C_D is the drag coefficient.

To determine the drag force, the drag coefficient needs to be determined first by finding out the air conditions, shape, and inclination of the object. The drag coefficient is commonly determined by experiments in the wind tunnel.

- **Lift to drag ratio**

The lift to drag ratio E is the amount of lift force F_L generated by airfoil divided by the aerodynamic drag force F_D which is created by moving through the air. Lift to drag ratio is usually determined by flight tests or testing in a wind tunnel.

$$E = F_L/F_{D.} \quad (2.3)$$

According to equation 2.1 and 2.2, the lift to drag ratio can be also expressed as:

$$E= C_L/C_{d.} \quad (2.4)$$

Lift to drag ratio is used to indicate the efficiency of the kite. If this ratio is high, it means the kite generates more lift force over drag force; therefore, the kite will stay in the air for a long time with no control of changing position. If the ratio is low, it means the kite has too much resistance due to the design. The kite will stay in the air for a short time, and it will require more control to stay in the sky [22], [23], [24].

- **Angle of attack**

The angle of attack is the angle between the reference body line (Chord line) and flow direction; it has a large effect on the lift force. The below diagram illustrates the angle of attack.

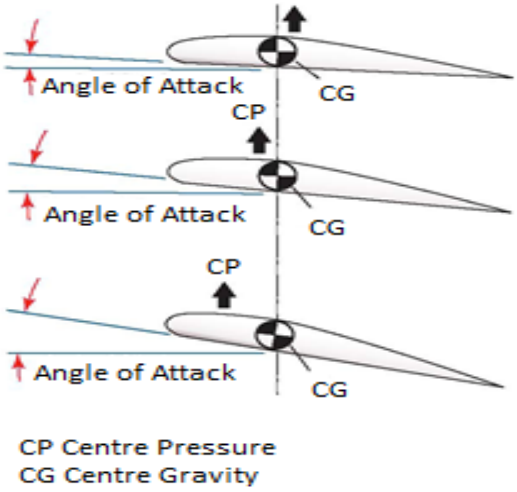

Figure 12. Angle of Attack. From The Secrets of Science. Retrieved from http://thesecretsofscience.com/center-of-pressure-in-symmetrical-airfoil. Reprinted with permission.

The angle of attack (AOA) considered as an initial kick for the kite to take off into the sky. If this angle is too high, then the kite will be subjected to loss of speed. For the symmetrical design of a surf kite, at zero angles of attack, it will not generate any lift force. By increasing the angle of attack, the air is deflected through a larger angle and the vertical component of the airstream velocity increases; it will generate the lift forces. By further increasing the angle of attack, the lift force will continue to grow until it arrives at a maximum point and further increasing of the angle will reduce the lift force. This point is called the critical angle of attack. Thus, after the critical angle of attack, if the angle is still increasing, the upper surface flow separates from the body and deflects less downwards; as a result, the life force will be decreased again. The diagram below shows the relationship of C_L,C_D and E with respect to AOA.

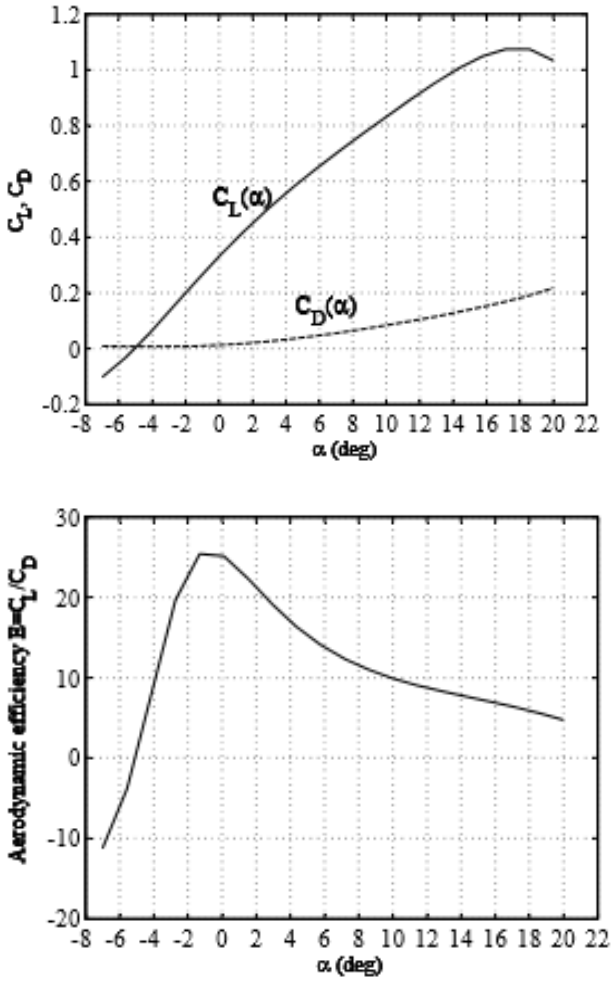

Figure 13 (a) C_L and C_D with respect to AOA; (b) Aerodynamic Efficiency **with respect to AOA** [25]

2.3.2 Tension force

The tension force is the only controlled input in the whole kite simulation system to control the kite trajectory. For simplicity, the cable is considered as a weightless rigid rod; therefore, the kite is only subject to a pure tension force, which has been exerted by aerodynamic forces trying to pull the kite away from a tethered point. The aerodynamic lift force is used to overcome the weight of kite, and the tension force is applied to overcome the aerodynamic drag force. The tension force acts through the towing point of the kite, which is in a slightly different position to the centre of the load.

2.3.3 Kite Weight

The kite's weight is perpendicular to the ground at centre gravity or balance point, as the black arrow indicated in figure 10.

The combination of all these four forces acts on different points along the centre beam of the kite; however, all of these forces reach equilibrium when the kite rises to its maximum height. The diagram below illustrates how the forces act on the kite from side view:

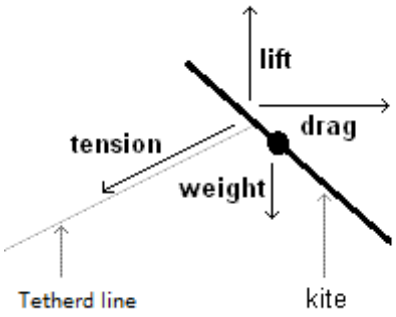

Figure 14 Equilibrium Kite Force

At fixed altitude of steady state position, the lift, and drag forces balance out the weight and tension and kite reach to the equilibrium position. The motion of the kite will be stable, which means it moves neither up nor down, the kite velocity is zero in the vertical axis. However, if the wind velocity or the controlled tension changed, the kite will fly into a new position accordingly. For instance, if the wind velocity increased, the lift and drag force increases, the lift force now is greater than the sum of the weight and tension forces, it results in the unbalanced force to push the kite moving upwards. On the other hand, as the kite climbs, the tension force increases to balance out the drag forces. Eventually, a new equilibrium point is

established in a slightly higher altitude. To keep the kite pulling the tethered line to generate power, the wind window must be introduced.

2.3.4 Wind Window

It is essential to understand what wind-window is since it determines the power of the kite and the flight trajectory. Clock type notation has been employed to indicate the kite location and displacement in the wind window. Figure 4 shows the view directly in front of the control object. Between 11 and 1 o'clock is considered the power zone where the kite will get most of the pull forces. Between 10 and11 and 1 and 2 is called the intermediate zone, which is used to launch the kite.

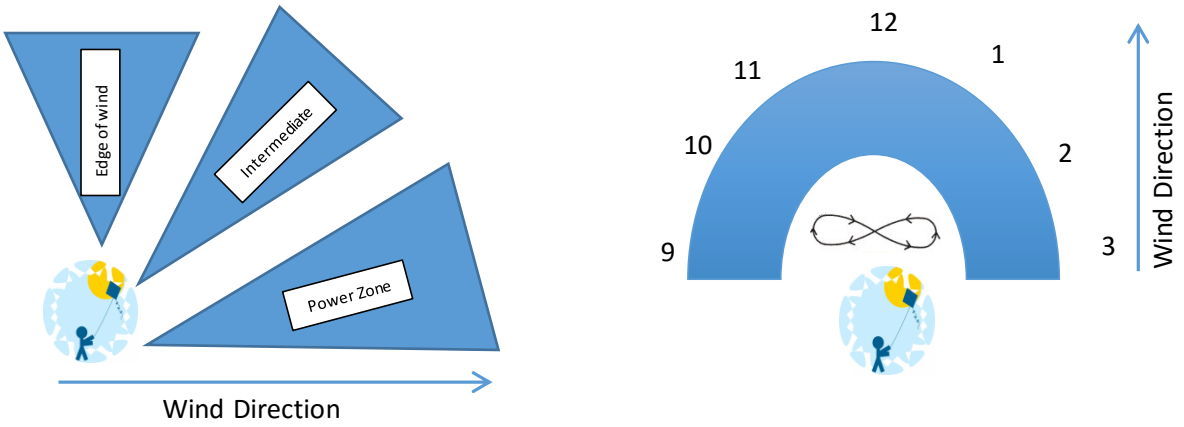

Figure 15 a) Wind window in clock notation b) Wind window side view

Since the earth is a sphere shape, the wind window has another area, which is the up and down side view demonstrated in figure 5. The side view also has three zones, which are the edge of the wind window, intermediate zone, and power zone. The power zone generates the substantial power. When using the kite to generate power, we want to control the kite so that it can stay in the power zone for a longer time, until the kite reaches to the edge of the wind window, then

retract the kite. As the kite climbs in altitude, power and speed will decrease. Then the kite will enter the intermediate zone, where the kite will fly steady in the sky while the wind strength is good. Eventually, the kite will enter the edge of the wind window, which provides no power to the kite. The kite will be in parking station and drop out of air [16]. In the kite generation project, this is the time to retract the kite and prepare for the next generation phase.

2.3.5 Trajectory of crosswind motion

When the kite flies straight downwind, it reaches the intermediate zone in a short period and parks at this zone. The kite has nearly no velocity on the earth and therefore generate very little tension force on the tethering cable. However, the goal of kite generation is to create a large constant traction force to pull the kite cable which then drives the ground station generator.

In order to generate consistent and reliable power, the kite needs to fly in a crosswind. The wind force can be separated into two vector components, which are the headwind component and crosswind component. The headwind component is in line with the travel direction, and crosswind component is perpendicular to the travel direction. When the kite is moving side from the wind direction, it creates an extra crosswind component on the kite to increase the apparent wind speed of the kite. Loyd's formula [26] suggests that the total power that can be generated is related to the apparent wind speed.

$$P=\frac{2}{27}\rho_a A C_L \left(\frac{C_L}{C_D}\right)^2 V^3 \quad (2.3)$$

P is the power, ρ_a is the air density, A is the kites effective surface area, C_L is the left coefficient , C_L/C_D is the lift to drag ratio and V is the true airspeed.

To create the crosswind motion, the kite should be steered left when it is in the central position. Initially, until it reaches the edge of the left wind window and then steere to the right so that the kite will fly to the edge of the right wind window, and then steere to the left again to repeat the whole process [17].

The resulting path of crosswind motion is shown in figure 14; the trajectory path called figure 8 had been identified as the most optimal flight trajectory [19]. Put simply, by creating crosswind motion; the kite can generate much stronger power in making mode for a longer

time compared with the straight up the track. Thus, the kite operation will have longer generating time than consuming (motor retraction) time.

Figure 16 Figure Eight Trajectories

3.0 Kite Model Based on Newton's Law

The Rigid body model is one of the simplest ways to represent a kite motion by ignoring the altitude dynamics and flexible bodies. This model typically used for initial analysis of flight trajectories and general performance analysis of kite systems [18]. It is especially useful to understand how kites work in the air during the beginning stage. Lift and drag forces are the only parameters that are used for aerodynamic modelling. By changing the roll angle (Ψ) of the kite, the motion of kite can then be controlled. The downside of this method is that it is hard to carry out the fine-tuning control of the kite.

3.1 System Equation

The right choice of system equation has to be made before physically modelling the kite system as this has a significant effect on the result. Due to the complexity of the kite, several simplifications have been carried out to achieve the appropriate modelling. In this case, Diehl's model [18] has been employed to suit the purpose. Diehl's model makes three assumptions: firstly, the kite aligns itself to the incoming airflow with no time delay. Secondly, the angle of attack remains the same during the whole flying cycle. Thirdly, the tethering cable considered as a rigid line with no sag [19]. In this case, all these assumptions are applied to the system modelling.

The previous chapter discussed that the kites are subject to four forces which are a lift, drag, tension and the kite's own gravity. The vector sum of lift force and drag force will be counted as overall wind force [20]. The kite will be in equilibrium when the overall force is equal to:

$$F=F_{grv}+F_{ten}+F_{wind} \quad (3.1)$$

Where, F_{grv} = mg and m is the mass of the kite. It referenced to the 3-dimensional coordinate system. This model will neglect the weight and aero force of the cable.

However, since the earth is a sphere shape, each of the forces will have three dimensions. The primary analytic tool used to describe the kite system on the earth will be the Fixed Cartesian coordinate system of X, Y, Z. The nominal wind speed vector V_a direction is aligned with the X-axis. The Cartesian system is shown in Figure 17:

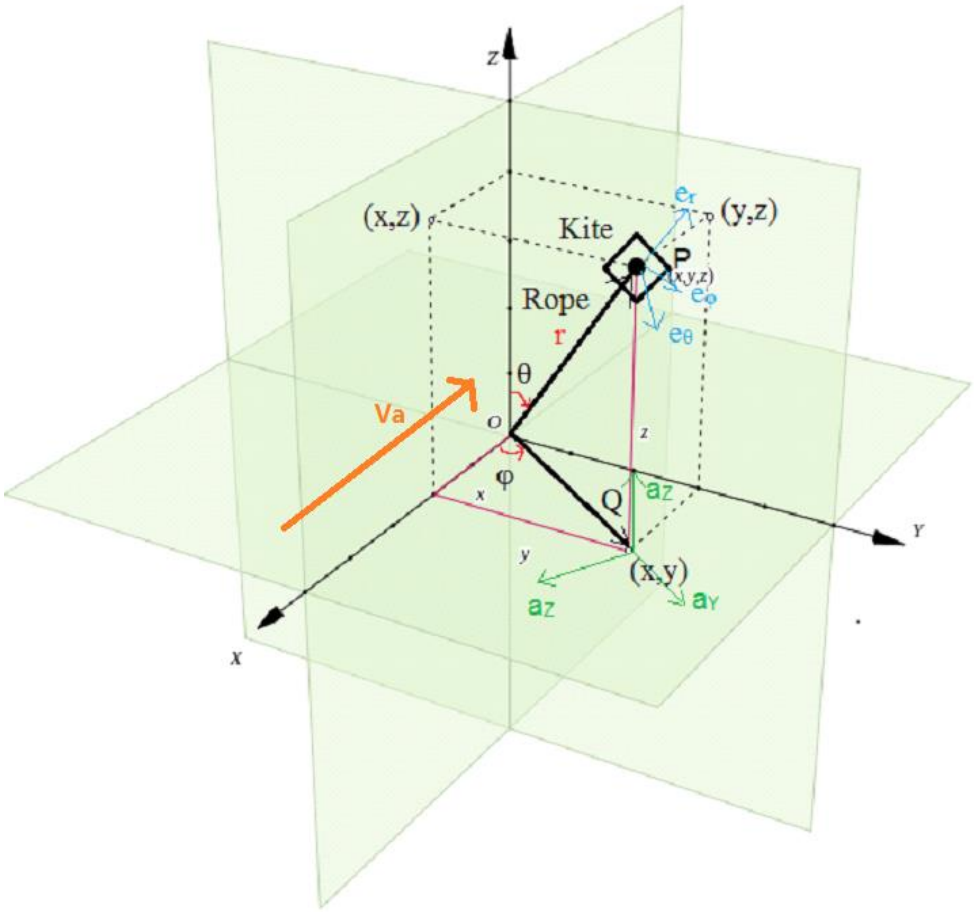

Figure 17 Coordinate system of kite with respect to local coordinate system, fixed Cartesian coordinate and spherical coordinate system

Where O represents the ground station, named as O frame, θ is the inclination angle, and φ is the azimuth angle.

3.2 Equation of Motion

Due to the complicated nature of the kite motion, it is useful to use two coordinate systems to describe the kite motion. The referenced original frame (ground control station) note as O frame and the kite body frame note as P. The global coordinate system (Cartesian coordinate system) will be used to indicate the ground control station, while, the kite position P is parameterized by two angles θ, φ and the leads for a constant line length r, with respect to the basis vectors of O frame Px Py and Pz have been employed to demonstrate the kite position. The kite position can be referenced back to the Cartesian coordinate system. Where r is the radius of the sphere, in this case, it is the length of the tethering line, θ is the inclination angle, which is referred to as the z-axis and φ is the azimuth angle to indicate the direction.

Therefore, to explain the kite position by assuming it as a point of P, it can be expressed in the following format:

$$P = \begin{pmatrix} P_x \\ P_y \\ P_z \end{pmatrix} = \begin{pmatrix} rsin(\theta)\cos(\varphi) \\ rsin(\theta)\sin(\varphi) \\ rcos(\theta) \end{pmatrix} \quad (3.2)$$

Where a lower case of x, y, z will be a scalar indication of the length from origin with respect to basis vectors of X,Y,Z; hence, the position vector can be expressed as above.

In order to translate the kite unit vector of the local coordinate to the base unit, we will need another help frame (coordinate system) **a** as the figure 17 illustrates above. Within this **a** frame, the origin will be located at the project point of kite Q at XY plane, unit vector a_Z will be aligned with the Z axis, unit vector a_Y will be the aligned in the direction of OQ and unit vector

a_X axis is going to be perpendicular to the YZ plane. This new frame initially aligned with frame o, but frame **a** is rotated about the vertical axis by angle φ. However, the angle φ will be negative by the right-hand rule (counter-clockwise rotation).

The kite will have its basic vector coordinate system. In this case, e-frame of e_r, e_θ and e_φ are used as unit vectors to express the kite's local coordinate system. The origin of this coordinate system is located at the kite's centre mass. The e-frame is initially aligned with frame a but also rotated by angle θ. Theta is the angle of rotation about a_X and e_θ.

After that, it is necessary to build up the relationship between the x, y and z and how it relates to r, φ, and θ . The key is to link $\hat{X}, \hat{Y}, \hat{Z}$ to $\overrightarrow{r^{op}} = r\,\hat{er}$ by dotting. Dot Product gives the angle between two vectors. For example, if X and Y are two vectors, then the angle 'A' between them is given by A=arc Cos [(X.Y) / xy], where x and y are the magnitudes of X and Y vectors. Note that the dot product of a vector (which is given by the sum of x, y and z components multiplied by its respective unit vectors) and a unit vector in a particular coordinate will produce the component of the vector in that co-ordinate. This is because the dot product of the unit vector in one coordinate with the other two coordinates is 0 as they are orthogonal to each other. [Cos 90(degrees) = 0]. x,y and z can be expressed as follows:

$$x=(r\hat{e_r})\cdot \hat{X} \tag{3.6}$$

$$y=(r\hat{e_r})\cdot \hat{Y} \tag{3.7}$$

$$z=(r\hat{e_r})\cdot \hat{Z} \tag{3.8}$$

The rotation matrices of dot product which noted as oRe from o (ground station) frame to **e** frame (kite) is a very complicated process due to the setup of the geometry. Therefore, **a** frame will be used to reduce complications.

The first rotation table will be oRa (from ground station o frame to a frame rotational matrices):

Table 1 Rotation table oRa

oRa	$\hat{a}_X$	$\hat{a}_Y$	$\hat{a}_Z$
$\hat{X}$	cos(φ)	-sin(φ)	0
$\hat{Y}$	sin(φ)	cos(φ)	0
$\hat{Z}$	0	0	1

Since $\hat{a}_Z$ and $\hat{Z}$ are always aligned, the dot product is 1, since $\hat{a}_Z$ is out of XY plane but $\widehat{XY}$ still in the ground plane, the dot product will be 0; similarly, $\hat{a}_X$ and $\hat{a}_Y$ are 0 with respect to $\hat{Z}$. Therefore, it can be simplified to a 2D plane where there is only $\widehat{XY}$ and $\hat{a}_X\hat{a}_Y$.

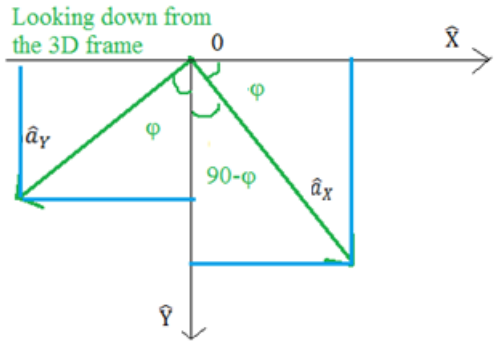

Figure 18 Simplified 2D Plane oRa

The dot product can be directly evaluated from the 2D plane by applying basic trigonometry.

The next step will be to find rotation matrices between the translational a frame and kite **e** frame:

Table 2 Rotation table aRe

aRe	$\hat{e}_\theta$	$\hat{e}_\varphi$	$\hat{e}_r$
$\hat{a}_X$	cos(θ)	0	0 sin(θ)
$\hat{a}_Y$	0	1	0
$\hat{a}_Z$	-sin(θ)	0	cos(θ)

This process is similar to the last step, only this time, take the $\hat{a}_Y$ as a rotational axis, in which **a** frame and **e** frame will rotate along with $\hat{a}_Y$. Therefore, angle φ and $\hat{a}_Y$ and $\hat{e}_\varphi$ can be rolled out and it can be simplified to 2D plane where there is only $\hat{e}_\theta$,$\hat{e}_r$ and $\hat{a}_X\hat{a}_Z$.

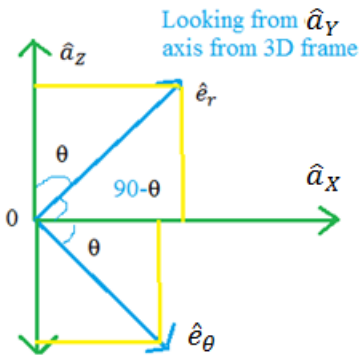

Figure 19 Simplified 2D Plane aRe

Then, to integrate the two 2D planes together to get the translational matrices for oRe;

$$oRe = oRa * aRe \tag{3.9}$$

Note that they have to be in the correct order of o frame to a frame and a frame to **e** frame; a frame is located inside. It can express as:

$$oRe = \begin{bmatrix} cos(\varphi) & -sin(\varphi) & 0 \\ sin(\varphi) & cos(\varphi) & 0 \\ 0 & 0 & 1 \end{bmatrix} * \begin{bmatrix} cos(\theta) & 0 & sin(\theta) \\ 0 & 1 & 0 \\ -sin(\theta) & 0 & cos(\theta) \end{bmatrix} \tag{3.10}$$

Table 3 Rotation table oRe

oRe	$\hat{e}_\theta$	$\hat{e}_\varphi$	$\hat{e}_r$
$\hat{X}$	cos(φ)cos(θ)	-sin(φ)	$sin(\theta)\cos(\varphi)$
$\hat{Y}$	sin(φ)cos(θ)	cosφ	$sin(\theta)\sin(\varphi)$
$\hat{Z}$	-sin(θ)	0	$cos(\theta)$

In this case, the Cartesian coordinate system of x,y,z is linked to the kite system with respect to unit vectors of $(\hat{e}_\theta, \hat{e}_\varphi, \hat{e}_r)$, it can be expressed as:

$$(\hat{e}_\theta\ \hat{e}_\varphi\ \hat{e}_r) = \begin{pmatrix} \cos(\varphi)\cos(\theta) & -\sin(\varphi) & sin(\theta)\cos(\varphi) \\ \sin(\varphi)\cos(\theta) & \cos\varphi & sin(\theta)\sin(\varphi) \\ -\sin(\theta) & 0 & cos(\theta) \end{pmatrix} \quad (3.11)$$

The kite coordinate system is used to define the rotational position of the kite with controlled tethering lines. Tension is always perpendicular to the kite surface and always aligned up with the vector; therefore, it is only exerting the force along the r axis.

Newton's laws of motion is defined:

$$F = ma \quad (3.12)$$

Where F is the force, m is the kite mass, and a is the kite body acceleration

Therefore, applying Newton's laws of motion to the kite in the local coordinate system of $(\hat{e}_\theta\ \hat{e}_\varphi\ \hat{e}_r)$, the overall force can be decomposed into the kite base vector of e_r, e_θ and e_φ , the force in each direction can be noted as:

$F_\theta = F^* e_\theta$

$F_\varphi = F^* e_\varphi$

$F_r = F^* e_r$ (3.13)

As for kite body acceleration, the position of the kite is defined in the spherical coordinate system by using inclination angle θ, the azimuth angle φ, and the length of the tethering line r.

therefore, taken the first derivative of these position vectors, the velocity, and acceleration can be found as:

$P=r\hat{e}_r$

$\dot{P}=\dot{r}\hat{e}_r+r\sin\theta\ \dot{\varphi}\ \hat{e}_\emptyset-r\dot{\theta}\hat{e}_\theta$

$$\ddot{P}=\frac{d\dot{P}}{dt}=\frac{F}{m} \tag{3.14}$$

Where m is the kite mass, F is the resulted force

To put in the spherical form:

$$\ddot{P}=\begin{pmatrix}F_\theta/m\\F_\varphi/m\\F_r/m\end{pmatrix};\ \begin{matrix}F_\theta/m\\F_\varphi/m\\F_r/m\end{matrix}\ \begin{matrix}=\ddot{\theta}r+2\dot{r}\dot{\theta}-\dot{\varphi}^2r\sin(\theta)\cos(\theta)\\=\ddot{\varphi}r\sin\theta+2\dot{\varphi}\dot{r}\sin\theta+2\dot{\varphi}\dot{\theta}r\cos\theta\\=\ddot{r}-\dot{\theta}^2r-\dot{\varphi}^2r\sin^2\theta\end{matrix} \tag{3.15}$$

To find the acceleration regarding $\ddot{\theta}$, $\ddot{\varphi}$ and $\ddot{r}$ is remain unchanged, then we can obtain:

$$\ddot{\theta}=\frac{F_\theta}{rm}-\frac{2\dot{r}\dot{\theta}}{r}+\sin\theta\cos\theta\ \dot{\varphi}^2$$

$$\ddot{\varphi}=\frac{F_\varphi}{rm\sin\theta}-\frac{2\dot{r}\dot{\theta}}{r}-2\cot\theta\ \dot{\varphi}\dot{\theta}$$

$$\ddot{r}=\frac{F_r}{m}+r\dot{\theta}^2+r\sin^2(\theta)\varphi^2 \tag{3.16}$$

Forces F_θ, F_φ and F_r include five forces which are kite gravity force, apparent force, kite aerodynamic force, aerodynamic drag force and the traction force. It can be expressed in the matrix vector form as kite gravity force $\vec{F}^{\text{grav}}$, apparent force $\vec{F}^{\text{app}}$, kite aerodynamic force $\vec{F}^{\text{aer}}$(matrix vector), aerodynamic drag force of the line $\vec{F}^{\text{c,aer}}$ and the traction force exerted by the lines on the kite of $F^{c,trc}$. It is worthy to note that in this model, the rope weight has been assumed to be zero, therefore, the aerodynamic drag force of the line $\vec{F}^{\text{c,aer}}$ can be ignored.

In this case, the gravity forces take the kite weight, the apparent forces are used to include the effects of an accelerating coordinate reference frame such as rotation of the earth, it includes centrifugal and inertial forces due to the kite movement. The detailed work can be found in [28] The kite aerodynamic force $\vec{F}^{aer}$can be derived by the computation of the lift force of $\vec{F}_L$ and drag force of $\vec{F}_D$. lift and drag force depend on the wind speed at e kite altitude, air density, kite speed with respect to the wind speed, kite surface area and the coefficient of C_L and C_D which in turn depend on the kite angle of attack which have been mentioned in chapter 2.3 and lastly the traction force is only exerted along the rope.

The relationship between these forces can be expressed in the local coordinates of $(\hat{e}_\theta, \hat{e}_\varphi, \hat{e}_r)$ as shown below:

$$F_\theta = F_\theta^{grav} + F_\theta^{app} + F_\theta^{aer}$$

$$F_\varphi = F_\varphi^{grav} + F_\varphi^{app} + F_\varphi^{aer}$$

$$F_r = F_r^{grav} + F_r^{app} + F_r^{aer} - F^{c,trc} \quad (3.17)$$

3.3 Gravity Forces

The kite itself subject to the gravitational and inertial force. Taking the assumpting of fixed rope length with pre-set trajectory, the gravitational force can be explained in the spherical coordinate as follow:

$$\vec{F}\text{grav} = \begin{bmatrix} F_\theta^{grav} \\ F_\varphi^{grav} \\ F_r^{grav} \end{bmatrix} = m \begin{bmatrix} sin\theta \\ 0 \\ -cos\theta \end{bmatrix} g \quad (3.18)$$

Therefore, equation 3.15 can be further reduced to:

$$F_{\theta} = mgsin\theta + F_{\theta}^{app} + F_{\theta}^{aer}$$

$$F_{\varphi} = F_{\varphi}^{app} + F_{\varphi}^{aer}$$

$$F_{r} = -\mathrm{mgcos}\theta + F_{r}^{app} + F_{r}^{aer} - F^{c,trc} \quad (3.19)$$

There are two frames of the reference system, one is the inertial or absolute frame of reference, which refers to a coordinate system fixed in space. The other system is called non-inertial frame of reference, which is a coordinate system that is not fixed in space, such as one defined with respect to rotating earth [32], [33], [34], [35]. For this project, kite motion is an earth-based coordinate system; therefore, Newton's motion law is used in the non-inertial frame reference with respect to earth rotating. To reconcile Newton's law, the apparent forces must be introduced. The complicated equation of apparent force will be listed in the following section.

3.4 Apparent forces

The apparent force has been introduced in above section due to the earth rotation. The constantly changing direction of the coordinate system will result in the apparent force acting on the kite. An apparent force is a vector force which includes centrifugal force and the Coriolis force [32], [33], [34], [35]. In this project, due to the kite configuration, only centrifugal inertial force is taken into consideration. That is, $\overrightarrow{\mathrm{Fapp}} = \overrightarrow{\mathrm{Fapp}}(\theta, \varphi, \mathrm{r}, \dot{\theta}, \dot{\varphi}, \dot{\mathrm{r}})$. The formula can be expressed as:

$$
\begin{aligned}
F_{\theta}^{app} &= m(\dot{\varphi}^2 r sin - \mathrm{r}\sin(\theta)\cos(\theta) - 2\dot{r}\dot{\theta}) \\
F_{\varphi}^{app} &= m(-2\sin(\theta)\,\dot{r}\dot{\varphi} - 2\mathrm{r}\cos(\theta)\dot{\varphi}\dot{\theta}) \\
F_{\mathrm{r}}^{app} &= m(r\dot{\theta}^2 - r\dot{\sin}^2(\theta)\dot{\varphi}^2)
\end{aligned}
\tag{3.20}
$$

Therefore, the equation 3.17 can further break down as:

$$
\begin{aligned}
F_{\theta} &= mgsin\theta + m(\dot{\varphi}^2 r sin - \mathrm{r}\sin(\theta)\cos(\theta) - 2\dot{r}\dot{\theta}) + F_{\theta}^{aer} \\
F_{\varphi} &= F_{\varphi}^{aer} + m(-2\sin(\theta)\,\dot{r}\dot{\varphi} - 2\mathrm{r}\cos(\theta)\dot{\varphi}\dot{\theta}) \\
F_{\mathrm{r}} &= -\mathrm{mgcos}\theta + m(r\dot{\theta}^2 - r\dot{\sin}^2(\theta)\dot{\varphi}^2) + F_{\mathrm{r}}^{aer} - F^{c,trc}
\end{aligned}
\tag{3.21}
$$

Because the traction force exerts align with r, therefore, $F^{c,trc} = F_{\mathrm{r}}$.

3.5 Aerodynamic forces of Kite

Aerodynamic force F^{aer} generated by the kiote is approximated as the sum of a lift vector L and a drag vector D as chapter 2 explined. $F^{aer}=F_L+F_D$, with the magnitudes of these force vectors represented as equation 2.1 and 2.2 in chapter 2. It can be see that the aerodynamic force is directly relate to the speed of effective wind speed. As the chapter 2 figure 11 indicate,

the nominal wind speed vector direction is aligned with the X-axis of fixed Cartesian coordinate system (ground control unit), and is denoted as $\overrightarrow{X_W}$. This aerodynamic model assumes that the nominal wind is the total wind speed vector, and the aerodynamic force $\overrightarrow{\text{Faer}}$ depends on the effective wind speed of $\overrightarrow{V_a}$, (the combination of lift and drag forces). If refering to the local coordinate system, the effective wind speed is equal to the nominal wind speed minus the kite speed with respect to the ground. The wind speed can be shown as:

$$\overrightarrow{V_a} = \overrightarrow{V_W} - \dot{P} = \overrightarrow{V_W} - \overrightarrow{V_K} \tag{3.22}$$

Where $\overrightarrow{V_W}=(v_w, 0,0)^T$ is the wind as seen from the global coordinate system, and $\dot{P}$ is the kite velocity. The kite speed $\overrightarrow{V_K}$ can be illustrated in the local coordinate system as:

$$\overrightarrow{V_K} = \begin{pmatrix} \dot{\theta} r \\ \dot{\varphi} \sin(\theta)\, r \\ \dot{r} \end{pmatrix} \tag{3.23}$$

The Wind itself will have a local coordinate system act on kite of $\vec{X}_w$, $\vec{Y}_w$, and $\vec{Z}_w$. The origin of the coordinate system will also be located at the center of gravity. Since we defined that the effective wind speed is aligned with the X-axis, the direction of this X_w is basis vector starting from the trailing edge of the kite to the leading edge of the kite. Z_w is the basis vector acting from the lift to right winding tip when looking into the incoming wind. Y_w is the basis vector fulfilling the right-handed system. So they all orthogonal to each other.

The unit vector of the wind in the X-axis can be illustrated in the local kite system as:

$$\vec{X}_w = -\frac{\overrightarrow{v_a}}{|\overrightarrow{v_a}|}$$

$$\vec{Z}_w \cdot \vec{X}_w = \vec{Z}_w \cdot \frac{\overrightarrow{v_a}}{|\overrightarrow{v_a}|} = 0 \tag{3.24}$$

The orientation of the axis Z_w against the lines axis which has been listed as unit vector e_r can be influenced by the length difference of ΔL of the two lines. If the distance between the

connectiong points is d, then the vector from the right to left connecting point is d Z_w, and the projection of this vector onto the lines axis should equal to ΔL. For example, $\Delta L = \mathrm{d}\, Z_w \cdot e_r$

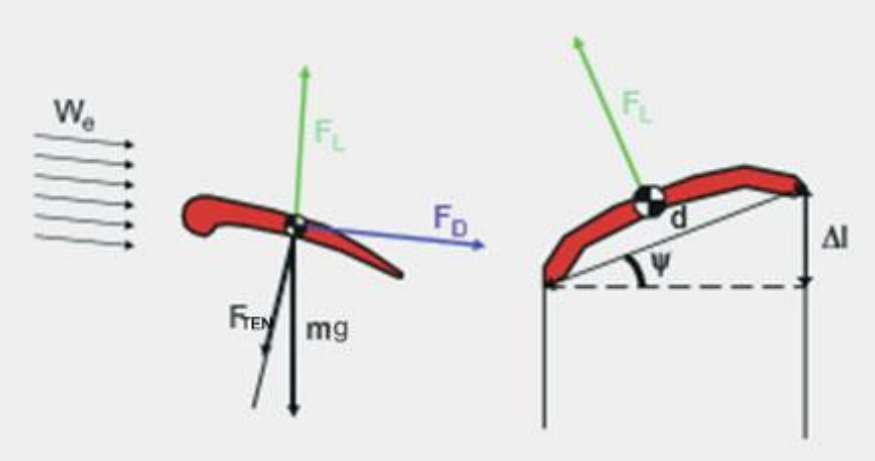

Figure 20 Kite Control Angle

Figure 18 above shows that d is the kite width, and ΔL is the length difference between the two lines. The roll angle, also known as bank angel or glide angle denoted as Ψ, influences the kite motions by changing the direction of the $\vec{F}_{aer}$.

As figure 20 indicated,

$$\Psi = \sin^{-1}(\frac{\Delta L}{d}) \tag{3.25}$$

Where Ψ is the control angle determines the orientation of Z_w, it complete the relation of:

$$\sin\Psi = \frac{\Delta L}{d} = Z_W e_r \tag{3.26}$$

Meanwhile, since we defined that the kite is always in the same orientation on the lines, therefore we have Z_w satisfying:

$$(\vec{Z}_w \times \vec{X}_w) \cdot e_r = \vec{Z}_w \cdot \frac{\overrightarrow{v_a}}{|\overrightarrow{v_a}|} \cdot e_r > 0, \tag{3.27}$$

After setup, the unit vector of the wind coordinates system, the projection of apparent wind vector V_a^p onto the tangent plane which is orthogonal to the rope.

Then $\left|V_a^p\right|$=EV_w^r; V_w^r=V_w·e_r

Where, V_w^r is the wind speed component along the rope, therefore, the projection of apparent wind velocity is the kite along e_r axix by kite coordinate system of e_θ and e_φ.

$$V_a^P = (V_a \cdot e_\theta)e_\theta + (V_a \cdot e_\emptyset)\, e_\emptyset = V_a - (V_a \cdot e_r)e_r \tag{3.28}$$

The orthogonal unit vectors of e_w t_o and e_r can be described as:

$e_w=\frac{V_a^P}{\|V_a^P\|}$; and $e_o=e_r \times e_w$; (3.29)

In this coordinated basis, the effective wind V_a has no component in e0 direction, as:

$$V_a=\|V_a^P\|e_w + (V_a \cdot e_r)e_r \tag{3.30}$$

Following figure 20, the effective wind along the e_r direction project on the kite can be simplified by introducing the ratio of γ , it will be:

$$\gamma = \sin^{-1}(\frac{V_a \cdot e_r}{\|V_a^P\|}\tan\Psi) \tag{3.31}$$

$$Z_w=e_w(-\cos\Psi\sin\gamma) + e_o(\cos\Psi\sin\gamma) + e_r\sin\Psi \tag{3.32}$$

To rewrite equation regarding γ in equation 3.32

$$Z_w \cdot v_a = -\cos\Psi\sin\gamma\left\|v_a^p\right\| + \sin\Psi\,(v_a \cdot e_r)=0 \tag{3.33}$$

Equation 3.25 can be verified by:

$$(v_a \times Z_w)\cdot e_r=(v_a \cdot e_w)\cos\Psi\cos\gamma\text{-}(v_a \cdot e_0)(\text{-}\cos\Psi\sin\gamma)$$

$$=\left\|v_a^p\right\|\cos\Psi\cos\gamma \tag{3.34}$$

Since we defined that the direction of v_a is always aligned with e_o, therefore, $v_a \cdot e_0 = 0$,

For the control angle Ψ and angle of γ in the range from -90 to 90 degree, equation 3.31 always positive.in this case, the orientation of the kite is determined by the control angle Ψ and the effective wind v_a. The vector of $X_w \times Z_w$ and X_w are the direction of the aerodynamic lift and drag respectively. To find the lift and drag force, the equation in previous chapter equation 2.1 and 2.2, we assumed that the lift coefficient and drag coefficient remains same.

$$F_L = \frac{1}{2} \times \rho \times ||Va||^2 \times A \times C_L$$

$$F_D = \frac{1}{2} \times \rho \times ||Va||^2 \times A \times C_D \quad (3.35)$$

Where V_a is effective of wind vector. And $V_a = V_w - V_k$;

Since the aerodynamic force on the kite is the sum of the lift and drag, it can express as:

$$F^{aer} = F_L + F_D = F_L(X_w \times Z_w) + F_D X_W \quad (3.36)$$

Or to put it in the sphere coordinate system, we will have

$$F_\theta^{aer} = F_L(X_w \times Z_w) \cdot e_\theta + F_D X_W \cdot e_\theta;$$

$$F_\varphi^{aer} = F_L(X_w \times Z_w) \cdot e_\emptyset + F_D X_W \cdot e_\emptyset; \quad (3.37)$$

Therefore, the equation 3.19 can be further broken down as:

$$F_\theta = mgsin\theta + m(\dot{\varphi}^2 r sin - r\sin(\theta)\cos(\theta) - 2\dot{r}\dot{\theta}) + F_L(Xw \times Zw) \cdot e_\theta + F_D X_W \cdot e_\theta$$

$$F_\varphi = m(-2\sin(\theta)\,\dot{r}\dot{\varphi} - 2r\cos(\theta)\dot{\varphi}\dot{\theta}) + F_L(X_w \times Z_w) \cdot e_\emptyset + F_D X_W \cdot e_\emptyset;$$

$$F_r = -mg\cos\theta + m(r\dot{\theta}^2 - r\sin^2(\theta)\dot{\varphi}^2) - F^{c,trc} \quad (3.38)$$

For system states in polar coordinates, the state of system x can be expressed

$x = (\theta, \varphi, r, \dot{\theta}, \dot{\varphi}, \dot{r})^T$ are the el states and control input is $u(t) = \Psi(t)$..

as equation 3.15, we can summarize the state of x in the first order ODE:

$$\dot{x} = \begin{pmatrix} \dot{\theta} \\ \dot{\varphi} \\ \dot{r} \\ \ddot{\theta} \\ \ddot{\varphi} \\ \ddot{r} \end{pmatrix} = \begin{pmatrix} \dot{\theta} \\ \dot{\varphi} \\ \dot{r} \\ \frac{g}{r} sin\theta + \frac{F_L(Xw \times Zw) \cdot e_\theta + F_D X_W \cdot e_\theta}{rm} + \frac{2\dot{r}\dot{\theta}}{r} + \sin(\theta)\cos(\theta)\,\dot{\varphi}^2 \\ -\frac{F_L(Xw \times Zw) \cdot e_\emptyset + F_D X_W \cdot e_\emptyset}{rm\sin\theta} - \frac{2\dot{r}\dot{\theta}}{r} - 2\cot\theta\,\dot{\emptyset}\dot{\theta} \\ -\frac{g}{r}\cos\theta + \dot{\theta}^2 - \sin^2(\theta)\varphi^2 \end{pmatrix} \quad (3.39)$$

3.6 Tethering Cable Forces

The only actuator control in the dynamic kite system achieved by manipulating the tethering line differences between two tethered line thus to generate the orientation angle Ψ. This project is only interested in the exertion of traction force; the weight of the line has been neglected [21]. By concerning the effect of the lines, the force F_T is always directed along the local unit vector e_r. The value of the F_T is always positive or equal to zero due to the pulling of the kite. According to the previous formula, F_T can be calculated as:

$$F_T = m(r\dot{\theta}^2 + r\sin(\theta)^2\dot{\emptyset}^2) - mg\cos(\theta) \quad (3.32)$$

The total force on the rope of F_T is the combination of the force exerted on the left-hand side of rope F_T^L and the force exerted on the right-hand side of rope F_T^R, so the kite can be controlled by changing the balance of forces on the rope [22]. Similarly, as above, both of the ropes can also be referenced to the kite body frame of the coordinate system as:

$$r_T^L = \begin{pmatrix} X_T^L \\ Y_T^L \\ Z_T^L \end{pmatrix};\ r_T^R = \begin{pmatrix} X_T^R \\ Y_T^R \\ Z_T^R \end{pmatrix};\ r_T = \begin{pmatrix} X_T^R + X_T^L \\ Y_T^R + Y_T^L \\ Z_T^R + Z_T^L \end{pmatrix} \quad (3.33)$$

Since this case based on the Diehl model [34], [35], [36], the rope can be traded as two rigid lines with no sag and a constant angle of attack. For the simplicity, the Y and Z frame of both sides of rope force can be dropped out since the displacement is small. Therefore it is only left with the X frame of X_T^L and X_T^R. It can be concluding that: $\Delta L = r_T^L - r_T^R = X_T^L - X_T^R$;

$$\Psi = \sin^{-1}\left(\frac{X_T^L - X_T^R}{d}\right) \quad (3.34)$$

In this local coordinate system, the tension force can be explained as several arguments of the nonlinear function:

$$F_T(t) = F_T(\theta,\ \phi, r, \dot{\theta},\ \dot{\phi}, \dot{r}, \overrightarrow{W_e}) \tag{3.35}$$

4.0 Kite Model Based on Kane's Equation

In this section, another mathematical model has been developed to describe simplified dynamics of the kite generation system. The kite can be treated as a single inverted pendulum model with length controlled by the tension that is free to rotate about the ground station. At the kite end, the cable is attached at the center of mass of the rigid kite body. The kite is free to rotate about the end of the pendulum. Then integrated this single inverted pendulum model into a six degree of freedom non-linear aircraft model. The aerodynamic model of the cable and cable elasticity are ignored.

4.1 Comparison with Newton's Method

There are several methods for obtaining equations of motion including Newton-Euler method, Lagrange equation, and Kane's equation. They are essentially equivalent. However, the ease of applying the various methods are different. Some are more suited for multi-body dynamics than others. Kane's equation is used to deriving the equation of motion in this section. Kane's equation originally developed for the dynamical equation of motion.

Newton-Euler method is comprehensive regarding all the forces and kinematic variables. However, it is inefficient as chapter 3 demonstrated when few of the system forces need to be solved. Lagrange's equations offer a method by ignoring all interactive and constraint forces that do not perform work; it provides a better efficiency than Newton-Euler method for the small multi-body system. The downside of this approach is the need to differentiate scalar

energy functions including kinetic and potential energy. Therefore, Kane's method combined the advantages of Newton-Euler method and Lagrange's methods.

4.2 Kane's Equation

Kane's method only using generalized forces without taking care of interactive and constraint forces between bodies. Generalized forces can be obtained from the applied forces acting on a system that has its configuration defined regarding generalized coordinates. And generalized coordinates refers to the parameters that describe the configuration of the system about some reference configuration. Furthermore, generalized velocities are the full-time derivative of the generalized coordinates of the system. By leaving the energy functions alone, differentiating for velocities and acceleration can be obtained by using an algorithm based on vector products. This method provides an efficient way of solving the dynamic equation for multi-body systems.

There are five procedures for applying Kane's method, firstly, defining all center of mass locations and applied forces areas. Secondly, select generalized coordinates, generate the expression for velocity and accelerations of all bodies. Thirdly, find the partial derivatives of velocity. Then, consider the generalized inertia forces and generalized active forces, the last step is to form the resulting equation of motion into matrix form of $\mathrm{M}\ddot{q} = B$, then reduce the equation of motion to state-space form for numerical integration.

According to Kane's equation of motion, it can be expressed as:

$$F_{qj}^{*} = F_{qj}; j = 1, \dots n; \tag{4.1}$$

$$F_{qj}^{*} = \sum_{i=1}^{n} m_i a_i \frac{\partial v_i}{\partial \dot{q}_j}; j = 1, \dots n; \tag{4.2}$$

$$F_{qj} = \sum_{i=1}^{n} F_i \frac{\partial v_i}{\partial \dot{q}_j}; j = 1, \dots n; \tag{4.3}$$

Where, F_{qj}^{*} are the generalized inertia forces; F_{qj} are the generalized active forces; n is the number of bodies; F is the vector of external forces.

The inverted pendulum model with unit vectors i,j,k in x,y and z plane, the inertial positions of kite mass, tether rope mass and the control pod with respect to the reference axes regarding the generalized coordinates showed below in figure 21 a):

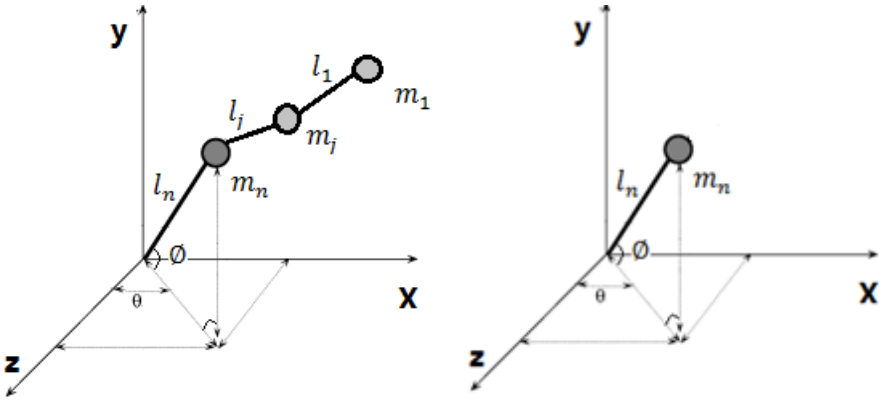

Figure 21 a) Inversed Pendulum Multibody Model; b) Inversed Pendulum Single body Model

Tether lumped masses with rigid links; External forces F applied at the lumped masses;

The angle of attack controls the kite. Neglected the attitude and flexible dynamics in this model;

Generalized coordinates are the angular rotation of each link $\emptyset_j$, θ_j, with j=1…n, and n is the number of masses, in this model, for the simplicity, only take the kite as number of mass, therefore, n=1 as figure 21 b) illustrated. Length of the links l_j(t) are a function of time, so there is no generalized coordinates when the line length is changed. However, in the future development, as the system getting complicate, the control unit and the rope weight will also be take into the consideration, then n will be equal to three.

The general position of each lumped mass in the kite model can be expressed as:

$$r = [l\cos\emptyset\sin\theta, l\sin\emptyset, l\cos\emptyset\cos\theta]+r; \quad (4.4)$$

Where l is the length of the tethering rope; r is the kite position; $\emptyset$ and θ is the rotation angle respectively.

Each lumped mass had its own local coordinate system but aligned with the global coordinate system. The corresponding velocities and accelerations are determined by differentiation of the poison vectors. Kane's equation is interest to find the nodal velocities and acceleration; it can be done by taking first full-time derivative of equation 4;

$$v = \begin{bmatrix} \dot{l}\cos\theta\sin\theta - l\dot{\emptyset}\sin\emptyset\sin\theta + l\dot{\theta}\cos\emptyset\cos\theta \\ \dot{l}\sin\emptyset + l\dot{\emptyset}\cos\emptyset \\ \dot{l}\cos\emptyset\cos\theta - l\dot{\emptyset}\sin\emptyset\cos\theta - l\dot{\theta}\cos\emptyset\sin\theta \end{bmatrix} \quad (4.5)$$

Where v is the velocities; $\dot{l}$ is the rope length generalized speed; $\dot{\emptyset}$ and $\dot{\theta}$ the rotate generalized speed. And the acceleration is the second full time derivative of velocities in equation 5, it can be represented as:

$$a = \begin{bmatrix} \ddot{l}\cos\emptyset\sin\theta - 2\dot{l}\dot{\emptyset}\sin\emptyset\sin\theta + 2\dot{l}\dot{\theta}\cos\emptyset\cos\theta - l\ddot{\emptyset}\sin\emptyset\sin\theta \\ -l\dot{\emptyset}^2\cos\emptyset\sin\theta - 2l\dot{\emptyset}\dot{\theta}\sin\emptyset\cos\theta + l\ddot{\theta}\cos\emptyset\cos\theta - l\dot{\theta}^2\cos\emptyset\sin\theta\,; \\ \ddot{l}\sin\emptyset - 2\dot{l}\dot{\emptyset}\cos\emptyset + l\ddot{\emptyset}\cos\emptyset - l\dot{\emptyset}^2\sin\emptyset\,; \\ \ddot{l}\cos\emptyset\cos\theta - 2\dot{l}\dot{\emptyset}\sin\emptyset\cos\theta - 2\dot{l}\dot{\theta}\cos\emptyset\sin\theta - l\ddot{\emptyset}\sin\emptyset\cos\theta - l\dot{\emptyset}^2\cos\emptyset\cos\theta \\ +2l\dot{\emptyset}\dot{\theta}\sin\emptyset\sin\theta - l\ddot{\theta}\cos\emptyset\sin\theta - l\dot{\theta}^2\cos\emptyset\cos\theta \end{bmatrix} \quad (4.6)$$

Where a is the acceleration; $\ddot{l}$ is the rope length generalized acceleration; $\ddot{\emptyset}$ and $\ddot{\theta}$ the rotate generalized accelerations.

According to the process of Kane's method described above, the third step is to find out the partial velocities; it has been done by taking the partial derivatives of v with respect to $\dot{l}, \dot{\emptyset}, \dot{\theta}$, in this way, the velocity vector can be projected onto the generalized speed. After taking the partial derivatives of equation 6:

$$\frac{\partial \mathrm{v}}{\partial \dot{l}} = [\cos\emptyset\sin\theta\,, \sin\emptyset\,, \cos\theta\cos\emptyset]$$

$$\frac{\partial \mathrm{v}_j}{\partial \dot{\emptyset}_k} = [-l\sin\emptyset\sin\theta\,, l\cos\emptyset\,, -l\sin\emptyset\cos\theta]$$

$$\frac{\partial \mathrm{v}_j}{\partial \dot{\theta}_k} = [l\cos\emptyset\cos\theta\,, 0, -l\cos\emptyset\sin\theta] \quad (4.7)$$

The fourth step is to find out the generalized inertial force and generalized active force. For generalized inertial force, according to equation 2, it can be expressed as:

$$F_l^* =$$

$$m\begin{bmatrix} \cos\emptyset\sin\theta\begin{pmatrix} \ddot{l}\cos\emptyset\sin\theta - 2\dot{l}\dot{\emptyset}\sin\emptyset\sin\theta + 2\dot{l}\dot{\theta}\cos\emptyset\cos\theta - l\ddot{\emptyset}\sin\emptyset\sin\theta \\ -l\dot{\emptyset}^2\cos\emptyset\sin\theta - 2l\dot{\emptyset}\dot{\theta}\sin\emptyset\cos\theta + l\ddot{\theta}\cos\emptyset\cos\theta - l\dot{\theta}^2\cos\emptyset\sin\theta \end{pmatrix} \\ +\sin\emptyset\left(\ddot{l}\sin\emptyset - 2\dot{l}\dot{\emptyset}\cos\emptyset + l\ddot{\emptyset}\cos\emptyset - l\dot{\emptyset}^2\sin\emptyset\right) \\ \cos\theta\cos\emptyset\begin{pmatrix} \ddot{l}\cos\emptyset\cos\theta - 2\dot{l}\dot{\emptyset}\sin\emptyset\cos\theta - 2\dot{l}\dot{\theta}\cos\emptyset\sin\theta - l\ddot{\emptyset}\sin\emptyset\cos\theta \\ -l\dot{\emptyset}^2\cos\emptyset\cos\theta + 2l\dot{\emptyset}\dot{\theta}\sin\emptyset\sin\theta - l\ddot{\theta}\cos\emptyset\sin\theta - l\dot{\theta}^2\cos\emptyset\cos\theta \end{pmatrix} \end{bmatrix} \quad (4.8)$$

$$F_\emptyset^* =$$

$$m\begin{bmatrix} -l\sin\emptyset\sin\theta\begin{pmatrix} \ddot{l}\cos\emptyset\sin\theta - 2\dot{l}\dot{\emptyset}\sin\emptyset\sin\theta + 2\dot{l}\dot{\theta}\cos\emptyset\cos\theta - l\ddot{\emptyset}\sin\emptyset\sin\theta \\ -l\dot{\emptyset}^2\cos\emptyset\sin\theta - 2l\dot{\emptyset}\dot{\theta}\sin\emptyset\cos\theta + l\ddot{\theta}\cos\emptyset\cos\theta - l\dot{\theta}^2\cos\emptyset\sin\theta \end{pmatrix} \\ +l\cos\emptyset\left(\ddot{l}\sin\emptyset - 2\dot{l}\dot{\emptyset}\cos\emptyset + l\ddot{\emptyset}\cos\emptyset - l\dot{\emptyset}^2\sin\emptyset\right) \\ -l\sin\emptyset\cos\theta\begin{pmatrix} \ddot{l}\cos\emptyset\cos\theta - 2\dot{l}\dot{\emptyset}\sin\emptyset\cos\theta - 2\dot{l}\dot{\theta}\cos\emptyset\sin\theta - l\ddot{\emptyset}\sin\emptyset\cos\theta \\ -l\dot{\emptyset}^2\cos\emptyset\cos\theta + 2l\dot{\emptyset}\dot{\theta}\sin\emptyset\sin\theta - l\ddot{\theta}\cos\emptyset\sin\theta - l\dot{\theta}^2\cos\emptyset\cos\theta \end{pmatrix} \end{bmatrix} \quad (4.9)$$

$$F_\theta^* =$$

$$m\begin{bmatrix} l\cos\emptyset\cos\theta\begin{pmatrix} \ddot{l}\cos\emptyset\sin\theta - 2\dot{l}\dot{\emptyset}\sin\emptyset\sin\theta + 2\dot{l}\dot{\theta}\cos\emptyset\cos\theta - l\ddot{\emptyset}\sin\emptyset\sin\theta \\ -l\dot{\emptyset}^2\cos\emptyset\sin\theta - 2l\dot{\emptyset}\dot{\theta}\sin\emptyset\cos\theta + l\ddot{\theta}\cos\emptyset\cos\theta - l\dot{\theta}^2\cos\emptyset\sin\theta \end{pmatrix} \\ -l\cos\emptyset\sin\theta\begin{pmatrix} \ddot{l}\cos\emptyset\cos\theta - 2\dot{l}\dot{\emptyset}\sin\emptyset\cos\theta - 2\dot{l}\dot{\theta}\cos\emptyset\sin\theta - l\ddot{\emptyset}\sin\emptyset\cos\theta \\ -l\dot{\emptyset}^2\cos\emptyset\cos\theta + 2l\dot{\emptyset}\dot{\theta}\sin\emptyset\sin\theta - l\ddot{\theta}\cos\emptyset\sin\theta - l\dot{\theta}^2\cos\emptyset\cos\theta \end{pmatrix} \end{bmatrix} \quad (4.10)$$

For the generalized active forces, the only control force is the tension on the cable T (neglect the weight of the cable) which exert alone l direction. According to the equation 3, it can be expressed as:

$$F_l = (F_{A_g} + [0 \quad 0 \quad -mg])\frac{\partial v}{\partial \dot{l}} - T$$

$$F_\emptyset = (F_{A_g} + [0 \quad 0 \quad -mg]) \cdot \frac{\partial v}{\partial \dot{\emptyset}}$$

$$F_\theta = (F_{A_g} + [0 \quad 0 \quad -mg]) \cdot \frac{\partial v}{\partial \dot{\theta}} \quad (4.11)$$

According to Kane's method, the generalized active force is equal to the initial generalized force. According to equation 4.1, 4.2, 4.3, 4.6 and 4.7 for a single pendulum model where n=1, the system model can be described as:

$$\mathrm{F}_l^* = m\begin{bmatrix} \cos\emptyset\sin\theta\begin{pmatrix} \ddot{l}\cos\emptyset\sin\theta - 2\dot{l}\dot{\emptyset}\sin\emptyset\sin\theta + 2\dot{l}\dot{\theta}\cos\emptyset\cos\theta - l\ddot{\emptyset}\sin\emptyset\sin\theta \\ -l\dot{\emptyset}^2\cos\emptyset\sin\theta - 2l\dot{\emptyset}\dot{\theta}\sin\emptyset\cos\theta + l\ddot{\theta}\cos\emptyset\cos\theta - l\dot{\theta}^2\cos\emptyset\sin\theta \end{pmatrix} \\ +\sin\emptyset\left(\ddot{l}\sin\emptyset - 2\dot{l}\dot{\emptyset}\cos\emptyset + l\ddot{\emptyset}\cos\emptyset - l\dot{\emptyset}^2\sin\emptyset\right) \\ \cos\theta\cos\emptyset\begin{pmatrix} \ddot{l}\cos\emptyset\cos\theta - 2\dot{l}\dot{\emptyset}\sin\emptyset\cos\theta - 2\dot{l}\dot{\theta}\cos\emptyset\sin\theta - l\ddot{\emptyset}\sin\emptyset\cos\theta \\ -l\dot{\emptyset}^2\cos\emptyset\cos\theta + 2l\dot{\emptyset}\dot{\theta}\sin\emptyset\sin\theta - l\ddot{\theta}\cos\emptyset\sin\theta - l\dot{\theta}^2\cos\emptyset\cos\theta \end{pmatrix} \end{bmatrix};$$

F_l=$(F_{A_g}[0 \quad 0 \quad -mg])\frac{\partial v}{\partial l} - T;$

$$\mathrm{F}_l^* = F_l. \tag{4.12}$$

$$\mathrm{F}_\emptyset^* = m\begin{bmatrix} -l\sin\emptyset\sin\theta\begin{pmatrix} \ddot{l}\cos\emptyset\sin\theta - 2\dot{l}\dot{\emptyset}\sin\emptyset\sin\theta + 2\dot{l}\dot{\theta}\cos\emptyset\cos\theta - l\ddot{\emptyset}\sin\emptyset\sin\theta \\ -l\dot{\emptyset}^2\cos\emptyset\sin\theta - 2l\dot{\emptyset}\dot{\theta}\sin\emptyset\cos\theta + l\ddot{\theta}\cos\emptyset\cos\theta - l\dot{\theta}^2\cos\emptyset\sin\theta \end{pmatrix} \\ +l\cos\emptyset\left(\ddot{l}\sin\emptyset - 2\dot{l}\dot{\emptyset}\cos\emptyset + l\ddot{\emptyset}\cos\emptyset - l\dot{\emptyset}^2\sin\emptyset\right) \\ -l\sin\emptyset\cos\theta\begin{pmatrix} \ddot{l}\cos\emptyset\cos\theta - 2\dot{l}\dot{\emptyset}\sin\emptyset\cos\theta - 2\dot{l}\dot{\theta}\cos\emptyset\sin\theta - l\ddot{\emptyset}\sin\emptyset\cos\theta \\ -l\dot{\emptyset}^2\cos\emptyset\cos\theta + 2l\dot{\emptyset}\dot{\theta}\sin\emptyset\sin\theta - l\ddot{\theta}\cos\emptyset\sin\theta - l\dot{\theta}^2\cos\emptyset\cos\theta \end{pmatrix} \end{bmatrix};$$

$F_\emptyset$=$(F_{A_g}[0 \quad 0 \quad -mg])\frac{\partial v}{\partial \dot{\emptyset}};$

$$\mathrm{F}_\emptyset^* = F_\emptyset. \tag{4.13}$$

$$\mathrm{F}_\theta^* = m\begin{bmatrix} l\cos\emptyset\cos\theta\begin{pmatrix} \ddot{l}\cos\emptyset\sin\theta - 2\dot{l}\dot{\emptyset}\sin\emptyset\sin\theta + 2\dot{l}\dot{\theta}\cos\emptyset\cos\theta - l\ddot{\emptyset}\sin\emptyset\sin\theta \\ -l\dot{\emptyset}^2\cos\emptyset\sin\theta - 2l\dot{\emptyset}\dot{\theta}\sin\emptyset\cos\theta + l\ddot{\theta}\cos\emptyset\cos\theta - l\dot{\theta}^2\cos\emptyset\sin\theta \end{pmatrix} \\ -l\cos\emptyset\sin\theta\begin{pmatrix} \ddot{l}\cos\emptyset\cos\theta - 2\dot{l}\dot{\emptyset}\sin\emptyset\cos\theta - 2\dot{l}\dot{\theta}\cos\emptyset\sin\theta - l\ddot{\emptyset}\sin\emptyset\cos\theta \\ -l\dot{\emptyset}^2\cos\emptyset\cos\theta + 2l\dot{\emptyset}\dot{\theta}\sin\emptyset\sin\theta - l\ddot{\theta}\cos\emptyset\sin\theta - l\dot{\theta}^2\cos\emptyset\cos\theta \end{pmatrix} \end{bmatrix};$$

F_θ=$(F_{A_g}[0 \quad 0 \quad -mg])\frac{\partial v}{\partial \dot{\theta}};$

$$\mathrm{F}_\theta^*=F_\theta. \tag{4.14}$$

After rearrange the formula, the acceleration of the rope tether rotations are:

$$\begin{bmatrix} \ddot{l}(\cos^2\emptyset\sin^2\emptyset + \sin^2\emptyset + \cos^2\emptyset\cos^2\theta) \\ +\ddot{\emptyset}l(-\cos\emptyset\sin^2\theta\sin\emptyset + \sin\emptyset\cos\emptyset - \cos\emptyset\sin\emptyset\cos^2\theta) \\ +\ddot{\theta}l(\cos^2\emptyset\cos\theta\sin\theta - \cos^2\emptyset\cos\theta\sin\theta) \end{bmatrix} = ((F_{A_g} + [0 \quad 0 \quad -mg])\frac{\partial v}{\partial l} -$$

$$T)(m^{-1})\text{-}\begin{pmatrix} \cos\emptyset\sin\theta\begin{pmatrix} 2\dot{l}\dot{\emptyset}\sin\emptyset\sin\theta + 2\dot{l}\dot{\theta}\cos\emptyset\cos\theta - \dot{l}\dot{\emptyset}^2\cos\emptyset\sin\theta \\ +2l\dot{\emptyset}\theta\sin\emptyset\cos\theta - \dot{l}\dot{\theta}^2\cos\emptyset\sin\theta \end{pmatrix} \\ +\sin\emptyset\,(2\dot{l}\dot{\emptyset}\cos\emptyset - l\dot{\emptyset}^2\sin\emptyset) \\ +\cos\emptyset\cos\theta\begin{pmatrix} -2\dot{l}\dot{\emptyset}\sin\emptyset\cos\theta - 2\dot{l}\dot{\theta}\cos\emptyset\sin\theta - l\dot{\emptyset}^2\cos\emptyset\cos\theta \\ +2l\dot{\emptyset}\dot{\theta}\sin\emptyset\sin\theta - l\dot{\theta}^2\cos\emptyset\cos\theta \end{pmatrix} \end{pmatrix} \tag{4.15}$$

$$\begin{bmatrix} \ddot{l}(-l\sin\emptyset\sin^2\theta\cos\emptyset + l\cos\emptyset\sin\emptyset - \cos^2\theta\sin\emptyset\cos\emptyset) \\ +\ddot{\emptyset}l(-l\sin^2\emptyset\sin^2\theta + l\cos^2\emptyset + l\cos^2\theta\sin^2\emptyset) \\ +\ddot{\theta}l(-l\cos\emptyset\cos\theta\sin\emptyset\sin\theta + l\cos\emptyset\cos\theta\sin\emptyset\sin\theta) \end{bmatrix} = ((F_{A_g} + [0 \quad 0 \quad -mg])\frac{\partial v}{\partial \dot{\emptyset}})(m^{-1})\text{-}$$

$$\begin{pmatrix} -l\sin\emptyset\sin\theta\begin{pmatrix} 2\dot{l}\dot{\emptyset}\sin\emptyset\sin\theta + 2\dot{l}\dot{\theta}\cos\emptyset\cos\theta - l\dot{\emptyset}^2\cos\emptyset\sin\theta \\ -2l\dot{\emptyset}\dot{\theta}\sin\emptyset\cos\theta - l\dot{\theta}^2\cos\emptyset\sin\theta \end{pmatrix} \\ +l\cos\emptyset\,(2\dot{l}\dot{\emptyset}\cos\emptyset - l\dot{\emptyset}^2\sin\emptyset) \\ -l\sin\emptyset\cos\theta\begin{pmatrix} -2\dot{l}\dot{\emptyset}\sin\emptyset\cos\theta - 2\dot{l}\dot{\theta}\cos\emptyset\sin\theta - l\dot{\emptyset}^2\cos\emptyset\cos\theta \\ +2l\dot{\emptyset}\dot{\theta}\sin\emptyset\sin\theta - l\dot{\theta}^2\cos\emptyset\cos\theta \end{pmatrix} \end{pmatrix} \tag{4.16}$$

$$\begin{bmatrix} \ddot{l}(l\cos^2\emptyset\sin\theta\cos\theta - l\cos^2\emptyset\sin\theta\cos\theta) \\ +\ddot{\emptyset}l(-l\cos\emptyset\cos\theta\sin\emptyset\sin\theta + l\cos^2\emptyset + l\cos\emptyset\cos\theta\sin\emptyset\sin\theta) \\ +\ddot{\theta}l(l\cos^2\emptyset\cos^2\theta + l\cos^2\emptyset\sin^2\theta) \end{bmatrix} =$$

$$((F_{A_g}[0 \quad 0 \quad -mg])\frac{\partial v}{\partial \dot{\theta}})(m^{-1})\text{-}$$

$$\begin{pmatrix} l\cos\emptyset\cos\theta\begin{pmatrix} -2\dot{l}\dot{\emptyset}\sin\emptyset\sin\theta + 2\dot{l}\dot{\theta}\cos\emptyset\cos\theta - l\dot{\emptyset}^2\cos\emptyset\sin\theta \\ -2l\dot{\emptyset}\dot{\theta}\sin\emptyset\cos\theta - l\dot{\theta}^2\cos\emptyset\sin\theta \end{pmatrix} \\ -\cos\emptyset\sin\theta\begin{pmatrix} -2\dot{l}\dot{\emptyset}\sin\emptyset\cos\theta - 2\dot{l}\dot{\theta}\cos\emptyset\sin\theta - l\dot{\emptyset}^2\cos\emptyset\cos\theta \\ +2l\dot{\emptyset}\dot{\theta}\sin\emptyset\sin\theta - l\dot{\theta}^2\cos\emptyset\cos\theta \end{pmatrix} \end{pmatrix} \tag{4.17}$$

Eventually, to rearrange the above equation to get the individual second order derivatives with respect to the rope length l, and rotation angle of $\emptyset$ and θ :

$$\ddot{l} = \left(\left(\left(F_{A_g} + [0 \quad 0 \quad -mg]\right)\frac{\partial v}{\partial \dot{l}} - T\right)(m^{-1})\right) + l\dot{\emptyset}^2 + l\dot{\theta}^2\cos^2\emptyset \tag{4.18}$$

$$\ddot{\emptyset} = \frac{\left(((F_{A_g} + [0 \quad 0 \quad -mg])\frac{\partial v}{\partial \dot{\emptyset}})(m^{-1}) - (2l\dot{l}\dot{\emptyset} + l^2\dot{\theta}^2\sin\emptyset\cos\emptyset)\right)}{l^2} \tag{4.19}$$

$$\ddot{\theta} = \frac{\left(((F_{A_g} + [0 \quad 0 \quad -mg])\frac{\partial v}{\partial \dot{\theta}})(m^{-1}) - \left(2l\dot{l}\dot{\theta}\cos\emptyset - 2l^2\dot{\emptyset}\dot{\theta}\cos\emptyset\sin\emptyset\right)\right)}{l^2\cos^2\emptyset} \tag{4.20}$$

Equations of 4.18, 4.19 and 4.20 demonstrated the pendulum equation of the single kite.

The last step of Kane's method is to find the state space form for numerical integration:

$$\dot{x}(\mathrm{t}) = \mathrm{f}(x, u, t) \tag{4.21}$$

Where x is the state vector; u is the control vector and t is time.

4.3 Electric Machine

After assessing the force acting on the kite by the tethering cable, the next step is to find the linkage between the electric actuator (in this case a DC motor and generator) and kite tension. In this model, a few assumptions are made to reduce the intricacy. Firstly, assume that the drum and the electric machine are physically attached; therefore, by applying control element to the

electric machine, the drum will then be controlled. Secondly, there is no vibration in the system due to the motor of the operation.

The analogue potentiometer used to control the motor by taking the ADC (analogue to digital converter) signal from the microcontroller.

4.3.1 Generator Mode

The generator inertia J_g and friction coefficient B, the DC generator equations with the equivalent circuit shown are:

$$J_g\ddot{\theta}_g = T - B\dot{\theta}_g$$

$$L_a\dot{I}_a = V_a - V_{emf} - R_aI_a$$

$$T = k_tI_a$$

$$V_{emf} = k_e\dot{\theta}_g \qquad (4.22)$$

Where V_a and I_a are the generated voltage and current, R_a and L_a is the armature winding resistance and inductance, θ_g is the angular displacement of the generator's rotor shaft, T is the applied torque and k_t is the torque constant, V_{emf} is the back emf voltage, and k_e is the back emf constant. Therefore, total power generation will be P=T* $\dot{\theta}_m$ assuming $k_e = k_t$ [23,24,25,26].

4.3.2 Motor Mode

For the motor inertia J_m and friction coefficient B, the DC motor equations with the equivalent circuit shown are:

$$J_m\ddot{\theta}_m = T - B\dot{\theta}_m$$

$$L_a\dot{I}_a = V_a - V_{emf} - R_aI_a$$

$T = k_t I_a$

$V_{emf} = k_e \dot{\theta}_m$ (4.23)

Where I_a is the motor armature current, L_a is the armature winding inductance, R_a is the armature winding resistance, θ_m is angular displacement of the motor shaft angle, V_a is the applied voltage to the motor, k_t is the torque constant, V_{emf} is the back emf voltage, and k_e is the back emf constant, where in general k_t=k_e. Moreover, the torque generated by the motor is given by $T = k_t I_a$ [23,24,25,26].

4.3.3 Intergradation

The tethering rope wound around the drum by friction; to eliminate the cable slip, the rope is wound tightly onto the drum. Therefore, the torque on the drum directly linked to the cable tension force of F_T. The whole drum unit is then mounted on the shaft of the electric machine with a coupling gear. According to above formula, T can transform into the same force as F_T. The generator/motor rotation speed is directly related to the rope pulling speed or winding speed, thus, it is related to the length of the rope, and angular displacement of the electric machine shaft angle is $\theta = l/r_{drum}$. Since the drum radius is a constant in this case, then $\dot{\theta} = \dot{l}/r_{drum}$; $\ddot{\theta} = \ddot{l}/r_{drum}$, the tension force can be represented in terms of length of rope as:

$T = J_{g/m}\ddot{\theta}_{g/m} + B\dot{\theta}_{g/m} = J_{g/m}(\frac{\ddot{l}}{r_{drum}}) + B(\frac{\dot{l}}{r_{drum}})$ (4.24)

The current equation is then being represented regarding rope length as:

$\dot{I}_a = (V_a - k_e\dot{\theta}_{g/m} - R_a I_a)/L_a = (V_a - k_e(\frac{\dot{l}}{r_{drum}}) - R_a I_a)/L_a$ (4.25)

4.4 Overall Model

The primary purpose of this project is to generate power; therefore, the generation phase should generate more power than the retraction phase. In this case, the algebraic sum of the power has been produced in the generation phase and the power consumed in the retraction phase results in the total net mechanical power output. The kite and wind dynamic model state space are listed below [28]:

$$x(t) = \left[\theta(t),\ \phi(t), r(t), \dot{\theta}(t),\ \dot{\phi}(t), \dot{r}(t)\right]^T \quad (4.26)$$

The generic system dynamics are:

$$\dot{x}(t) = f(x(t), \Psi(t), \dot{r_{ref}}(t) V_a) \quad (4.27)$$

The kite will be controlled by the roll angle of Ψ. The roll angle is Ψ= arcsine (ΔL/d), where d is the kite span length which is a constant number. Thus, this control has been achieved by measuring the difference between the two tethering lines.

Later on in the system, the bank angle will be introduced to the system to indicate the flight trajectory of the kite. Similar to the roll, the bank angle is a static angle display at the moment, whereas, the roll angle is a dynamic measurement including the directional vector. Roll rate will decide how fast of the kite should move to achieve the defined bank angle. Therefore, in a stable system, bank angle is same as roll angle, while in an unstable system, the instantaneous roll angle is not same as bank angle.

This overall mathematic model is a highly non-linearised system. Therefore, it is very hard to be modelled and observed. It is necessary to make a few assumptions and constraints in this multi-variable system so that it can be controlled and observed. The following chapter will discuss how to simplify the operation of the system to achieve the goal.

5.0 System Simulation by Using Newton Method

This section describes the overall system operation from controlling the trajectory of the kite to motor/generator operation. The overall system will have five key parts: aerodynamic part, kite body, mechanical part, electric machines and control system. Within the aerodynamic part, the wind force, gravity and air pressure will be calculated and translated into the same coordinate system as the kite and then act as a direct force to move the kite. The mechanical part will have three parts, which are two control tether cables (left and right) wound around two drums; there will be a drum brake coupled to the drum. Each of the drums will physically connect to the end shaft of the electric machines, which are two DC motors/generators. In the end, there will be a control system controlling the motor operation and the drum brake. The detailed operation process is illustrated below. In this case, kite operation will have three phases, which are known as traction phase, crossfeed traction phase and retraction phase. These will be explained respectively according to the diagram below:

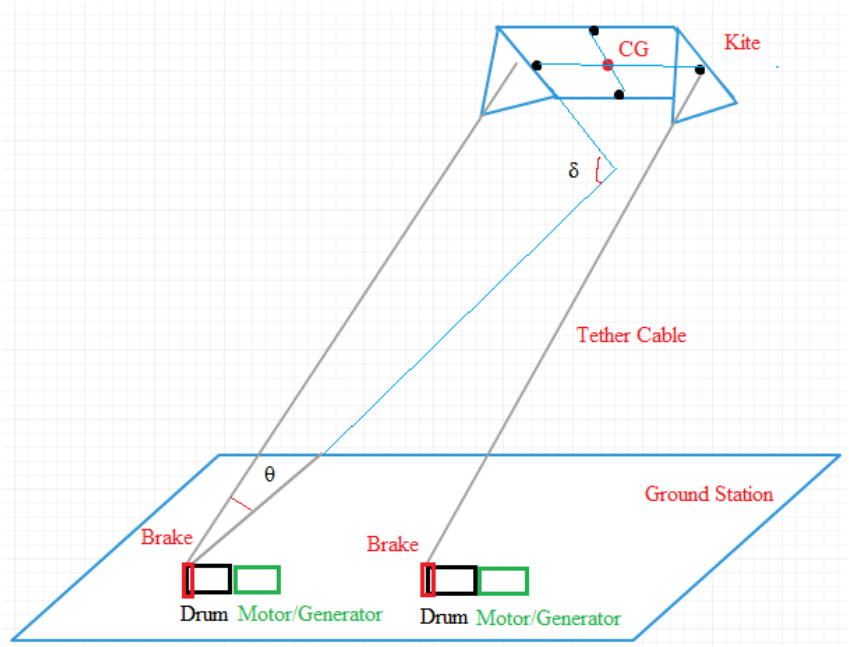

Figure 22 Kite Angle

5.1 Traction phase

In this report, the kite will be modelled as rigid body subject only to gravity and wind forces. Then another four points are distributed equally from center gravity (CG) so that the kite can be traded as a plane with an area of S. The kite used in this project has a wingspan distance of two meters. The wind direction (wind tunnel test condition) here is defined as always perpendicular to the kite surface, and the kite will move along with the angle of δ. The tether cable will be traded as two rigid body lines attached to the left end of the kite and the right end of the kite. The tether cable and the referenced ground will have angle θ.

After the kite has launched, (the launching process is not within the scope of this project), the kite will be in the initial traction phase. Which means the kite will pull both tether lines, hence rotating both generator shafts to produce power at the same time until one side of the cable length reaches the preset values. In this case, the left cable will be set to the initial conditions, therefore, when left cable (L) reaches the preset value, the drum can be stopped by applying the drum brake force, thus, the left generator will stop. The right generator will go further for

some time (distance) until the right cable (R) reaches the preset distance. The right drum brake will then be applied to the drum to stop rotating.

Hence, the different length of these two ropes will result in the angle of Ψ as seen in figure 16 in the horizontal plane (YZ plane). Due to this angle, the kite position is no longer in an equilibrium position; it will move sideways due to the normal component of the wind force. At the same time, while the kite is moving sideways, the left side of the rope is released so that it is equal length to the right side of the rope. Therefore, the kite will reach another equilibrium position in a different location. The kite will then located on the left-hand side of the original track.

The angle Ψ determines how far a kite will fly horizontally before it starts to fall. If this angle is too small, it will not generate the sufficient displacement or if the angle is too big it will result in the kite tipping over. The angle should ideally to be 30 degrees.

Therefore by applying the simple maths, for a kite with a wingspan of two meters, in order to create an optimal 30 degrees of Ψ, $\sin^{-1} \Delta L/d$ =30; then, ΔL = L_L-L_R= 1m. Figure 20 a shows the initial traction phase of kite, in which the left side and right side of the rope will be pulled at same time. Figure 20 b showed when the left side of the rope reaches 20 meters, the drum brake will clamp on to stope and right side of the rope will continue to go for further 1 meter to create the angle Ψ, which result the kite flight toward to the left side, at the same time, release the left side of rope so that both rope have a stheme length of 21 meters, the kite aerodynamic will then adjust by itself to find another equilibrium in a new displacement.

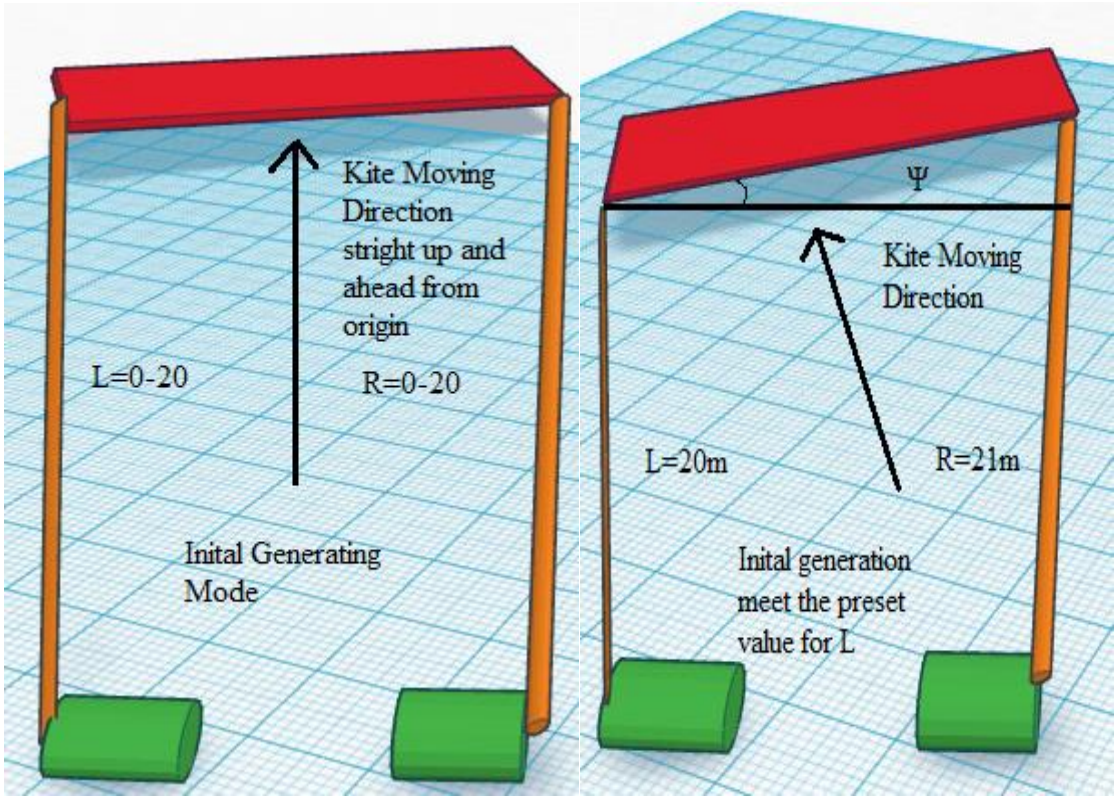

Figure 23 (a) Initial traction phase (b) Traction phase kite movement

5.2 Cross Feed Traction Phase

The crossfeed traction phase starts with the kite in the left hand.

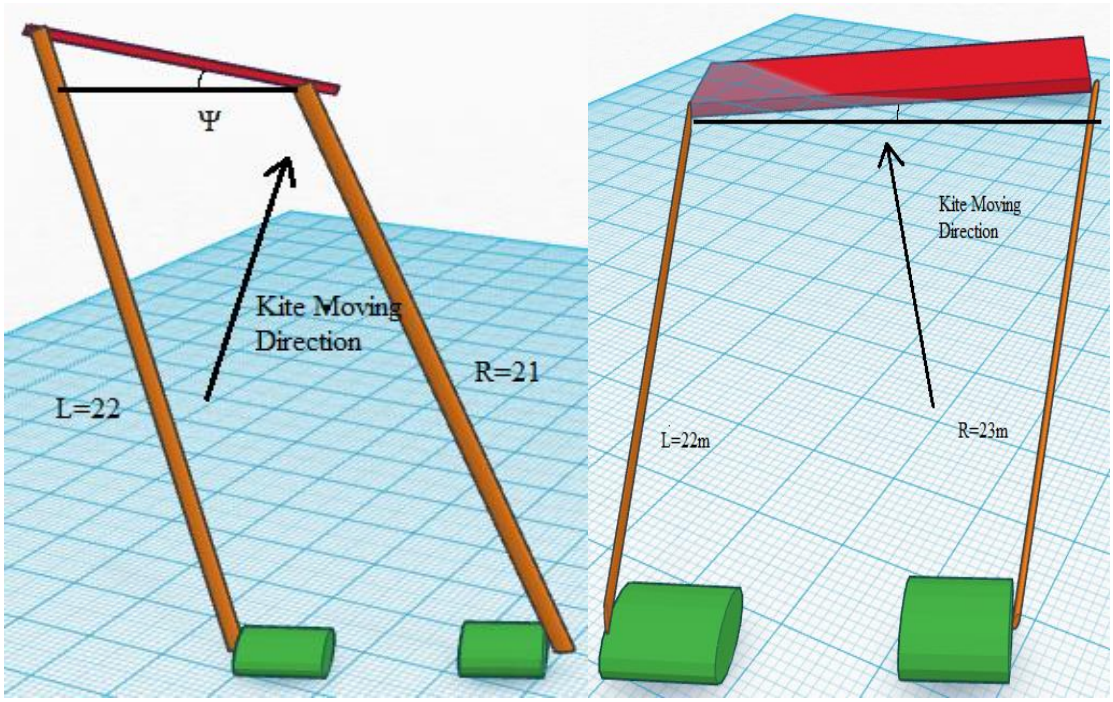

Figure 24 (a) Cross feed traction kite left (b) Cross feed traction kite right

By allowing the left-hand side of the rope to pull (generation mode) for 1 meter while the right-hand side drum is being held, the kite then will move to the right-hand side. Once the left-hand side of the rope reaches 22 meters, the drum brake will be applied on the drum again. Meanwhile, the right-hand side of the drum brake is freed until rope R reaches the same length as the left-hand side of the rope, which is 22 meters. The kite will then move to the right-hand side from the original track.

After the kite arrival at the equilibrium position on the right-hand side, the right-hand side of the drum brake will be released again so the right-hand side of the rope will pull for another 1 meter. Due to the component of the wind, the kite will move towards to left-hand side again, while the left-hand side of the brake is released for 1 meter so that it will be equal to the right-hand side of rope length which is 22 meters. The kite will reach a new equilibrium position.

5.3 Retraction Phase

The crossfeed traction phase will repeat until the left-hand side of the rope length first reaches the maximum, in this case, 40 meters. Only this time, the right-hand side of the brake will not release the right hand of the rope; the kite can no longer form an equilibrium position and will start to fall with an angle Ψ. The retraction phase will begin to act; the same two DC generators now will behave like a motor to wind back the rope at the same speed.

The Ψ angle will ensure that the tension force exerted by the kite aerodynamic on the rope will be at the minimum. (low lift force and low drag force). In this phase, the motor will need to use as least power as possible to retract the kite and work as fast as possible to prevent the kite falling speed from being quicker than the retraction speed. At the same time, both motors need to work at same speed and time.

When the left-hand side of the rope reduces to 5 meters again, both sides of the motor will stop working and transfer to generation mode again. The left-hand side of the drum brake will be applied to the left-hand side of the drum, and release the right-hand side of the drum for another 1 meter so that L=R=5 meters and the kite can be balanced out at its equilibrium state. At this stage, the operation of the generator is repeated and so on. Figure 22 below illustrates one complete cycle of the traction and retraction phase:

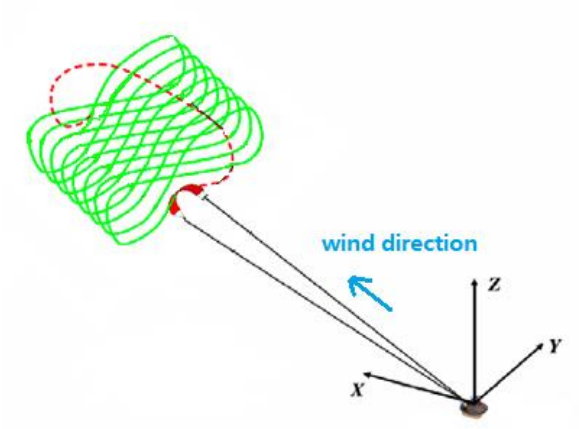

Figure 25 Kite Flight Control Trajectory

5.4 Base Unit

As the system described before, the whole kite unit (include kite, two drums, and two electric machines) will be mounted on the rotating dish station. In this case, while the kite changes in the direction of the trajectory, the whole base unit will be moving accordingly.

For the traction phase, at the time when both ropes have been pulling at the same time, the base unit is in steady condition. Once the length difference has occurred, the base unit will then turn to the direction of the pulling side, in this case, when L=20m, the drum brake will clamp on to stop the generator being pulled. Meanwhile, the right-hand side of the rope will go for a further 1 meter. At the time being, the angle has been created; then the kite will be fly toward to the left-hand side. Hence, it will pull the base unit to a certain angle. After the R reaches 21m, L will then released to the same 21m. At this time, the left-hand side of the rope is equal to the right-hand side of the rope again. After the aerodynamic force balances out on the kite, the base unit will stop turning and settle in the new position of the steady state.

The reason for introducing this 2-degrees of freedom base unit in the whole system is to reduce kite movement from a 3-dimensional plane to a 2-dimensional plane. In this new regime, the base unit coordinate frame will always follow the kite coordinate system, therefore, when studying the movement of the kite, the y-axis will then be coupled out, which leaves only the XZ plane.

In this case, the coupled angle Gama γ will then be introduced into the system. This angle measures the angular displacement of base unit movement from the original O frame of the coordinate system. The function can be presented regarding roll angle of the kite and wind velocity as:

$$\gamma(t) = (\Psi(t), We)$$

Where in this case, wind velocity We are always perpendicular to the kite surface. The overall system is displayed below:

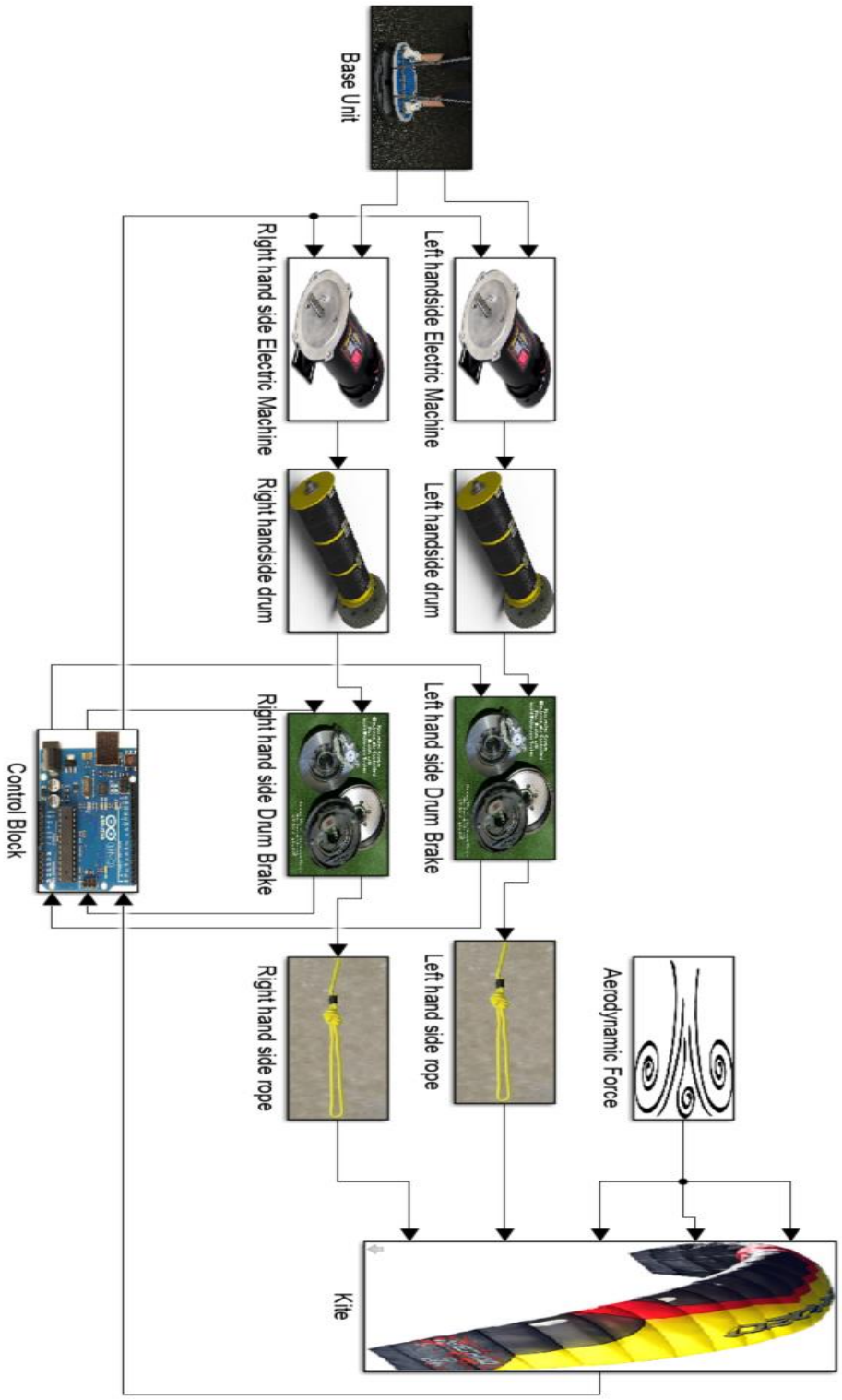

Figure 26 Overall Physical System Model

5.5 System Expectation

The overall system should be observable by the operator in terms of the rope length for both sides, the roll angle of the kite and the gamma angle of the unit base as shown in figure 24 below:

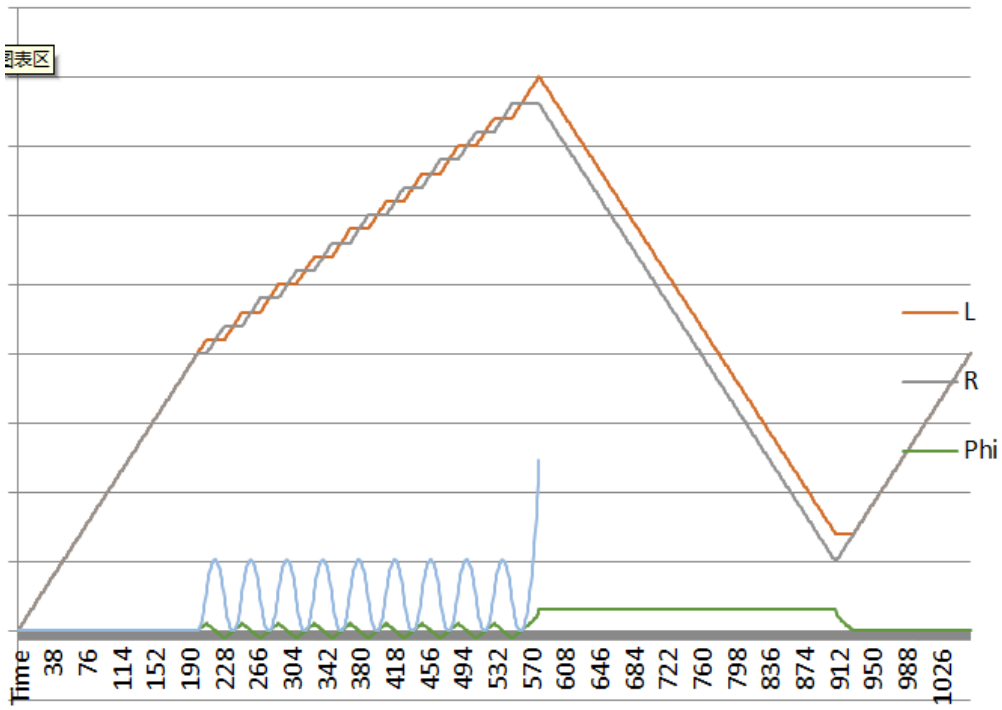

Figure 27 System Critical Observation Date

As the above diagram suggests, in the initial traction phase, both sides of the ropes have been released at the same time. It takes 210ms on the left-hand side of the rope to reach 20 meters and 10ms for the right-hand side of the rope to go for a further 1 meter. The roll angle of phi starts from zero and rises as soon as there is a length difference between the two ropes. At the same time, the base angle of gamma starts to raise, which indicates the base unit is yawing in the horizontal level. A linearized triangle wave can then represent the ideal roll angle function of the kite. The peak to peak oscillating angle will be between 30 degrees and -30 degrees. It can be expressed as (4n-1)th of additive harmonic times -1 on top of the sinusoid wave.

$$\varphi(t) = \frac{8}{\pi^2}\sum_{k=0}^{\infty}(-1)^k \frac{\sin(2\pi(2k+1)ft)}{(2k+1)^2}$$

5.6 System Implementation

For the kite to be controlled like chapter four described, we first have to design and implement a kite model that would simulate a path that a kite would potentially take when it is up in operation. In addition, we need to understand the amount of drag and lift force being exerted on the kite itself to design the rope and generator in the future.

5.6.1 Assumptions

The first assumption for the kite model being the kite body is mechanically rigid. This means the kite model is a solid rectangle that all points on the body moves in the same direction and rotates with the same angle

The second assumption being the kite is un-tethered, this means that the Kite does not have any rope or load on the kite. This simplifies the kite model mathematically as only the motion of the kite is considered.

Thirdly, it is assumed is that the kite model would be designed without air friction consideration, as the mathematical equations that govern this would require a real experiment with the kite to figure out the friction coefficient of the kite body before a good general air-friction equation can be obtained.

5.6.2 Kite Initial Setup

The kite has a defined length of 2 meters, the height of 0.8 meters, and depth of 0.05 meters. The kite has a mass of 0.2kg. The kit has a set of xyz coordinate relative to the base of the kite (the launch area) and initially the kite will be at this point (0,0,0). The kite also has a set of velocity and acceleration vectors that affect the next xyz position of the kite. A separate set of

xyz velocity and acceleration vectors are kept to simulate sensors being present on the kite; these values are calculated after the kite xyz positions are updated.

We utilise both the Spherical (r, θ, φ) and Cartesian coordinate system (x, y, z) as a means of modelling the kite's position. With the two coordinate systems relations as below:

Spherical to Cartesian:

```
x = r*sin(theta)*cos(azi);
y = r*sin(theta)*sin(azi);
z = r*cos(theta);
```

Cartesian to Spherical

```
r = sqrt((x^2)*(y^2)*(z^2));
theta = acos(z/(sqrt((x^2)+(y^2)+(z^2))));
azi = atan(y/x);
```

5.6.3 Kite Initial Pre-Flight Position

Realistically, the kites are 'launched' into the air through the use of a mechanical force. In practice, this is done through pushing the kite up into the air. With a mechanical propulsion of the kite, it decided that the kite can be pushed with enough force to a 1-meter radius from zero position. It is assumed that the propulsion would press the kite upward with a reasonable θ and φ value. Below shows a graph of all the possible kite positions that a reasonably designed initial propulsion system would push the kite.

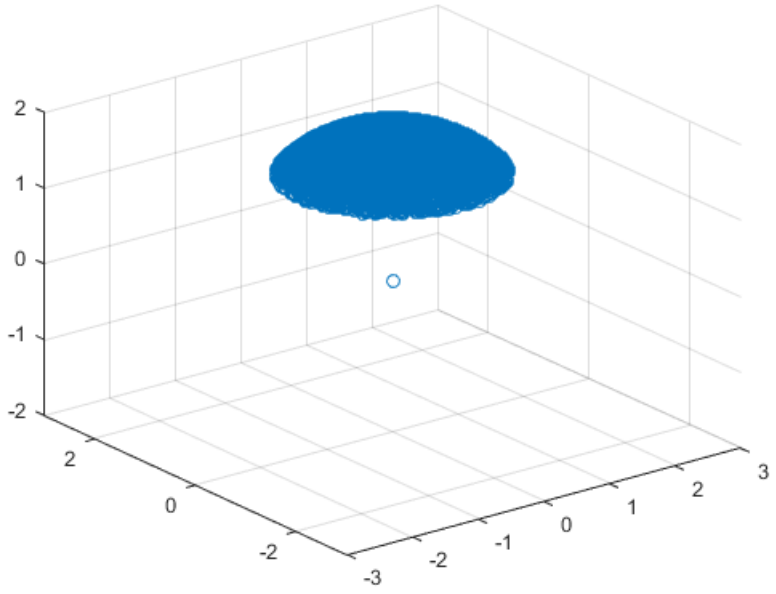

Figure 28 Possible kite initial positions

5.6.4 Wind Vector Design

After the initial kite, the position has been defined to be one of the possible positions as shown above. The wind vector and the relationship on the kite are considered. The wind vector affects the Cartesian coordinate of the kite, below shows an example of the kite model being affected by a randomly generated wind vector that changes with every new Cartesian coordinate was updated. Please note that the wind vector was defined to be quite small to see if the kite's Cartesian coordinates would update in all scenarios.

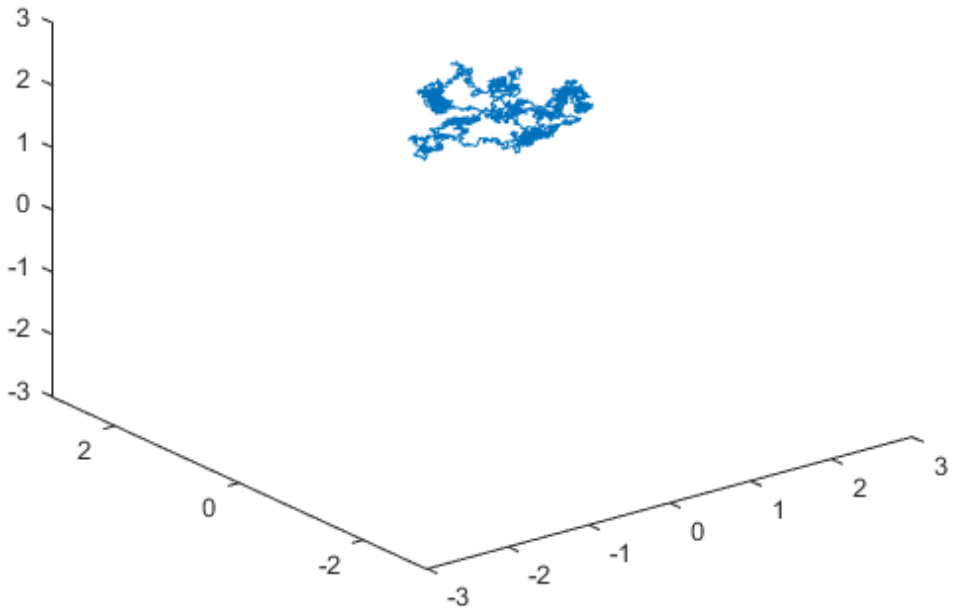

Figure 29 Isometric view of a kite affected by a random wind vector

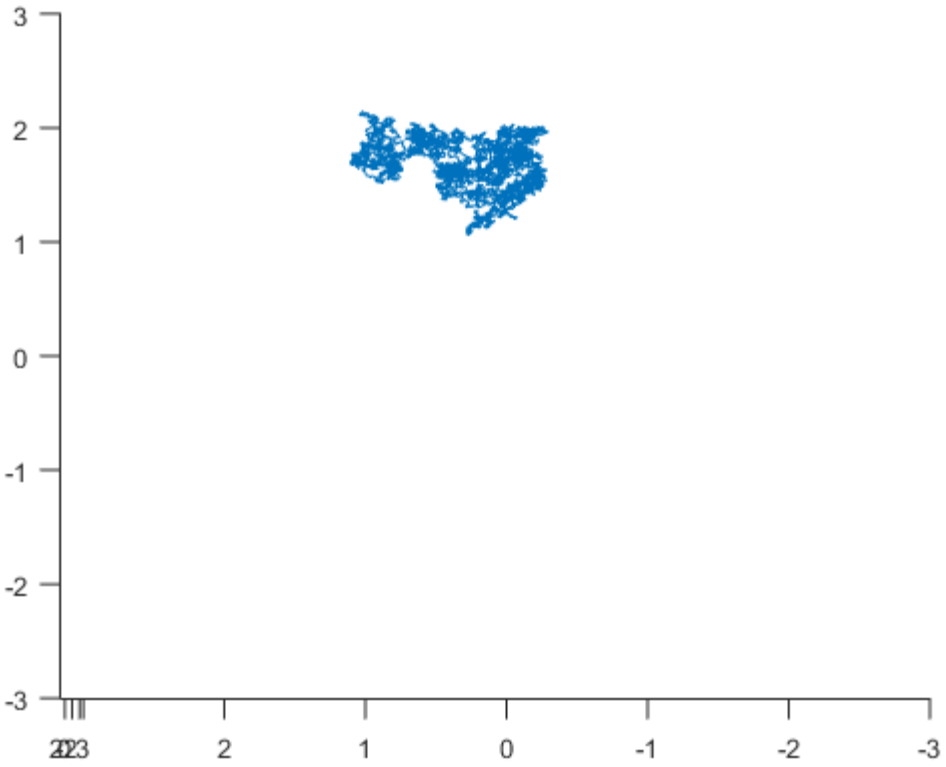

Figure 30 Side view of a kite affected by a random wind vector

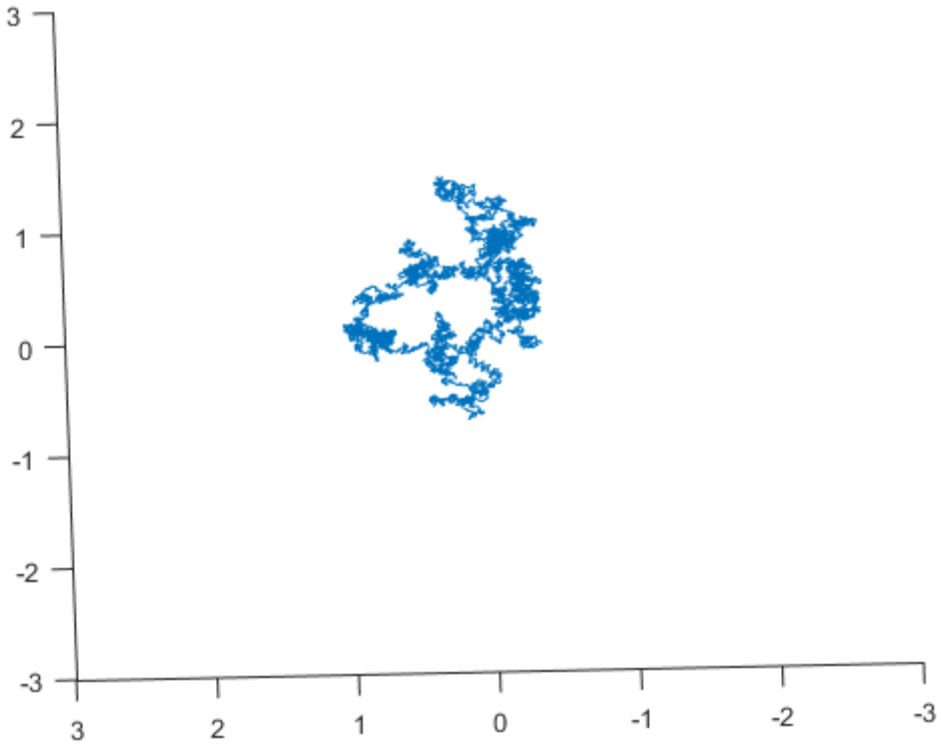

Figure 31 Top view of a kite affected by a random wind vector

5.6.5 Acceleration Design

As the wind vectors have been successfully implemented, the acceleration actions on the kite can be considered, acceleration on the kite that we do consider are the drag and lift accelerations.

The drag acceleration equation has derived as follows:

A_d = (0.5 x air pressure x wind vector^2 x drag coefficient x cross sectional area of the kite) / kite mass

The lift acceleration equation have been derived as follows:

A_L = (0.5 x air pressure x wind vector^2 x lift coefficient x kite length x kite height x angle of attack) / kite mass

The angle of attack is the kite's angle relative to the wind vector's angle.

The difference between the lift acceleration vector and the drag acceleration vector in addition to the gravitational acceleration vector forms the overall acceleration vector that acts upon the kite's overall velocity vector

The resulting kite model becomes split into two potential scenarios as shown below:

Scenario A: Kite going towards infinity

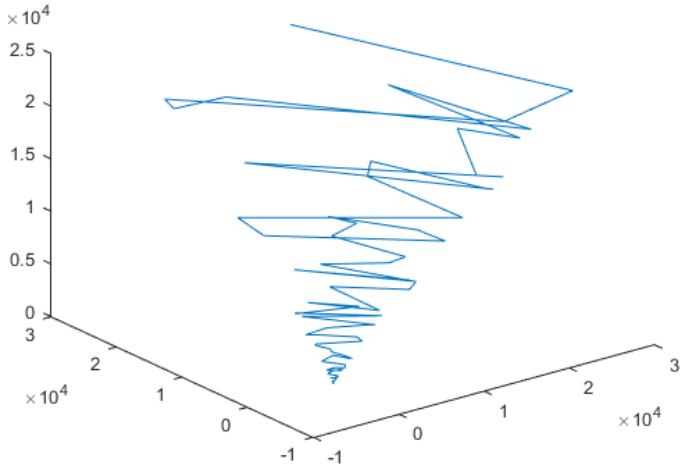

Figure 32 a) Isometric view of kite going towards infinity

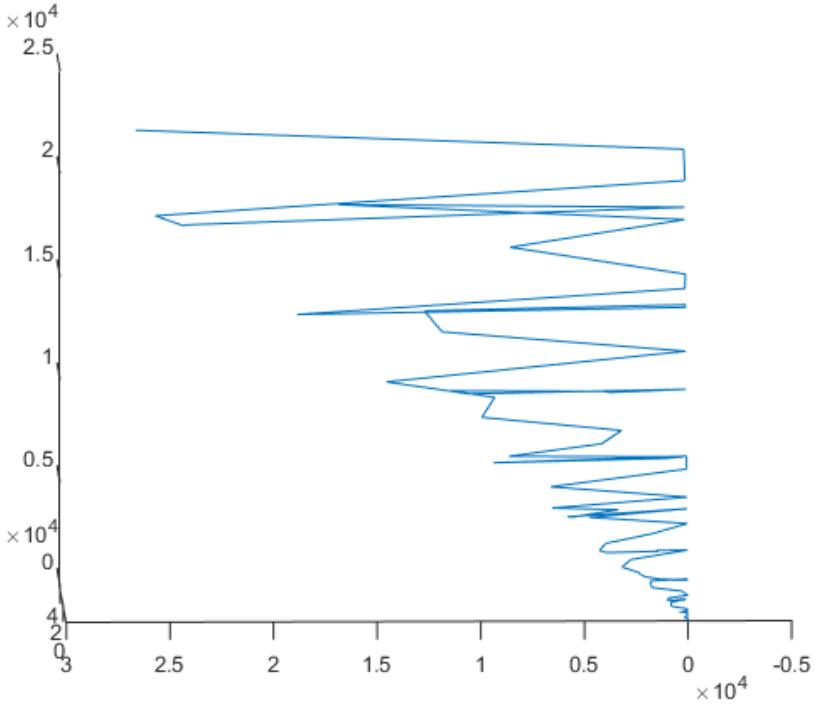

Figure 32 b) Side view of kite going towards infinity

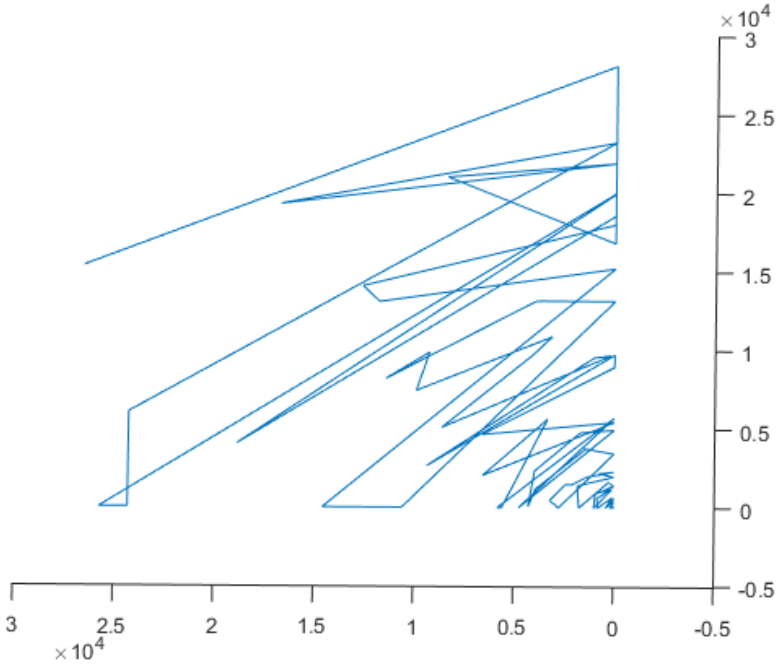

Figure 32 c) Side view of kite going towards infinity

Scenario B: Kite going towards negative infinity

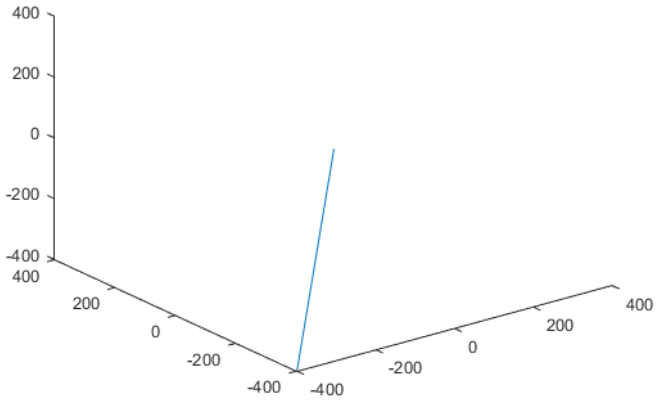

Figure 33 a) Isometric view of kite going towards negative infinity

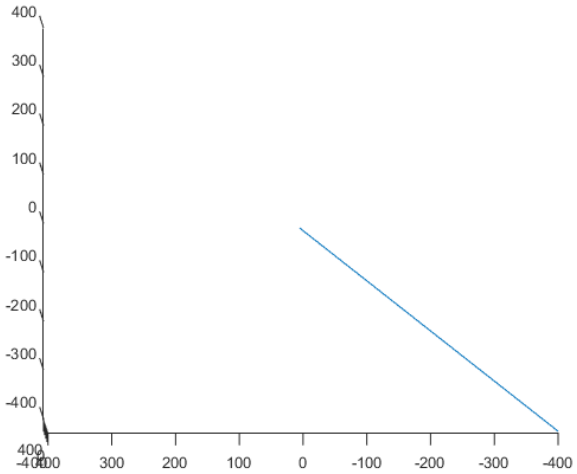

Figure 33 b) Side view of kite going towards negative infinity

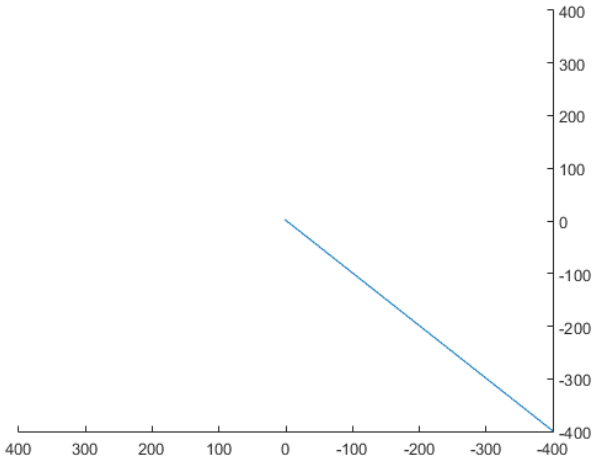

Figure 33 c) Top view of kite going towards negative infinity

The kite either flies towards infinity or negative infinity due to the uncontrolled nature that the kite was allowed to move in and disregarding the air friction acting on the kite. However, the outcome from these two scenarios shows that the kite going towards positive infinity means the kite would be sustained in the air. The kite going towards negative infinity represents that, under this scenario, the kite would have crashed into the ground.

The two situations arise due to the kite model simulating a different wind vector each time. With the wind vector value exceeding a critical value will sustain the kite up in the air while the vector not exceeding the critical wind value would not maintain the kite.

5.6.6 Controlling the kite pathway

By utilising the kite's orientation angle Ψ, we can anticipate and control the lift acceleration enough to completely adjust the kite's trajectory to what is desired. For kite power generation, a zig-zag figure-eight trajectory is concluded to be the best trajectory used.

The best control methodology, in this case, is to define the ideal trajectory, then change the orientation angle through the use of tethered kite ropes, then compare the ideal trajectory position coordinates to the current position coordinates to establish control error, depending on the control error adjust the orientation angle again to control the kite onto the ideal trajectory.

The trajectory in which the kite is controlled as shown as below,

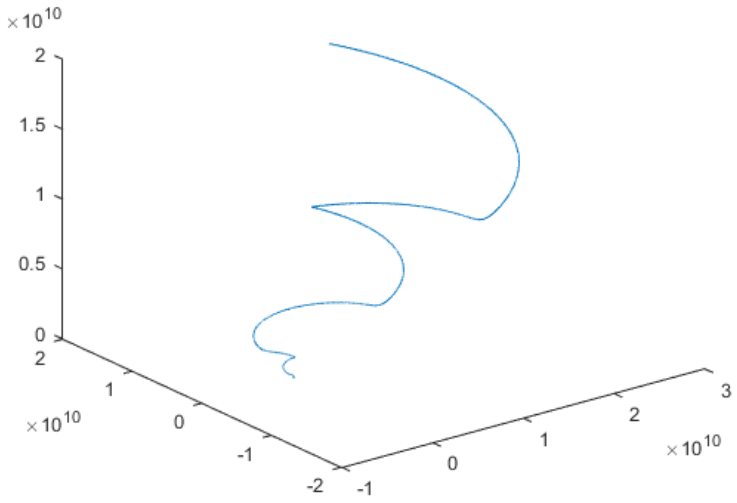

Figure 34 a) Isometric view of controlled kite trajectory

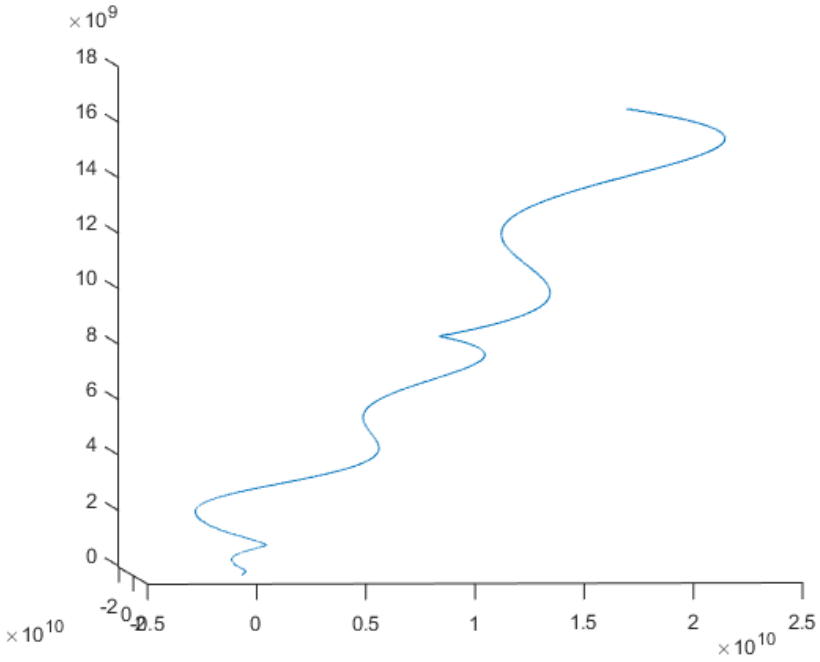

Figure 34 b)Side view of controlled kite trajectory

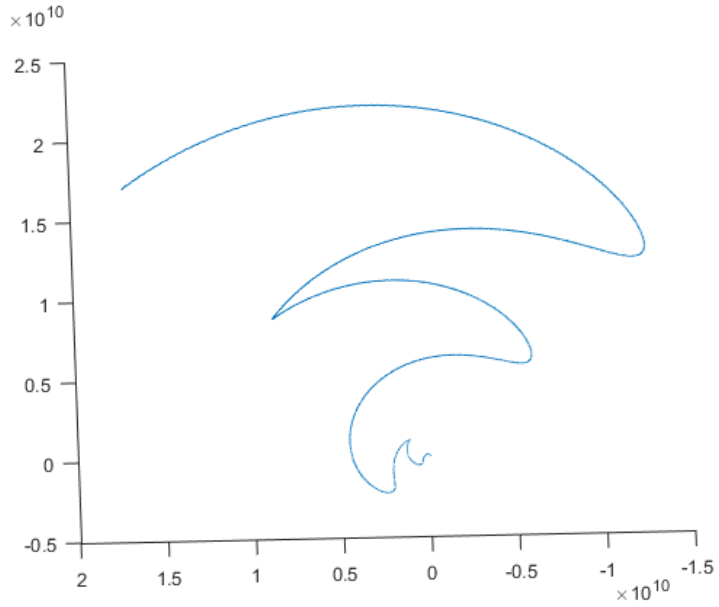

Figure 34 c) Top view of controlled kite trajectory

5.6.7 Disadvantage of Newton's method

To successfully control the kite trajectory to a figure eight is a piece of work that requires a lot more parameters and data to control. Incorporating air friction into the uncontrolled kite trajectory, this would increase the number of times the kite would crash, but for an uncontrolled kite, the critical wind vector value would be more accurate to a real kite environment. To add

in rope weight and additional parameters of the motor load are also needed to gauge the feasibility of the whole system for power generation. However, it will require a significant amount of mathematics computation. Therefore, to build more feasible kite model, Kane's method will be used in this project.

6.0 System Simulation By Using Kane Equation

This chapter discusses the implementation of the mathematical model for the surf kite power generation in physical modelling by using Aerospace/Aerosim Blockset and Simscape. The typical physical model includes the following components:

Kite and Aerodynamic: Represents a rigid body with mass, coordinate system and center of gravity, calculates the kite position and altitude from forces and moments and calculates aerodynamic, gravity, tension forces and moments. On the other hand, the simulation environment will also include in this block; it provides wind and power environment.

Adjustment and Control: Finding the best setting for glider aircraft to represent as a surf kite.

Sensor: Measures position, force, and angular velocity.

Electric Machines and Mechanics: Represent motor, generator, drum, drum brake, gear, base rotation unit and joint and actuator link between two body parts with a customised degree of freedom and calculate displacements based on the actuator.

Visualisation: 3D scope to observe the kite position.

The integrated dynamics of the wind environment and kite, sensor, motor, drum, and generator will be presented in detail according to the following design process:

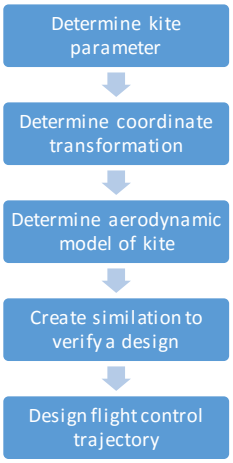

Figure 35 Design Process

6.1 Kite and Aerodynamic

Kite model is adopted from the Aerosonde UAV (Unmanned aerial vehicle) modelling under the gliding mode. It uses 6-DOF (degree of freedom) block from Aerospace block library. The aircraft parameter is aerosonadecfg.mat, and it will create the aerosondeconfig.s script. The detailed of the configuration has been showed in Appendix i, ii, iii, iv, ix.

Kite configuration has extracted from the MatLab config_template.m, which can be found in the samples directory. This custom kite MatLab script allowed setting up the kite's aerodynamic, mass and inertial parameters. After defining all the parameters, this script can be run at the MatLab command space, and then the parameter file of the KiteGlide.mat will be created. The entire variable will be displayed in the workspace at the right-hand side of MatLab operation screen.

Since the rigid body model has been chosen for this project, it is essential to reference the point to the arbitrary body frame. The orientation of the body coordinate system (refer to the local kite reference coordinate system) should follow as, X pointing forward, Y pointing inside the coordinate system and Z pointing downwards.

6.1.1 Kite Parameter Configuration

The original configuration includes five parts, which are aerodynamics, propeller, engine, inertia and other parameters. When adapted to the kite mode, the propeller, engine and other parameters can be taken away. Therefore, aerodynamics and inertia are the only parameters that need to be taken into consideration.

For the aerodynamic parameter, the following will need to be defined: the reference point, aerodynamic parameter bounds, and aerodynamic reference parameters, lift coefficient, drag coefficient, pitch moment coefficient, roll moment coefficient and yaw moment coefficient. The detailed block diagram can be found from Appendix xi to Appendix xxi. The side force, in this case, will be ignored since Diehl's model has been used in this application.

The reference point is used to specify the location with respect to the kite coordinate system; in this case, the position of the fixed ground control stationary will be the reference point. The value of the benchmark will be one by three-row vectors defined in the x, y and z coordinate system.

The aerodynamic parameter bounds used to keep the output model as a linearised model; it is used to limit the kite in terms of the airspeed and angle of attack. Since it is a bound value, it is set as one time two vectors of minimum and maximum values. For the Dihedral's model, the sideslip will be ignored, and the angle of attack will remain the same at all times.

Aerodynamic reference parameters are used to define the reference of the kite area, span, and chord. Lift coefficient, drag coefficient, pitch moment coefficient, roll moment coefficient and yaw moment coefficient can be determined by referring to the Aerosim user guide.

The kite inertial script will define the kite mass, the center of gravity location and moments of inertia. The empty aircraft mass will be set as 8.5 Kg, the position of the center of gravity of

the kite is a one times three vector of x=0.156, y=0 and z=0,079 coordinate with respect to the origin. The moment of inertia theoretically should have six vectors referring to the kite coordinate system, which are e_x, e_y, e_z, e_{xy}, e_{xz} and e_{yz}. However, since the kite is symmetrical on x-z plane, it can be reduced to one times four vectors, and they are e_x=0.7795, e_y=1.122, e_z=1.752, and e_{xz}=0.1211. Please refer to the kite glider in appendix ii and Aerosonde configuration in Appendix iii for details.

6.1.2 Kite Force Intergradation

This can be simply described using the block diagram below, the combination of all of these forces (wind force and kite force) can be computed in the equation of motion block, and this will generate the kite states such as the position, velocity, altitude and angular velocities. All the generated information will be sending out through sensors so that the receiving end of cable control can be adjusted to obtain the kite in the right trajectory.

Figure 36 Block diagram of Kite Block Contain

To find out the overall equation of motion xvii, it will require six blocks to form the equation of motion:

- Forces block (appendix xiii, xx)
- Moments block (appendix xvi, xvii, xviii, xix)
- Kinematics block (appendix xvii)

- Quaternions to Euler (appendix xvii)
- Quaternions to DCM (body inertial DCM from Quaternions) (appendix xvii)
- Customed cable control block (Appendix v, vi, vii)

The complete block can be found in Appendix xvii, xviii, xix, xx and xxi. These blocks have constructed according to the previous mathematic model. The kite block configuration and customized cable control block have being presented in the script version. The detailed script code can be found in appendix iv, v, vi, vii, viii, ix.

6.1.3 Kite Block Inputs

The kite model block takes the input of:

1. Cable control; take input from another block
2. The Wind; take input from another block
3. Aero control; take input from another block
4. Kite parameter, which includes empty aircraft mass, empty center of gravity location, empty moments of inertia, propulsion force application point and aerodynamic force application point
5. Stability derivations, which include all aerodynamic derivatives as per radian of lift coefficient, drag coefficient, side force coefficient, pitch moment coefficient, roll moment coefficient, yaw moment coefficient, mean aerodynamic chord of kite, kite span, and kite area
6. Derivative of wind
7. Standard atmosphere computation data; take input from NASA data bank
8. Cable parameters, which include the cable linear density, and the control flag
9. Mass scaling; take input as 1
10. Length scaling; take input as 100
11. Time scaling; take input as 1.

6.1.4 Kite Block Output

The kite model block sends the output of:

1. Euler Angle; used to display the kite rotations, this value can reflect the bank angle of kite, attitude of the kite and the heading direction of the kite
2. The output position of kite coordinate system of X Y Z
3. Cable tension; calculated from the double derivative of the area. However, due to the complexity of the overall kite function where several variables need to be derived, the partial derivative of all functions will be used.
4. Aero coefficient
5. Wind velocity; this result is associated with angle of attracting, wind axes and velocity from body axes
6. Mach; the kite speed divided by the speed of sound, kite flight speed is slow compared to the aircraft; therefore, it always flies under subsonic conditions, the compressibility of air can be ignored.
7. Wind tunnel dynamic pressure noted as P_{dyn}, which equals to the density of air times square of wind tunnel velocity and divided by two, expressed as $P_{dym}=0.5*\rho V^2$.

The kite model has two feedback controls:

1. The system state from X_{dot} to X, this includes the general function representing system dynamics. Details can be found in chapter 4.
2. The aerodynamics of the kite.

The overall kite block display is shown in figure 38 and 39:

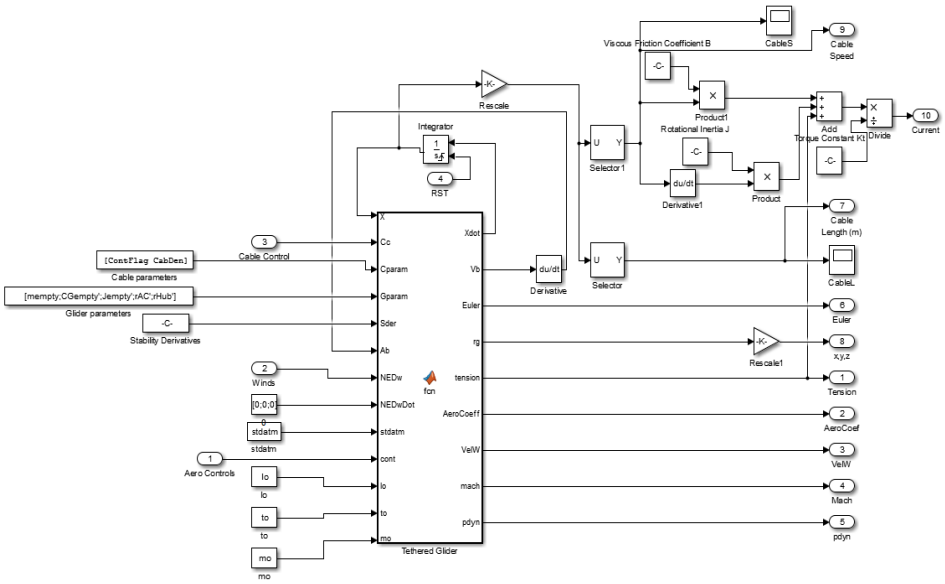

Figure 37 Kite Block – Script Version

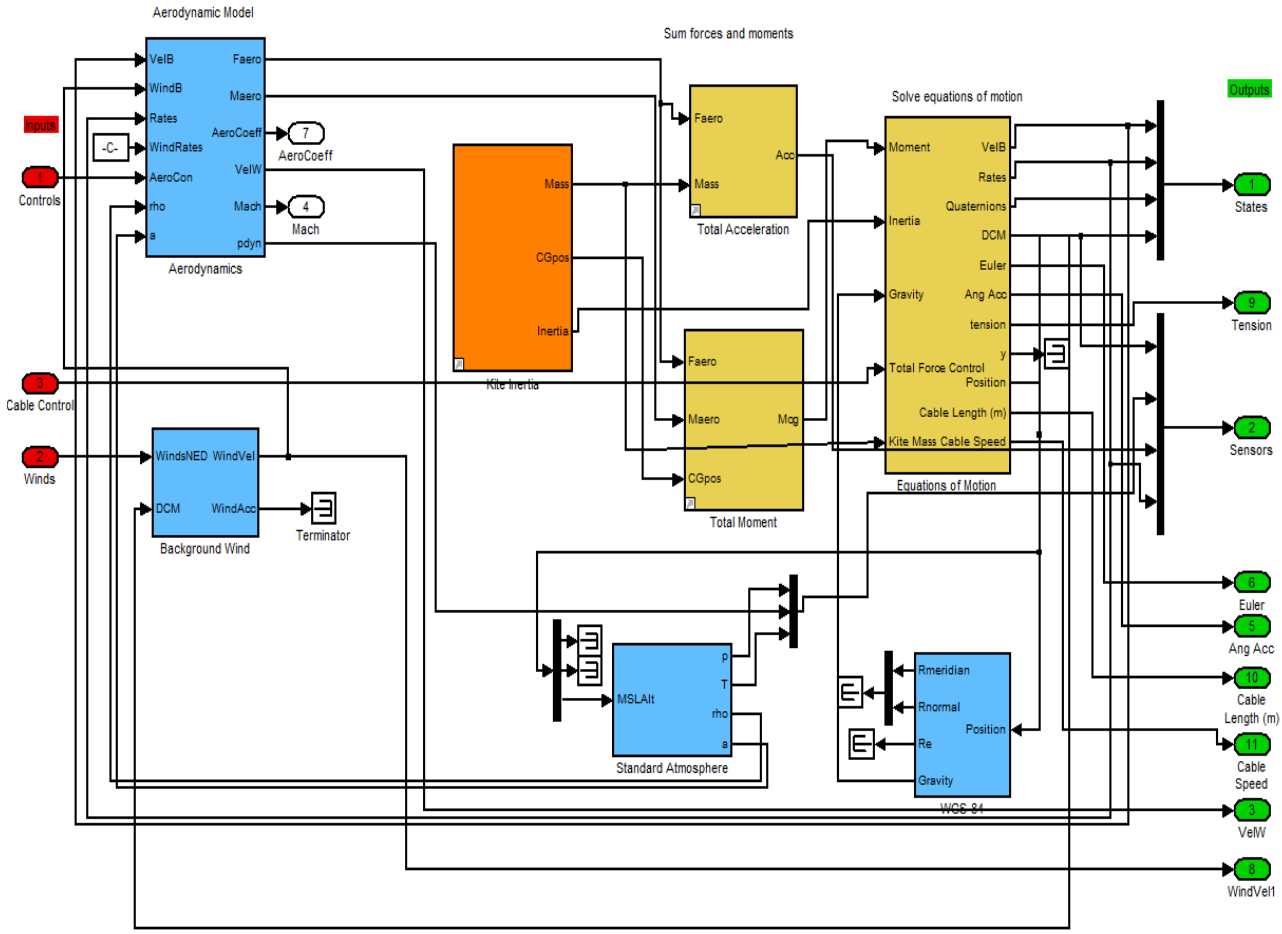

Figure 38 Kite Block – Aerosim Block

6.2 Aircraft Block Adjustment

6.2.1 Aileron Control

The kite model was originally adopted from glider aircraft in Aerosim when to choose Kane Equation method presented in chapter 4, therefore, it required fine tuning to ensure the best set up parameters for aileron, elevator, and rudder, so that when using the glider as a kite, it can provide the longest gliding time like the kite without any external control. The input of bank angle will be used to control the output behaviors of the aileron.

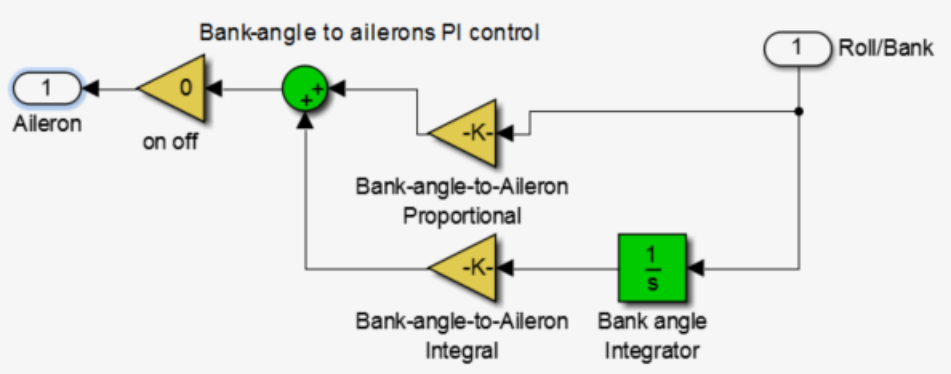

Figure 39 PI Control of Aileron

The bank angle has been evaluated from the Euler angle in the current glide mode; it can be stabilised by feeding the bank angle into the aileron through Proportional and Integral (PI) close loop control. PI control is used to eliminate the steady state error caused by proportional control. The Integral control will help to reduce the steady state error; the transfer function can be expressed as:

$$\frac{X(s)}{F(s)} = \frac{K_p s + K_i}{s^3 + 10s^2 + (20 + K_p s + K_i)} \quad (5.1)$$

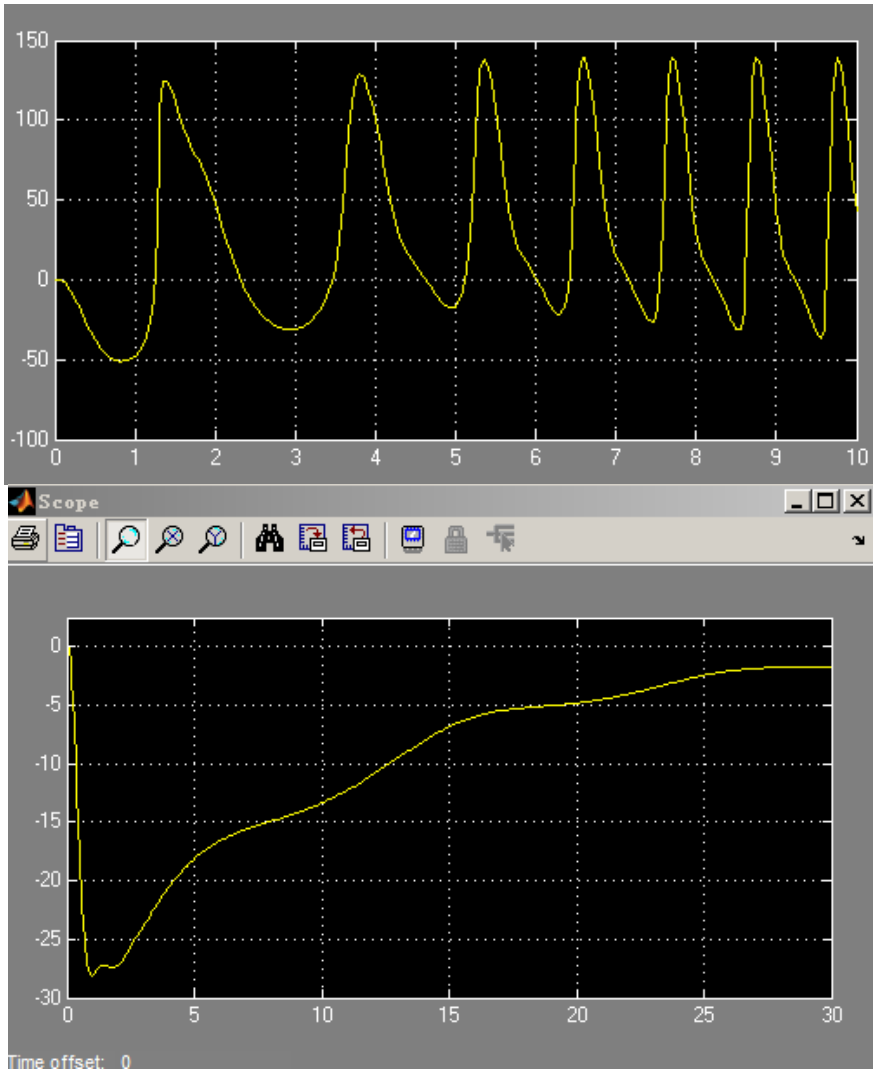

Figure 40 a) Open Loop Control Bank Angle b) Close Loop Control **Stabilized Bank Angle**

As the simulation results suggest, the bank angle has been stabilized after 27s, by applying PID auto tuning in Matlab control tool box, Kp has been set as 0.5*pi/180 and Ki has been set as 0.05*pi/180 to achieve stabilization.

6.2.2 Elevator Control

After the bank angle settles, the next step is to control the pitch angle:

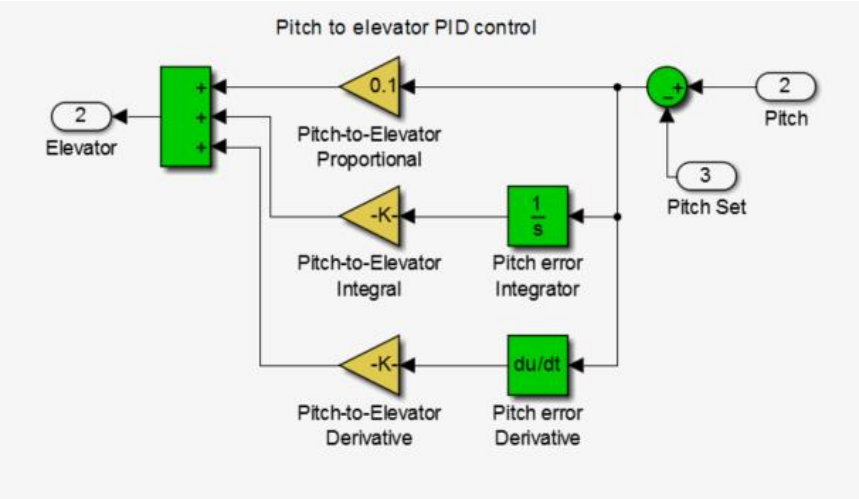

Figure 41 PID Control of Elevator

The elevator has been controlled by the Proportional-Integral-Differential (PID) controller for the pitch angle, which has evaluated from the Euler angle. The PID controller has the most accurate control since it has the zero steady state error. Short rising time provides the fast response and is stable with no oscillations. On the other hand, PID control can be used with higher order process meaning more than one input, in this case, both pitch angle and pitch set angle can be taken as input. PID closed loop transfer function can be expressed as:

$$\frac{X(s)}{F(s)} = \frac{K_d s^2 + K_p s + K_i}{s^3 + (10 + K_d)s^2 + (20 + K_p)s + K_i} \tag{5.2}$$

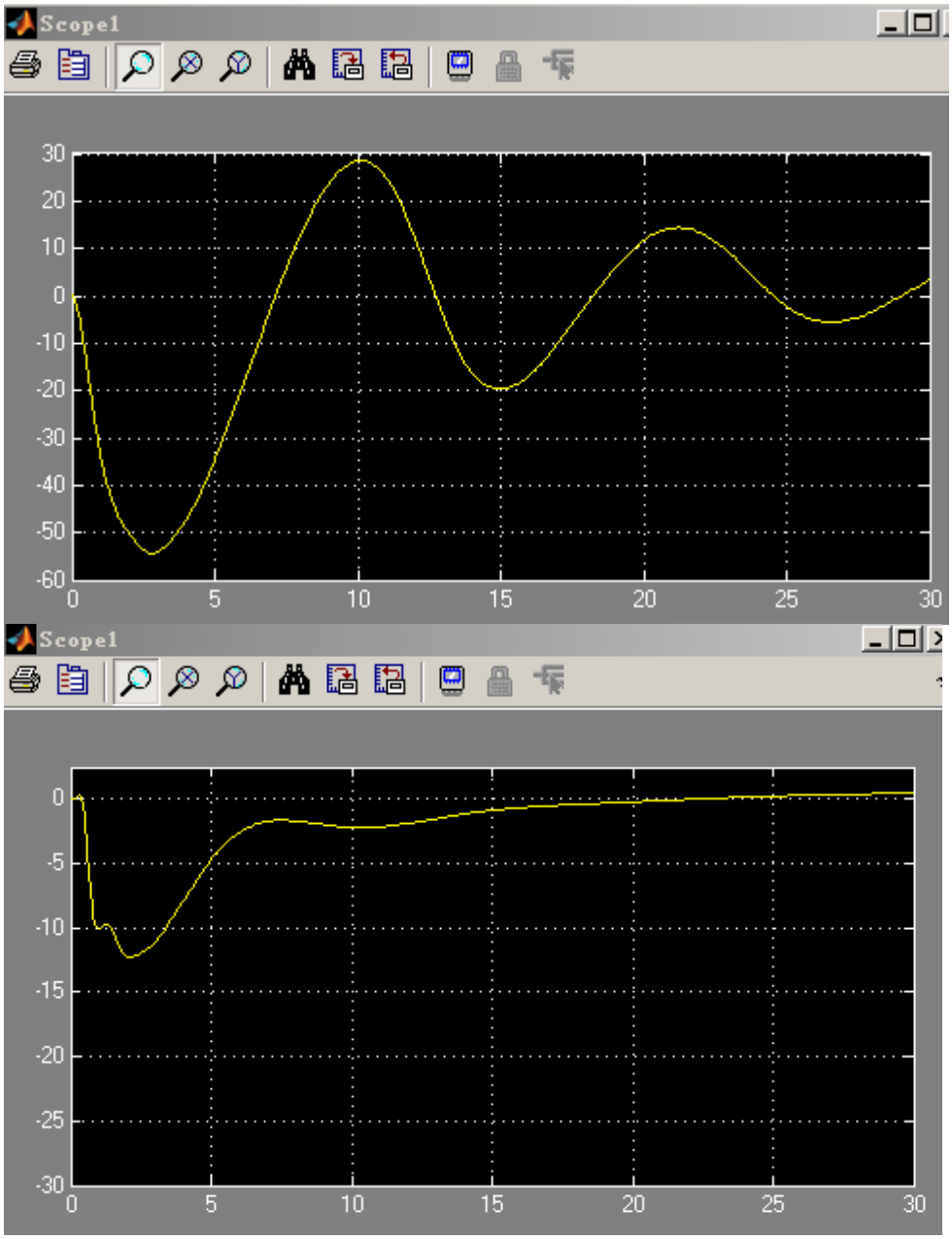

Figure 42 a) Open loop **Phugoid Oscillation of Pitch angle** b) PID **Phugoid Oscillation of Pitch angle**

As the simulation result suggests, the pitch angle is stable to a 25 degree. By applying PID auto tuning in Matlab control tool box, Kp has been set as -0.1, Ki has been set as -0.005 and K_D have been set as -0.05 to achieve stabilization.

6.2.3 Rudder Control

After the bank angle and pitch angle settle, the next step is to control the yaw angle:

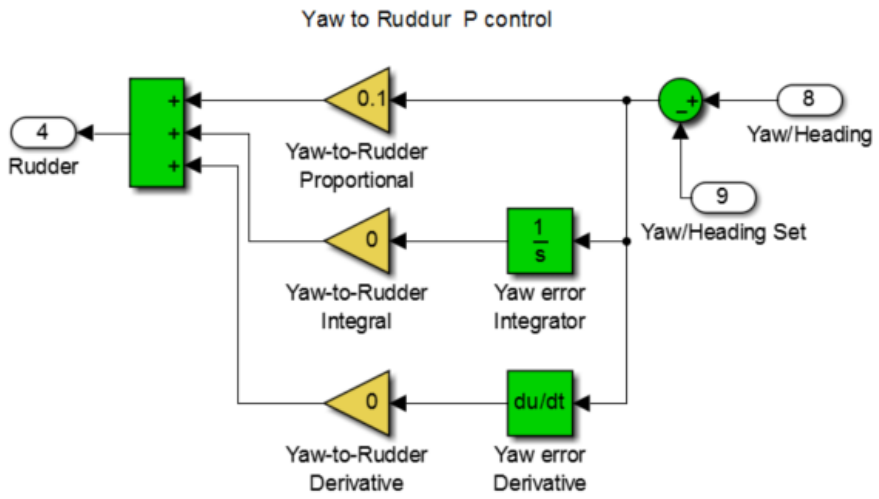

Figure 43 P Control of Rudder

The yaw angle has been evaluated from the Euler angle. In the current glide mode, the rudder has been controlled by P Proportional close loop control from the yaw angle. P control is the most popular controlling method in the first order system; it is used to stabilise the unstable process. The benefit of using P control is its fast response time. However, it can only come close to the set point; it will never reach the set point. PID closed loop transfer function can be expressed as:

$$\frac{X(s)}{F(s)} = \frac{K_p}{s^2+10s+(20+K_p)} \qquad (5,3)$$

The yaw angle is stable to a 30 degree by applying PID auto tuning in Matlab control tool box; Kp has been set as 0.1.

In Matlab control tool box, the auto PID tuning algorithm chose a crossover frequency based on the plant dynamics and designs for a target phase margin of 60^0. When to change the design

focus, the algorithm attempts to adjust the gains while maintaining the minimum phase margin. Essentially, it is necessary to find out the optimal design of glider (aircraft) in terms of aerodynamic force so that it can be represented as a kite. In turn, it can be gliding in the air for a longer time without control at all. A classic PID controller has been employed to stabilise the glider as a kite.

6.2.4 Cable Control

As discussed earlier for the two-line controlled kite, the cable control is only capable of controlling the roll angle and leaves the yaw and pitch angle free. Hence, the kite can fly a prescribed trajectory in the sky by manipulating the roll angle; the roll angle is then induced by creating different lengths of kite tethering cable. In comparison to the glider, ailerons are used to control the roll angle of aircraft. Therefore, only how the aileron works on the glider is of interest.

Ailerons are two loose rectangular thin pieces attached at the trailing edge of the wing on both sides. They are used to determine the roll angle of aircraft, thus control the flight direction, using tilting the wing tips up or down. They come as a pair but work in opposite directions, one side tilting up while the other hand tilts down. For example, to pilot aircraft to roll to the left, the control stick needs to turn to the left, then it results in the right aileron deflecting down to create more lift force on the right side and the left aileron deflecting up to create less lift force on the left side. This unbalanced lift force as a whole causes the plane to rotate about its major axis.

This is very similar to the two-line kite operation. To control the kite to roll to the left, the left side will need to pull back so that the left side will have less lift force, which immediately

causes the right side to have more lift force; the kite will then be controlled to roll to the left. The control of cable is also opposite in direction. The kite does not have the aileron, elevator or the rudder; therefore, after stabilising the kite, the input of the pitch angle and the yaw/heading angle will remain unchanged.

On the other hand, the PID roll controller has been employed to control the lift force generated by the wind. The aileron control becomes aero control, and the cable control needs to be added to the original control block to keep the kite stable in the air and flying on its prescribed trajectory. The rope length difference changed by DC machines.

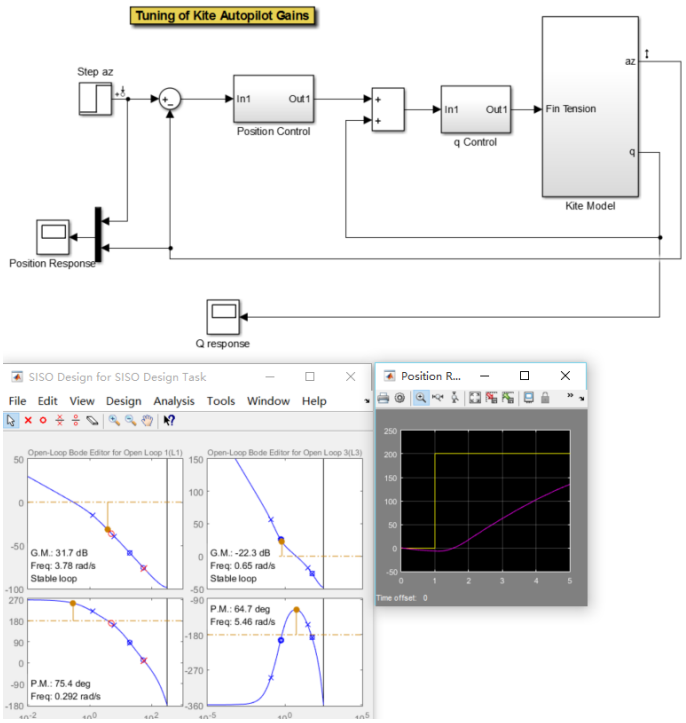

Figure 44 Turning of Kite Autopilot Gain for Cable Control

The complete kite block is presented in figure 46:

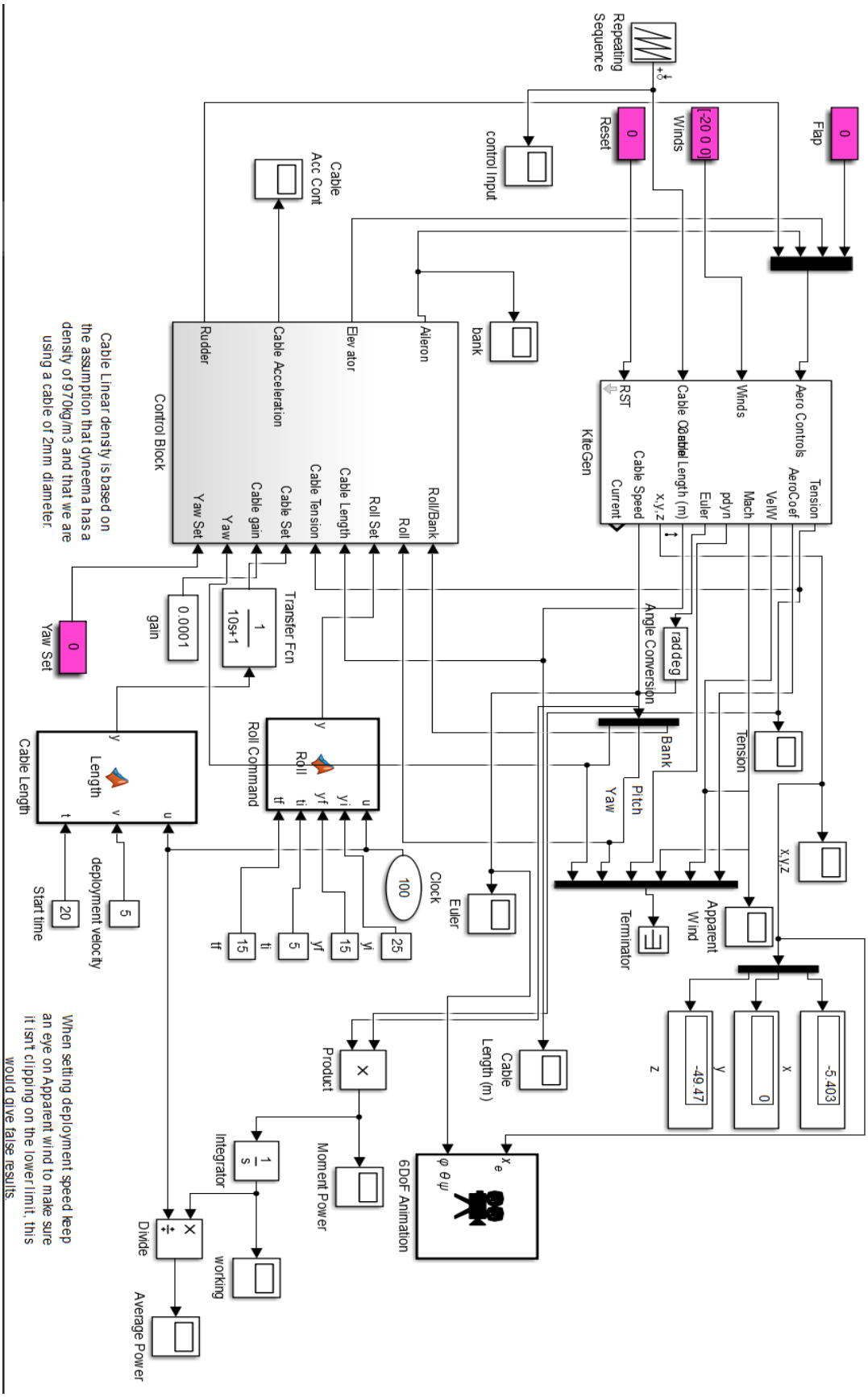

Figure 45 Overall Kite Block Early Version

6.3 Sensors

To control the kite so that it can adjust the flight by itself, the sensor is a fundamental part of the success this project. As humans maneuver the kite, we use our eyes to determine the kite location, wind direction, and velocity, feel the force exerted on the control bar and the speed of the kite at that moment. After obtaining enough current information, our brains will then make a decision to pull the left or right line to control the kite. In this project, to judge the position of the kite, the wind direction, and velocity, the force exerted on the control unit, and the speed of the kite will be determined by employing several sensors.

6.3.1 Position Sensor

Four GPS sensors are required to measure the kite position. Three of them are mounted on the kite, and one reference fits on the moving base unit. For the sensors mounted on the kite, one is at the joint where the left-hand side tip of the kite meets the left tethering cable, one is at the joint where the right-hand side tip of the kite meets the right tethering cable; and the last one is mounted on the center gravity (CG) of the kite. The sensor mount on the CG point determines the position of the kite, and sensor on each tip of the kite can ascertain the length of the rope.

6.3.2 Angle Sensor

Two sets of angle sensors are required to measure the angular velocity and displacement. By mounting the angle sensor on the line, it can detect the tethering cable azimuth angle (Φ) and inclination angle (θ). The other angle sensor is mounted on the base unit; it detects the azimuth angle (γ) of the rotational base turn. In this case, the feedback angle determines the mechanism of the drum brake condition. The other set of angle sensors is mounted on the drum to detect the angle displacement of the shift at each turn.

6.3.3 Force Transducer

Two force transducer sensors are required on each end of the tethering cable at the joint between the kite and the line to measure the forces on both cables. The signal is transmitted back to the ground control unit; the current rope tension can feed back to the local controller, and then regulate the speed of electric drive (motor or generator).

Some of these sensors are not designed for this project; however, the aim of this project is to build an underlying platform for future studies, and therefore, mounting these sensors on the kite will provide previous feedback information for later research.

6.4 Electric Machine

From above design plan, the motion of the system control unit is a three-phase cycle; traction phase, crossfeed traction phase and retraction phase. In the traction phase, the wind power releases the rope of the kite, and the kinetic energy runs electric machine as generators, driven by the movement of the drums. When the specified maximum rope length is reached, the motor begins to roll the rope, and then the drivers operate as motors, which is called the retraction phase. To drive the kite to a position which is suitable to start another traction phase, the electric motor needs to consume a tiny amount of the previously generated energy.

The kite starts flying in the wind direction of the unrolling the ropes; it causes the electric machine to work as a generator to produce power. Once the left-hand side of the drum stops at the rope length of L_{max}-ΔL, the right-hand side of the rope then unwinds for an extra rope length of ΔL. This causes the kite to move in the negative X direction. After the right-hand side of the rope reaches the length of L_{max}, the motors start to roll back the ropes in the retraction phase.

The model consists of a generator control block, a motor control block, and a DC machine subsystem. When the generator control block and motor control block finish running, their output is transmitted to the Multiport Switch with Cable Length Signal. After algorithm, Simulink-PS Converter block receives the signal and transfers it as a physical signal to the DC machine subsystem. As stated in the introduction, the kite has two drums to control its state, so in this model, there are two generators control blocks to deliver signals to different motors.

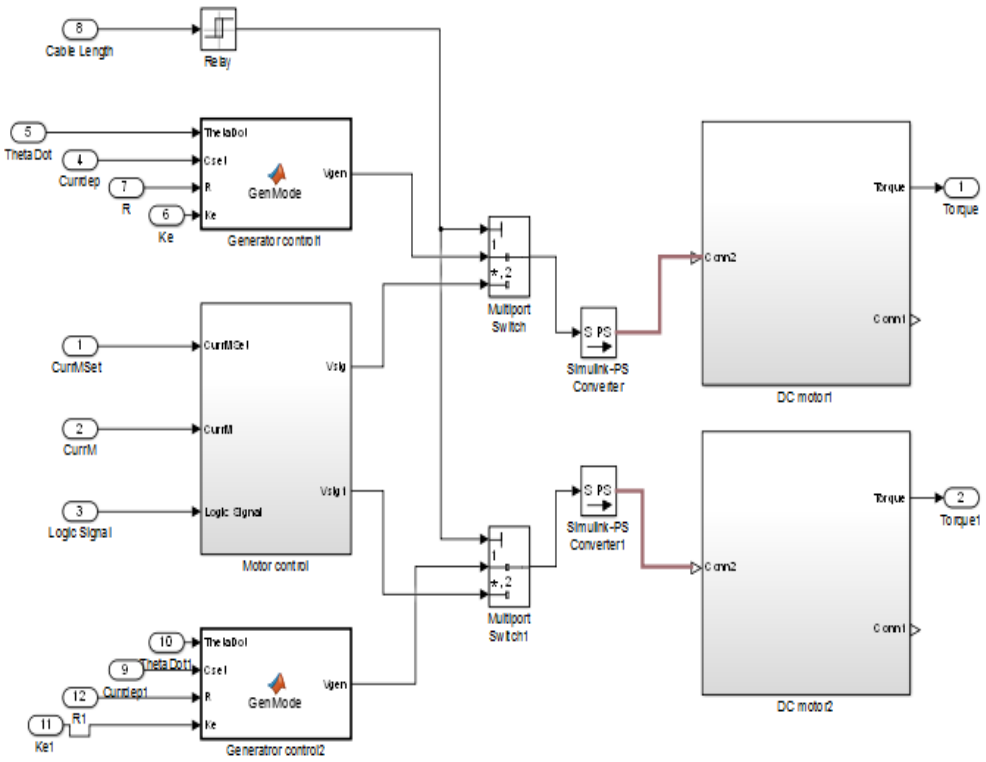

Figure 46 Electrical Machine and Control

6.4.1 DC motor model

The model shows the physical connection of motor circuit diagram. When the Controller Voltage Source receives the voltage signal, the Rotational Electromechanical Converter actuates the armature of the motor and starts to reroll the rope.

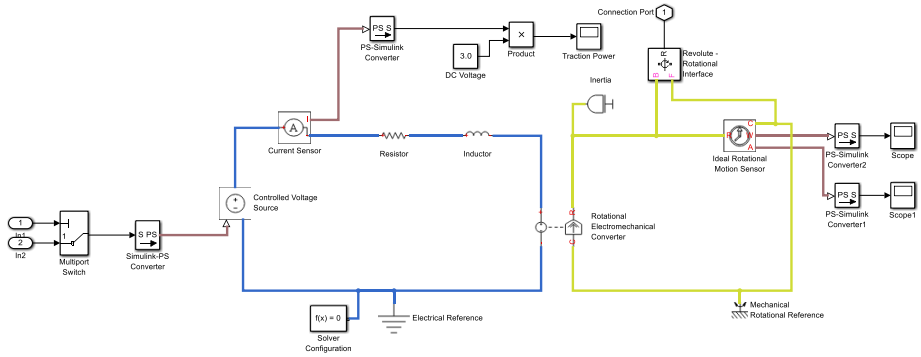

Figure 47 Motor Mode

6.4.2 DC Generator model

The generator is taking the torque input from the kite and rotating the armature to generate power.

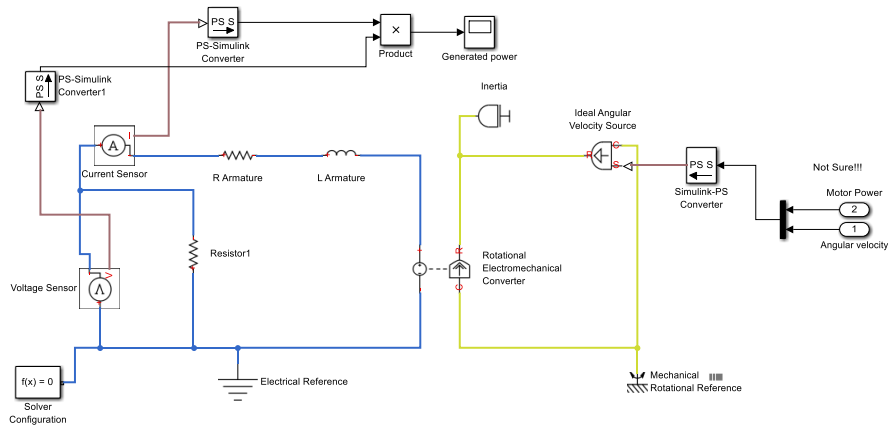

Figure 48 Generator Mode

6.4.3 Electrical Machine Control

In the motor control block, there are two input current values to the system; current measure set is a fixed current value, and current measure is a real-time current value evaluated from the kite. Simultaneously, a logic signal inputs to the derivative as shown in figure 50; this signal controls whether the integrator is reset. When the integrator is reset, the Proportional-Integral is started. After controlling, Volt Saturation storage is used to limit saturation values. Thus the result (voltage signal) is clearer.

Moreover, because two motors are physically connected to the kite, the two motor control block should receive the same input signals. Therefore, the outputs of the two motor control blocks are synchronised.

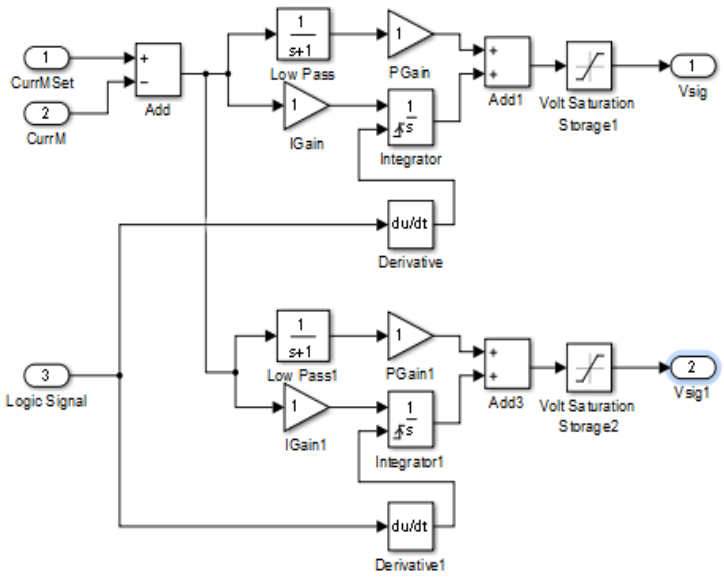

Figure 49 Control for Retraction Phase

The generator control block is a self-defined function which uses to switch between motor mode and generator mode. The function made a comparison between back emf (Ke*ThetaDot) and applied voltage (Cset*R). If back emf is greater, it means the system is in the traction phase, and the generator will then generate V_{gen} according to the steady state generator equation [31]. If the applied voltage is greater, which means that the system is in the retraction phase; there will be no output voltage from the generator. The overall system will take command from the control block for retraction phase. The code can be expressed as:

```
function Vgen = GenMode (ThetaDot, Cset,R,Ke)
%#codegen
if Ke*ThetaDot>Cset*R
   Vgen=-Ke*ThetaDot+Cset*R;
else
   Vgen=0;
End
```

This function confirms the system has the ability to control the voltage signal in a reasonable range; the test result is shown in figure 40:

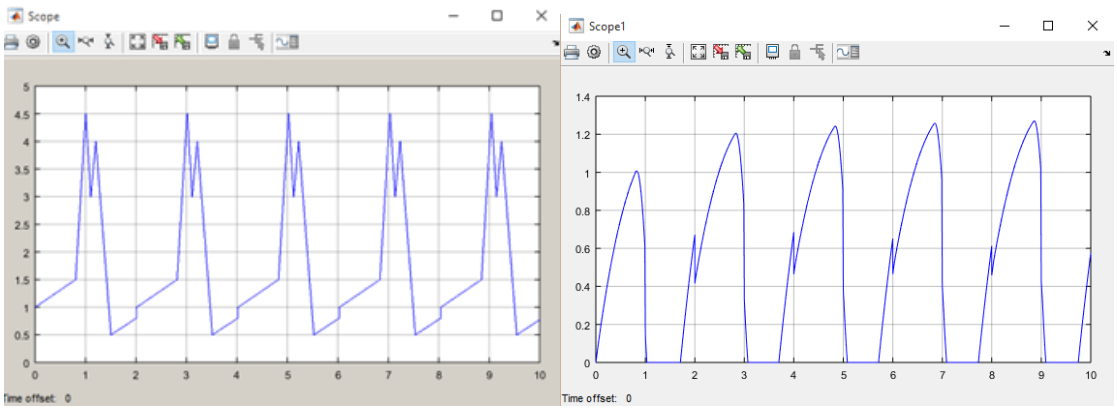

Figure 50 a) Input Current from Kite b) Controlled Voltage

The drum and drum brake are connected to the electrical machine; the generator will then be controlled by applied external brake force to achieve crossfeed traction phase.

6.4.4 Drum Brake

In the traction phase, the sum of line tension during flight is about 300N when flying through the power zone. This data has been obtained by a manual flight test; the kite parameters are shown in Table 4. When no steering input is given, the line forces were estimated to be equally large. During active steering, the line that is drawn in experiences more major forces than the line that is released. Based on measurements, a maximum force ratio of 2:1 was assumed for lines. According to this assumption, the line being drawn in experiences the nominal force of 2/3 of 300N (200N), whereas the other line transmits the remaining 100N (400N), to provide the possibility of attaching a larger kite and for safety reasons, a safety factor of Sf=2 was introduced. The forces were thus doubled for the dimensioning process.

Table 4 Filed Test Date

Parameter	**Value**
Kite Mass	8.5kg
Wind Span	2.89m
Wind Speed	18m/s
Tension Force	276.7N

In this case, the drum brake can be set as 600 N. When the cable has been sent out to one meter; the drum brake will then clamp on the rotational drum to stop the pulling force. When the other side of the cable reaches one meter, it will release the drum brake to go for another one meter. The drum brake can be constructed in SimMechnics as:

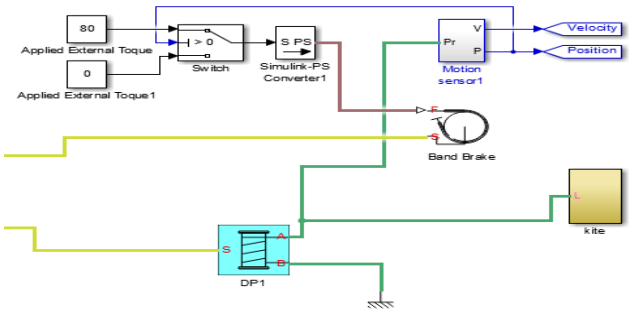

Figure 51 Drum Brake Block Diagram

6.4.5 Base Unit

A base unit used to reduce the system complexity by transferring the 3D movement to a 2D movement. It holds all the physical parts such as two electric machines; two sets of rope drum have been built under SimMechnics environment. The base unit will be used as a local reference point, and it turns according to the movement of the kite.

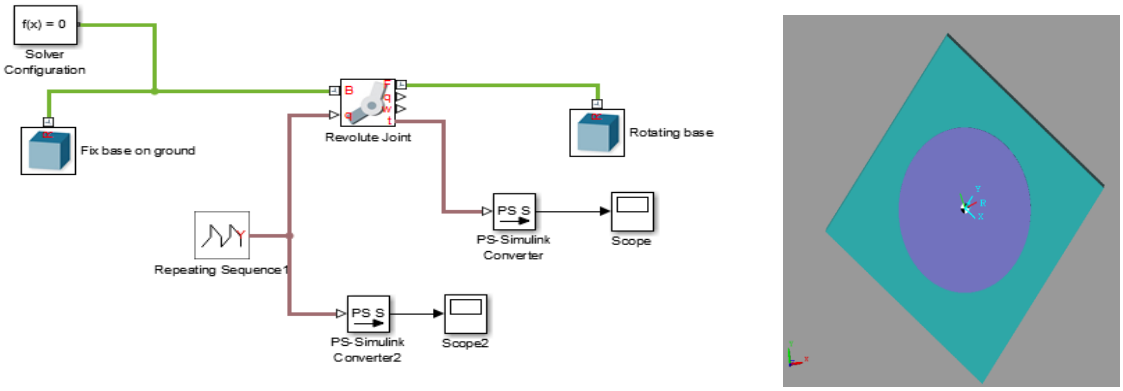

Figure 52 a) Base Unit Design b) 3D Base Unit

The base unit has two parts; the rectangle shaped base is fixed on the ground, and a circular rotational dish is mounted on top of it. These two components have been connected through the revolute joint. This joint has one degree of freedom represented by one revolute primitive; the joint constrains the originals of the two body frame to be coincident and the z-axes of the base and follower frames to be simultaneous, while the follower x-axis and y-axis can rotate around the z-axis. This joint not only offers linkage between two physical body parts but also

takes Simulink input signals to actuate the circular dish and senses the rotating plate position, angular velocity, and actuator torque. In this project, the base unit will take the overall tension force evaluated from the kite as input and rotate the rotating dish accordingly.

6.5 Visualisation

It is necessary to make an observation on how the kite flies in the sky and display the trajectory to the user. This can be done by several ways; the user can interpret the system by using the simple 2D scope in MatLab toolbox, or there is a more straightforward way to visualise the flight trajectory in three dimensions.

3D XYZ visualisation tool provides a more efficient way to communicate with the user. It can concentrate on support for perceptual and cognitive operations that enable users to detect the expected and discover the unexpected in complex information spaces. With the help of 3D XYZ scope, it can be readily determined if the system is flying in the designated trajectory or how to adjust it.

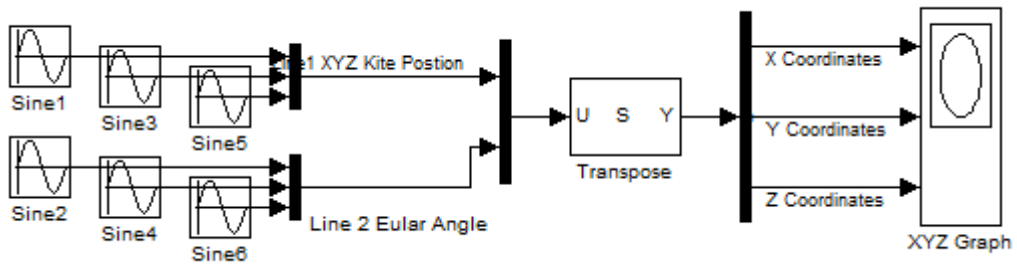

Figure 53 3D XYZ Scope

The detailed 3D script file is attached at Appendix xxii; this scope has been built based on the S-Function in MatLab toolbox. In short, it enables MatLab script file to be translated to the custom block under Simulink. It draws a line from the previous input point, which is stored using discrete states, and the current point. It then stores the current point for use in the next invocation. The plotting diagram can be adjusted in terms of the x,y and z-axis, minimum and maximum, the number of lines to display and sample time. The results will be explained in the next chapter.

7.0 Results and Findings

This section presents and discusses the results of the introduced modelling approach to see whether it leads to a realistic and fast result. The individual components of the model have been tested separately and validated in the previous chapters. Field testing of this model is beyond the scope of this thesis because the primary goal of this thesis is to introduce a fundamental modelling approach. Until now, no fully validated model has been developed due to lack of available test data. More experimental data has become available over the last couple of years, but validation methods are still in development. It is tough to compare the measurement data and simulations with other research results because, for instance, it is difficult to measure the deformations of the kite or to reproduce the exact measurement conditions in the computer model. Without field tests, it is still possible to say something about the validity of the model by comparing it to other models and comparing the results to known facts about kite behaviour.

7.1 Results

The simulated results are presented in this section. With the reduction of out of plane motion, only two dimension variables are included in this model, and results are shown in Table 5.The parameters used for this test are:

Table 5

Parameter	**Value**
Kite Mass	8.5kg
Wind Span	2.89m
Wind Speed	18m/s
C_L	0.3
C_D	0.04

7.1.1 Kite Movement

Figure 55 below illustrates the altitude and X direction of the kite position with respect to time. During the traction phase, due to the aerodynamic force, the kite will climb and move towards the downwind. The trap cut indicates that the cable is doing the crossfeed until the cable reaches maximum length, then the retraction phase will start at the 30s. The graph shows that the kite rapidly moves upwind until it reaches a quasi-equilibrium state, then the next traction phase will start again.

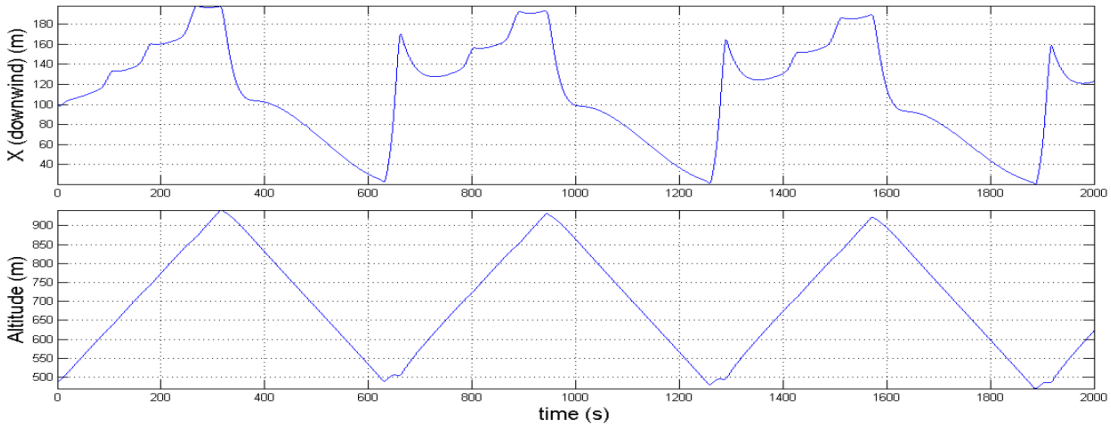

Figure 54 Kite Position without Control

Figure 56 below shows the tether tension and roll angle. **It is clear that the tension exerted on the line is directly proportional to roll angle.**

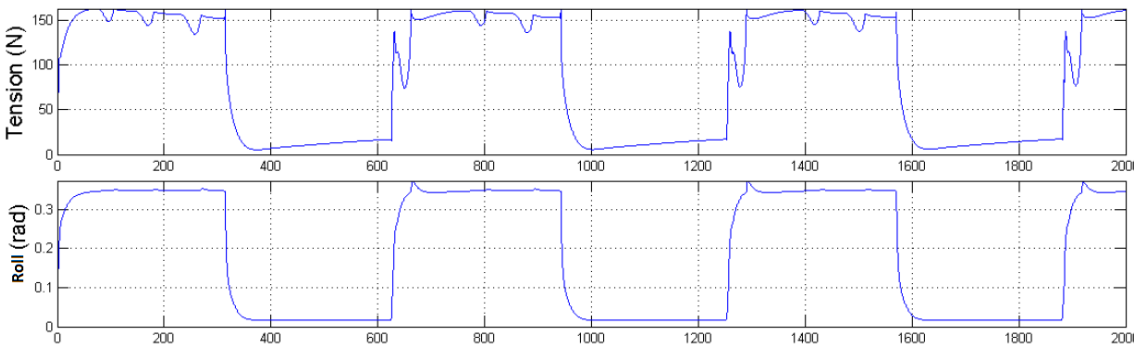

Figure 55 Cable Tension without Control

7.1.2 Power Generation

The power can be calculated out by using the section 3.6.1 mathematic formula P=T*$\dot{\theta}_m$. Since there is no gear ratio in between (ignore the drum radius in test), the angular displacement of the generator rotor shaft $\dot{\theta}_m$ is directly proportional to the cable speed. Therefore, the power can be presented as:

Power=Tension*Cable Speed

Figure 57 shows the average power generation over the simulation time is approximately 100W.

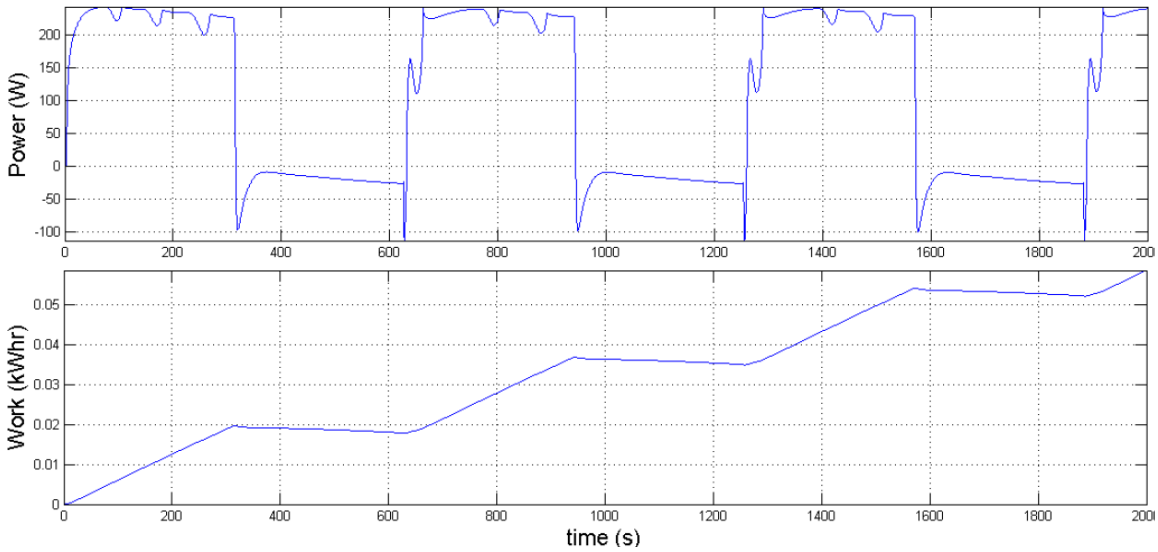

Figure 56 Power Generation without Control

For the first 300s, it is a traction phase; the power that has been generated is around 200W. The cupped shape at the 80s, 160s and 240s are when the kite been has been steering to a different location. The retraction phase starts at 320s; the electric machine now acts as a motor, it consumes approximately 100W to retrace the kite back to the original position.

This result suggests that it is possible to generate power by the current system model.

7.1.3 Optimal Power Control

The kite model is adopted from UMA glider in Aerosim; hence, the first step is to modify the glider to kite and stabilise it. Numerical experiments have been carried out to find the right gain to stabilise the glider through classic PI, PID and P control on aileron, elevator, and rudder. The detailed tuning process presented in chapter four and five. This section is then focused on introducing the test results of the machine control over the tethering cable. The electrical machine has been controlled by the applied voltage, aimed to maximise power generation. The switching control between traction and retracting phase has also been used to minimise the transient spark.

The machine electrical parameters are as follows in Table 6:

Table 6

Parameter	**Value**
B (Viscous Friction Coefficient)	0.00027
Ke back emf constant	0.04434
Kt torque constant	0.0491
Ra Armature Resistance	0.177Ohm
Ia Peak Current	29A
V_{max}	25V
Il Current Limit	12.5A
Jm motor inertial	670e-6
Drum radius	0.021m
Gear Ratio	10/3

The test results below in figure 58 show Kite X direction Position, Kite Altitude, Machine Current, Machine Voltage, Cable Tension, Roll Angle, Power Generation and Average Power. The simulation set generation current as 20A in traction phase and set motor current as 5A in retraction phase. When comparing with the previous test results, the power generation efficient has been improved from 50% to 60%. **Cable control through classic PI tuning achieved a good result of improving generation power efficacy.**

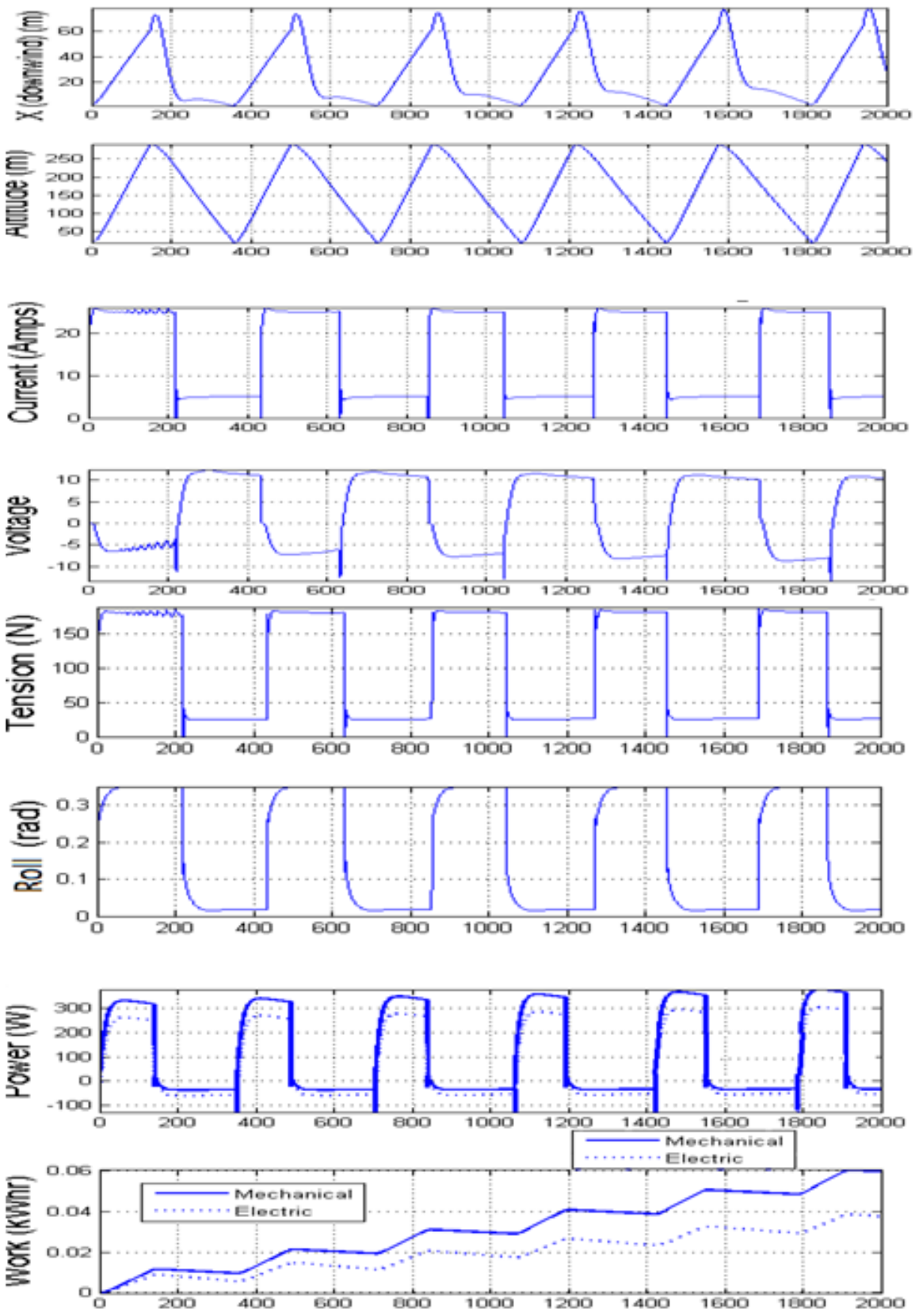

Figure 57 a) Kite X direction Position b) Kite Altitude c) Machine Current d) Machine Voltage e) Cable Tension f) Roll Angle g) Power Generation h) Average Power

7.1.4 Flight Trajectory Control

This section presents the results of kite flight trajectory by classic one input feedback controller. The input element is the kite roll angle; the detailed explanation can be found in chapter 3.7. The trajectory is shown from the moment the controller is turned on. The kite has been steered to flight in a rough figure eight trajectory; however, the controller fails to steer the kite in the precisely prescribed figure-eight trajectory.

The current feedback controller is not fast enough to control the highly dynamic kite movement. Firstly, kite movement is a highly non-linearized system. Thus it is very hard to identify the optimal setting parameters to be controlled by a simple linearized feedback controller. Secondly, the electrical machine has physical limitations in terms of the rotation speed and response time. Therefore, the kite control needs a feed-forward controller like fast model predictive control.

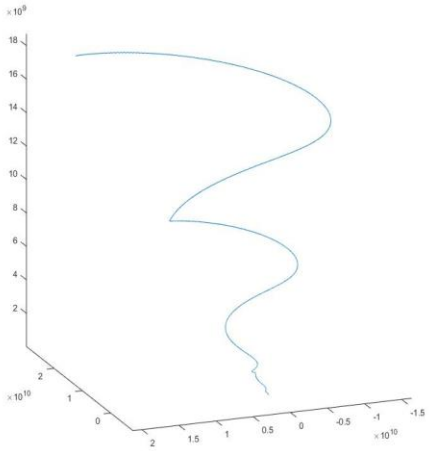

Figure 58 Tested Flight Trajectory

7.1.5 Validation of Forces Model

The Diehl's model shows that the line force can be expressed as:

$$F_{ten}=m(r\dot{\theta}^2 + r\sin(\theta)^2\,\dot{\emptyset}^2)\text{-}mg\cos(\theta)+F_r^{aer}$$

Figure 60 below presents the simulation result (in green) compared with the calculated line tension result. The test parameters are as follows in Table 7:

Table 7 Force Test Data

Parameter	**Value**
Kite Mass	1.5kg
Wind Span	1.89m
Wind Speed	18m/s
Tension Force	27.67N
C_L	0.6
C_D	0.16

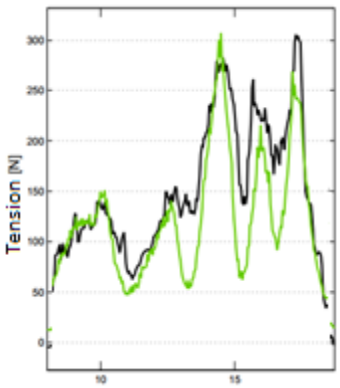

Figure 59 Calculate Tension VS Simulation Tension

The calculated result is very well correlated with the simulation result in the force magnitude. On the other hand, it also suggests that at the time when the kite changes the direction of flight trajectory at the time of 11s, 14s, 16s, 18s, 21s 23s, the mathematic model only predicts half of actual force. This can be explained by the mathematic model assuming the lift coefficient and drag coefficient remain the same thought out the whole flight process; however, **the lift drag coefficient is not same all the time.**

7.1.6 System Stability

This section reviews the overall system response characteristics. The system is firstly linearized using MatLab tool for control design. The order of the system is found to be 14. The transfer function is expressed as:

s^13 + 37.6 s^12 + 608.2 s^11 + 6411 s^10 + 4.697e004 s^9 + 2.097e005 s^8 + 6.854e005 s^7 + 7.165e005 s^6 + 2.525e005 s^5+ 2.8e004 s^4 + 273.7 s^3 - 5.52e-005 s^2 - 9.046e-019 s 0.1027 s^9 + 10.76 s^8 + 114.7 s^7 + 51.61 s^6 - 1074 s^ - 5.261e004 s^4 - 3.871e004 s^3 - 7664 s^2 - 64.38 s + 4.35e-013

y13: ----------

- s^12 + 37.6 s^11 + 608.2 s^10 + 6411 s^9 + 4.697e004 s^8 + 2.097e005 s^7 + 6.854e005 s^6 + 7.165e005 s^5 + 2.525e005 s^4 + 2.8e004 s^3 + 273.7 s^2 - 5.52e-005 s + 6.509e-019

Pole-Zero Map was used to visualise the properties of the system. Hence it determines if the system is stable or not. As figure 61 below suggests, **the overall kite system is a marginally stable system, which depends on the initial conditions. However, due to the complexity of the fast kite dynamic, the linear control system is not suitable for this system.**

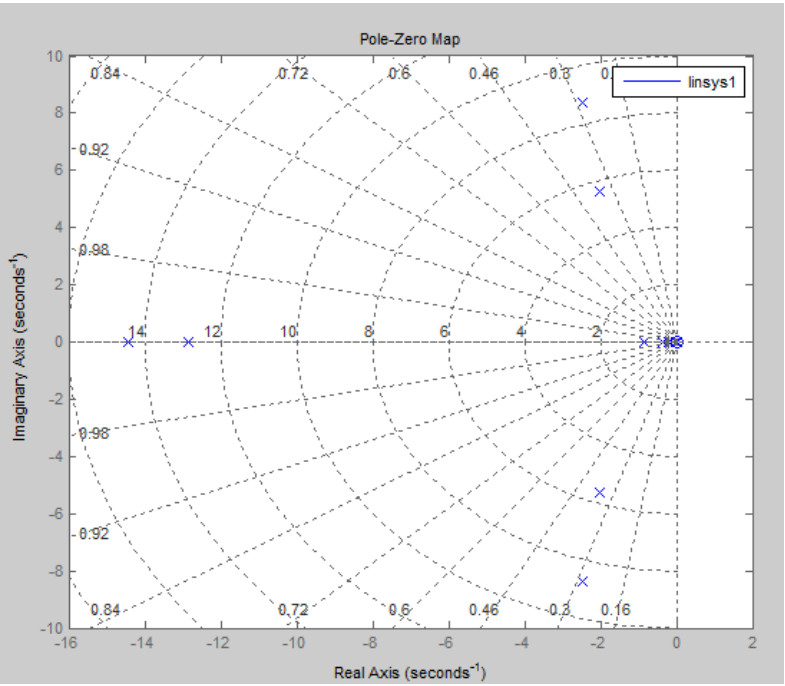

Figure 60 System Pole-Zero Map

7.2 Findings

The achievements of this project can be summarised as:

- **Identified that the tension exerted on the line is directly proportional to roll angle.**
- **Proved it is possible to generate power by current system model.**
- **Found that cable control through classic PI tuning achieved a good result of improving power generation efficacy.**
- **Disproved the current feedback controller design; it is not fast enough to control the highly dynamic kite movement**
- **Compared the calculated results; they are very well correlated with the simulation results in the force magnitude. However, lift drag coefficient is not the same all the time.**
- **Demonstrated overall kite system is a marginally stable system, which mainly depends on the initial conditions. However, due to the complexity of the fast kite dynamic, the designed linear control system is not suitable for this project.**
- **Identified that this system required the predictive control method to cope with this fast motion.**

8.0 Summary and Conclusion

This thesis started by reviewing different types of kites and identifying a two-line power kite as the study object. It then investigated the aerodynamic behaviours of two-line power kites, after developing the mathematic models uses Newton method and Kane's equation to suit this project, designed blueprint has developed for overall power generation system according to the kite's dynamic characteristics. Next, it developed a simulation model for power generation cycle by employing Simscape and Aerosim/Aerospace. The simulation involved reducing system complexity, trimming the system to a simple one variable (kite bank angle induced by difference length of two ropes) feedback control, adopting and adjusting the glider model aircraft as a kite, designing a drum, drum brake, and base unit mechanism and controlling an electrical machine.

The underlying platform has successfully built for further development. In this sense, this result fulfilled the goal of this project. On the other hand, there are numbers of assumptions and constraints were made. These limitations are setting wind speed as constant, setting the angle of attack as constant, ignoring the weight of rope, ignoring the damping factor of the rope, trading the kite as point of mass without considering the deforming of the kite body, ignoring the DC machine's vibrational influence and ignoring the drum friction factors. It is clear that the real test results will vary regarding stability, observability, and controllability.

However, according to Box, *"Essentially, all models are wrong, but some are useful."* [32] In this case, this model can be utilised to explain, predict and understand how kite generation systems work and provide a foundation for building a physical autonomous kite control system to achieve power generation.

9.0 Future work

Utilizing the motor controller that was developed and simulated, the work of integrating the most advanced controller into a full kite model simulation should be done to verify the dynamic system fully. When simulating a kite, it is critical to pick the right kite model to use for simulation as each kite's trajectory and simulation parameters would be different under the same environment circumstances. The motor controller unit would have been best to be used in a simple simulation to start off with and ramp up the kite complicity.

Once the simulation of the full kite model including the motor controller unit has been fully configured and simulated, it is time to build the actual system. The bill of materials would include at least three motors from the model above: One for the base turning table to move in the direction of the kite relative to the base tether, and one or two motors to reel the kite in when required. The generator would also be connected to the line reel when the motor is not running to ensure power can be generated in all kite generated movement. Then to construct the kite that is as close to the model as possible.

Once the whole kite system is realistically built, the kite would require additional location sensors on the kite actual and the generator output connected to a load circuit, with voltage and current measured the whole time. Once these additions made to the system, a test flight should be arranged so kite location 3D data can be mapped and the generated voltage and current performance data obtained. These data would help refine the generation efficiency, and the real location data would improve model simulation.

When the kite has been perfected to some degree of stability, and the power output is satisfactory, collaborations with larger companies such as KiteGen, NTS Gmbh, or Makani

power can be considered for industrial-sized development. Such a development would be useful to foster an academic-industry relationship and larger scale viability of deployment and verification of the kite method for sustainable power generation.

Glossary

r line length, m

S/A area of kite, m^2

d wingspan, m

t time, s

m mass of kite, kg

g gravitational constant, $m \cdot s^{-2}$

ρ Air density, $kg \cdot m^{-3}$

T line tension, N

F_L lift force, N

C_L lift force coefficient

F_D drag force, N

C_D drag force coefficient

AOA angle of attack, degree

F total force on kite, N

F_g gravitational force on kite, N

F_{ten} force exerts by kite, N

x, y, z Cartesian coordinates of O frame, m

P kite position vector in O frame, m

θ, φ, r spherical co-ordinates of o frame, rad, rad,m

$\dot{\theta}$, $\dot{\varphi}$, $\dot{r}$ spherical co-ordinates of o frame speed, $rad \cdot s^{-1}$, $rad \cdot s^{-1}$, $m \cdot s^{-1}$

$\ddot{\theta}$, $\ddot{\varphi}$, $\ddot{r}$ spherical co-ordinates of o frame accelerations, $rad \cdot s^{-2}$, $rad \cdot s^{-2}$, $m \cdot s^{-2}$

e_x, e_y,e_z unit vector of e-frame with the local coordinate of the kite in x, y z-axis

F_{aero} aerodynamic force on kite, N

F_{app} apparent force, N

W_0 nominal wind speed vector, $m.s^{-1}$

We effective wind speed, $m.s^{-1}$

q Quaternion vector

u control vector

x(t) state vector

$\dot{x}$(t) Time derivative of the state vector

ΔL Length difference between two rope/cable/tethering line, m

L_L left-hand side of the rope, m

L_R right-hand side of the rope, m

Ψ Kite bank angle/ glide angle/steering angle, rad

p, q, r roll rate, pitch rate and yaw rate, used in aerosim $rad \cdot s^{-1}$, $rad \cdot s^{-1}$, $rad \cdot s^{-1}$

$\delta_e, \delta_a, \delta_r$ Elevator, aileron and rudder deflection used in aerosim

$\emptyset, \theta, \alpha$ Roll angel, pitch angel and angel of attack used in aerosim rad, rad, rad

P_{dyn} wind tunnel dynamic pressure pa in aerosim

rho air density $kg \cdot m^{-3}$ in aerosim

J_g Generator inertia in simscape

B friction coefficient in simscape

R_a Armature winding resistance Ω in simscape

L_a Armature winding inductance H in simscape

θ_g Angular displacement rad/s in simscape

T Applied Torque τ in simscape

k_t Torque constant in simscape

V_{emf} Back emf voltage V in simscape

k_e Back emf constant in simscape

I_a Motor armature current A in simscape

J_m Motor inertia in simscape in simscape

Bibliography

1) U.S. Energy Information Administration, *International Energy Statistics,* Retrieved from http://www.eia.gov/cfapps/ipdbproject/iedindex3.cfm?tid=2&pid=2&aid=2&cid=ww,&syid=1980&eyid=2012&unit=BKWH

2) Jacobsson,S & Bergek,A. (2004). Transforming the energy sector: the evolution of technological systems om renewable energy technology. Industrial and Corporate Change. V13, n5, 815-849

3) The Institution of Engineering and Technology, *Archives Biography: Michael Faraday.* Retrieved from http://www.theiet.org/resources/library/archives/biographies/faraday.cfm

4) Niagara Faills Info, *Schoellkopf Power Plant.* Retrieved from http://www.niagarafallsinfo.com/history-item.php?entry_id=1435&current_category_id=242

5) Bright Hub Engineering, *Compare the Efficiency of Different Power Plants.* Retrieved from http://www.brighthubengineering.com/power-plants/72369-compare-the-efficiency-of-different-power-plants/

6) The Shift Project Data Portal, *Breakdown of Electricity Generation by Energy Source.* Retrieved from http://www.tsp-data-portal.org/Breakdown-of-Electricity-Generation-by-Energy-Source#tspQvChart

7) A Pioneer is Vindicated in *Kiplinger's Personal Finance*, Jan 1981. page 24

8) Union of Concerned Scientists, *Environmental Impacts of Hydroelectric Power.* Retrieved from http://www.ucsusa.org/clean_energy/our-energy-choices/renewable-energy/environmental-impacts-hydroelectric-power.html#.VbX_MPmqqko

9) Wind-power Program, *The Betz limit*. Retrieved from http://www.wind-power-program.com/betz.htm

10) Union of Concerned Scientists, *Environmental impacts of Hydroelectric Power*. Retrieved from http://www.ucsusa.org/clean_energy/our-energy-choices/renewable-energy/environmental-impacts-hydroelectric-power.html#.VbX_MPmqqko

11) My Best Kite, *Types of Kites*. Retrieved from http://www.my-best-kite.com/types-of-kites.html

12) Flickr, Akiyoshi, O, Rokkaku Kite. Retrieved from https://www.flickr.com/photos/drachen/8035132083

13) Wind power sports, *Delta kites*. Retrieved from http://www.windpowersports.com/kites/prism/stowaway-delta.php

14) Nosewmac, *Roller Kite*. Retrieved from http://www.nosewmac.com/kite-album/taped-kites/roller.html

15) Gombergkites, *G-Kites-Advanced Flaying Products*. Retrieved from http://www.gombergkites.com/g-advanced.html

16) Prism Kite Technology, *Tensor 5.0*. Retrieved from http://www.prismkites.com/products-pk-tensor50.php

17) Loyd, M. (1980), Crosswind Kite Power. *Journal of energy.* 13,41,43

18) Archer,C. & Caldeira, K. (2009). Global Assessment of High-Altitude Wind Power, *Energies. v2, n2,* 307-319

19) Ockels, W. (2001), Laddermill, a novel concept to exploit the energy in the airspace, *Aircraft Design*, *81-97*

20) Milano, P. (2012), Wind Energy Report 2012, *Collana Quaderni AIP,* 9.

21) Kleidon, F. & Miller, A & Gans, L. (2011), Jet stream wind power as a renewable energy resource: Little power, big impacts. *Earth System Dynamics, v2,n2,* 201-212

22) Surfer today, *How does a kite fly* (2015). Retrieved from http://www.surfertoday.com/kiteboarding/11494-how-does-a-kite-fly

23) National aeronautics and space administration (NASA), Glenn research center, *Newton's Laws of motion*. Retrieved from https://www.grc.nasa.gov/www/K-12/airplane/newton.html

24) American flyers, *Principles of Flight*. Retrieved from https://www.americanflyers.net/aviationlibrary/pilots_handbook/chapter_2.htm

25) RAANZ, *Forces acting on the microlight*. Retrieved from http://raanz.org.nz/wiki/pmwiki.php?n=TM.Principals

26) Loyd, M. (1980). *Crosswind Kite Power*, Lawrence Livermore National Laboratory, Livermore, Calif. Retrieved from http://homes.esat.kuleuven.be/~highwind/wp-content/uploads/2011/07/Loyd1980.pdf

27) Ippolito, M. KiteGen Research, *Response to 'Jet stream wind power as a renewable energy source: Little power, big impacts.* Retrieved from http://www.kitegen.com/en/2012/03/22/the-max-planck-is-scared-to-fly/

28) Ghivarello, M. KiteGen, *Carbo-Kite.* Retrieved from http://kitegen.com/2012/03/13/carbo-kite/

29) Hennon, C. Atmospheric Sciences, University of North Carolina Asheville, North Carolina. Retrieved from http://www.atms.unca.edu/chennon/notes/atms310/apparent_forces.pdf

30) Breukels, J. (2010). An Engineering Methodology for Kite Design, *Uitgeverij BOXPress, Oisterwijk,* 21, 47-49, 57, 83, 87

31) MacKite, *Kiteboarding FAQs: The Wind Window.* Retrieved from http://www.mackiteboarding.com/kiteboarding-wind-window.htm

32) Dawson, R. (2011), Kite Turning (Masters Thesis), *University of Canterbury, Christchurch, New Zealand.*

33) Wind Systems Mag, *Kiting for Wind Power.* Retrieved from http://windsystemsmag.com/article/detail/392/kiting-for-wind-power

34) Ruitterkamp, R. & Ockels, W. & Williams, P. & Lansdorp, B. (2008) Modelling, Simulation, and Testing of Surf Kites for Power Generation. *AIAA Modelling and Simulation Technologies Conference and Exhibit.* 45,47

35) Ockels, W. & Williams, P. & Lansdorp, B. (2007) Modelling and Control of a Kite on a Variable Length Flexible Inelastic Tether. *AIAA Modelling and Simulation Technologies Conference and Exhibit.* 48,49

36) Schimehl, R. & Ockels, W. & Terink, E. & Breukels, J. (2011) Flight dynamics and stability of a tether inflatable kiteplane. *Journal of Aircraft, v48, n2.* 45, 503-513

37) Breukels, W. & Ockels, J. (2008). Analysis of complex inflatable structures using a multi-body dynamic approach. *Collection of Technical Papers – AIAA/ASME/ASCE/AHS/ASC Structures, Structural Dynamics and Materials Conference.*

38) The Mathworks, *How Simscape Simulation Works.* Retrieved from http://au.mathworks.com/help/physmod/simscape/ug/how-simscape-simulation-works.html?refresh=true

39) The Mathworks, *How Simscape Models Represent Physical Systems.* Retrieved from http://au.mathworks.com/help/physmod/simscape/ug/how-simscape-models-represent-physical-systems.html

40) The Mathworks, *Choosing a Solver*. Retrieved from http://au.mathworks.com/help/optim/ug/choosing-a-solver.html

41) Miller, S. The Mathworks, *Modelling Physical Systems as Physical Networks with the Simscape Language*. Retrieved from https://www.mathworks.com/tagteam/63431_Physical_Networks_In_Simscape_PDF.pdf

42) Chuna, S. & Yen, C., & Chen, J (2009). Coupling behaviour of wire ropes subjected to tensile impulses. *Journal of Engineering Mechanics, v135, n 8,* 796-801

43) Canale, M. & Fagiano, L. & Milanese, M. (2007), A multibody dynamics approach to a cable simulation for kites, *IEEE Control Systems Magazine, v27, n 6,* 25-38, 83

44) Maneia, G. (2012). Aerodynamic study of airfoils and wings for power kites applications (Masters Thesis). *Politecnico di Torino, Italy.*

45) Silvennoinen, P. & Argatov, R. & Rautakorpi, I. (2009). Estimation of the mechanical energy output of the kite wind generator. *Renewable Energy v34, n6.* 1525-1532

46) Argatov, R. & Silvennoinen, I. (2012). Asymptotic modelling of unconstrained control of a tethered power kite moving along a given closed-loop spherical trajectory. *Journal of Engineering Mathematics, v72, n 1.* 187-203

47) Box, G. & Draper, N. (1987). Empirical Model-Building and Response Surfaces, *Wiley ISBN 0471810339.* 424